Cytoplasmic Domains in ClC Channels and Transporters

Structure and Function

Dissertation
zur Erlangung der naturwissenschaftlichen Doktorwürde
(Dr. sc. nat.)

vorgelegt der

Mathematisch-naturwissenschaftlichen Fakultät der
Universität Zürich

von
Sebastian Meyer
aus
Deutschland

Promotionskomitee

Prof. Dr. Raimund Dutzler (Leitung und Vorsitz)
Prof. Dr. Julia Fritz-Steuber
Prof. Dr. Tilman Schirmer

Zürich 2008

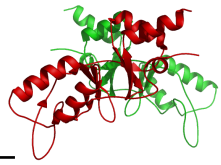

Acknowledgements

I am grateful to many people for help, both direct and indirect, in completing this thesis and making my time at the University of Zürich most entertaining.
First and foremost, I would like to thank Prof. Raimund Dutzler for giving me the opportunity to work on this challenging, interdisciplinary project and providing an excellent scientific environment.
I am very thankful to Prof. Julia Fritz-Steuber and Prof Tilman Schirmer for scientific discussions and kindly agreeing to take part in this project by forming my PhD thesis committee.
Furthermore I would like to thank my scientific collaborators Prof. Konstantin Pervushin and Dr. Simon Alioth for the scientific exchange during our shared project.
For the support in robotic crystallization I am indebted to Beat Blattmann and Annette Haisch, for help and advice concerning electrophysiological experiments I would like to thank Dr. Ian Forster.
I am grateful to all the members of the Dutzler laboratory for their support and especially Sara Savaresi for her enthusiasm in our mutual projects over the last four years.
Moreover I would like to thank all the colleagues at the institute who have helped me along the years with scientific advice or have contributed in providing the necessary infrastructure, without whom this project would not have been possible.
For all the support outside the laboratory I am grateful to my family, especially my parents, and Sara for all the encouragement and love. Furthermore I would like to thank all friends, old and new ones, that have been with me and made my time in Zürich most enjoyable. Special thanks to Swami for our many recreational BBQ events, Sara and Dani for inspiring coffee breaks, the "Jass" mates for many nice Endstationen, Thilo and Annette for challenging running and the lunch squad for purely nonscientific research.
My apologies if I have inadvertently omitted anybody, who has contributed to the success of this work.

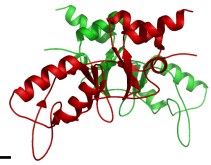

Contents

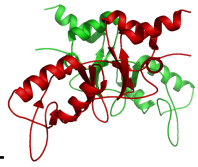

List of Figures

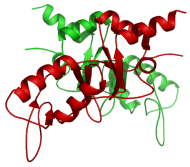

Abstract

ClC chloride channels and transporters are found in virtually every living cell and they are key players in a variety of physiological processes. The nine family members expressed in human are involved in diverse physiological functions ranging from the stabilization of membrane potentials, transepithelial transport of salt and water to the acidification of intracellular vesicles. Their essential roles in the organism are emphasized by hereditary diseases arising from ClC malfunction like myotonia, Dent's disease, Bartter's syndrome or osteopetrosis.

Structures of two bacterial homologs serve as a structural framework for the transmembrane region of the protein family. However, these crystal structures do not account for large cytoplasmic domains that are inherent to all human ClCs. These intracellular parts of the protein have been shown to be crucial for protein function and to be involved in the functional regulation of chloride transport. The precise role of these cytoplasmic domains in the context of the ClC family is unclear, although they have been associated with processes like the regulation of channel gating or ligand binding. Despite these functional implications only limited biochemical and no structural information on the organization of these domains was available. Therefore it was the aim of my PhD project to structurally and functionally characterize the cytoplasmic domains of ClC channels and transporters.

These domains were studied in the context of two members of the ClC family, the voltage-gated chloride channel ClC-0 from *Torpedo marmorata* and the human secondary active transporter ClC-5.

The structure of the isolated domains from ClC-0 provided the first atomic model of the ClC intracellular domains, thus revealing the structural organization of the protein including the organization of the two cystathionine-β-synthase (CBS) subdomains present in all eukaryotic ClCs. In addition it was established by analytical ultracentrifugation that the isolated cytoplasmic domains assemble as protein dimers in solution,

thereby extending the dimeric arrangement observed for the transmembrane domains. The structural studies on the domains from ClC-0 led to the discovery of extended natively disordered sequence stretches in the intracellular domains of a branch in the ClC family. In a study in collaboration with Prof. K. Pervushin from the ETH Zürich the dynamic properties of these functionally relevant segments have been characterized with nuclear magnetic resonance techniques.

The work conducted on the human transporter ClC-5 led to the structures of the isolated domains in complex with bound ATP and ADP. This is the first structure of any CBS domain protein with its nucleotide ligand revealing a novel ATP binding site and the molecular determinants of nucleotide recognition. The affinities of the cytoplasmic domains for adenosine nucleotides were determined and, under certain conditions, a modulation of ClC-5 activity could be correlated with nucleotide binding in electrophysiological measurements. Additionally, the crystal structure of the cytoplasmic domains revealed a novel dimeric arrangement.

In summary, the studies presented in this work provide the first high resolution structures for these important regulatory modules in ClC proteins. Structural and functional characterization revealed the oligomeric assembly of these domains, as well as the molecular interaction with adenosine ligands and aspects of their regulatory effects, an emerging facet of ClC modulation.

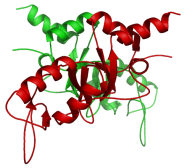

Zusammenfassung

Die Familie der ClC Chlorid Kanäle und Transporter sind an einer Vielzahl von wichtigen zellulären Prozeßen beteiligt und in nahezu allen lebenden Zellen zu finden. Die neun im Menschen vorkommenden Homologe tragen maßgeblich zu verschiedensten physiologischen Mechanismen bei, beginnend bei der Stabilisation von Membranpotentialen, über den Transport von Salzen und Wasser durch Zellepithele bis zur Ansäuerung von intrazellulären Kompartimenten. Ihre Wichtigkeit für den Organismus wird deutlich durch verschiedene erblich bedingte Krankheiten, die auf Fehlfunktionen in ClC Proteinen beruhen, wie Myotonie, die Syndrome Dent und Bartter sowie Osteopetrose.
Die Kristallstrukturen von zwei prokaryotischen ClC Homologen dienen als Modelle für den strukturellen Aufbau der membranständigen katalytischen Domäne der Proteinfamilie. In diesen Strukturen fehlen jedoch große zytoplasmatische Domänen, die Teil aller humaner ClC Proteine sind. Diese intrazellulären Domänen sind essentiell für die Funktion der Proteine und zudem an der Regulation des Chloridtransports beteiligt. Die genaue Funktionsweise dieser Proteindomänen in den ClC Kanälen und Transportern ist noch ungeklärt, obwohl sie mit der Regulation der Kanalaktivität oder auch mit Ligandenbindung in Verbindung gebracht wurden. Trotz dieser ersten Hinweise auf ihre funktionelle Rolle gab es nur wenige biochemische, und so gut wie keine strukturellen Informationen über ihre Organisation. Aus diesem Grunde war es Ziel meiner Doktorarbeit die zytplasmatischen Domänen der ClC Familie strukturell und funktionell genauer zu untersuchen.
Diese Untersuchungen wurden am Beispiel von zwei ClC Proteinen durchgeführt, dem spannungsabhängigen Chloridkanal ClC-0 aus *Torpedo marmorata* sowie dem humanen sekundär aktiven Transporter ClC-5.
Die Struktur der isolierten Domänen aus ClC-0 stellt das erste Modell mit atomarer Auflösung der intrazellulären Domänen der ClC Familie dar. Die Kristallstruktur gibt Aufschluß über den Aufbau der Domänen und zeigt die Organisation von zwei Sub-

domänen, die nach der Cystathionin-Synthetase (CBS) benannt sind. Diese Subdomänen kommen in allen eukaryotischen ClC Proteinen vor. Zudem konnte in dieser Studie mit Hilfe von analytischer Ultrazentrifugation gezeigt werden, daß die isolierten Domänen, ähnlich wie die katalytischen Membrandomänen, in Lösung dimerisieren. Des weiteren wurden anhand dieser strukturellen Untersuchungen innerhalb der zytoplasmatischen Proteinregionen von ClC-0 Bereiche entdeckt, die als intrinsisch ungeordnete Sequenzen vorliegen. Diese Sequenzbereiche sind nur in einer Untergruppe der ClC Proteine zu finden, scheinen aber wichtige Motive für deren Funktionsregulation zu beinhalten. In einer Zusammenarbeit mit Prof. K. Pervushin von der ETH Zürich wurden die dynamischen Eigenschaften dieser Proteinsequenzen mit Kernspinresonanzspektroskopie genauer charakterisiert.
Die am humanen Transportprotein ClC-5 vorgenommenen Untersuchungen führten zu den Kristallstrukturen der isolierten zytplasmatischen Domänen im Komplex mit ATP sowie ADP. Diese stellen die ersten Strukturen von Proteinen dar, die die molekulare Interaktion von CBS Subdomänen mit ihren Nukleotidliganden zeigen. Die Bindungsaffinitäten der Domänen für Adenosinnukleotide wurden durch Gleichgewichtsdialysen bestimmt. Zudem konnte in elektrophysiologischen Messungen unter bestimmten Bedingungen eine veränderte Aktivität des ClC-5 mit dem Bindungsverhalten des Liganden korreliert werden. Darüber hinaus ist in der Kristallstruktur erstmals die Dimerisierung zweier intrazellulärer ClC Domänen zu sehen.
Alles in allem zeigen die in dieser Arbeit vorgelegten Studien die ersten hoch auflösenden Kristallstrukturen dieser wichtigen Proteinmodule mit regulativer Funktion in der ClC Protein Familie. Die strukturelle und funktionelle Charakterisierung dieser Domänen führte zur Aufklärung verschiedener wesentlicher Sachverhalte. So wurde die Oligomerisierung dieser Proteinteile , die Interaktion mit Adenosinliganden auf molekulare Ebene sowie Aspekte ihrer regulatorischen Wirkung beschrieben.

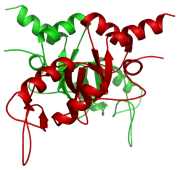

Outline

The 'Introduction' section gives a concise overview of the field of ClC channels and transporters touching on the general features like physiological functions, molecular architecture and ion conduction and selectivity. A more detailed perspective on the importance of the cytoplasmic domains in ClCs is given at the current status of research including the work presented in the later sections. The 'Results' section is structured into two chapters, one dealing with the work on the cytoplasmic domains from the voltage-gated chloride channel from ClC-0, the other describing the work on the cytoplasmic domains from the secondary active transporter ClC-5. Each chapter includes a short introduction sketching the status of the research prior to the studies and an aim formulating the key questions for each study. The core of the chapters are the experimental results that have led to three publications in peer reviewed journals. The articles are included in the thesis as they have been published, in the case of the work on the cytoplasmic domains of ClC-0 in Structure[1] and the Journal of Molecular Biology[2] and for the work on the domains from ClC-5 in Nature Structural and Molecular Biology.[3] In addition to these documents some supplementary information is appended giving more detailed methodological information and further results.

The section 'Concluding Remarks and Outlook' is intended to sum up the major findings of these studies, placing them in the context of the current questions in the ClC field. The unresolved issues concerning the detailed mechanisms and functions of ClCs lead to an outlook on the possible future strategies.

The 'Appendix' includes a chapter on the cloning, expression, and biochemical characterization of an archaebacterial ClC homolog, an intergral membrane protein that was studied towards the aim of resolving the structural organization of the cytoplasmic domains in the context of the catalytic pore domain.

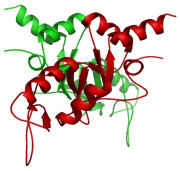

Chapter 1

Introduction

1.1 Principles of Ion Transport

Every living cell is surrounded by a lipid membrane separating the cytoplasm from the environment. The hydrophobic core of the membrane serves as a barrier that is impermeable to solutes, thereby allowing the cell to keep its interior separated from the extracellular surrounding. In order to exchange solutes with the environment life had to develop specific proteins that catalyze the movement of solutes across membranes. Using these proteins the cell is able to generate defined conditions needed for the different cellular processes in the cytoplasm or intracellular compartments.
In addition to the translocation of metabolites, the selective transport of ions across biological membranes is an essential feature of all living cells. Much of the metabolic energy of the cell is spent by molecular pumps to establish ion gradients, which in turn drive many of the fundamental tasks performed in the cell. The movement of potassium, sodium, calcium and chloride underlies important processes like solute and electrolyte uptake, chemical and electric signaling or cell volume homeostasis. Organisms have evolved a variety of different proteins that catalyze the translocation of ions across the hydrophobic core of cellular membranes.

Channels and Transporters Generally, two different classes of ion transport proteins are distinguished based on their thermodynamically different modes of action. Ion channels are permitting the passive diffusion of ions along their electrochemical gradient, while transporters use energy either from ATP hydrolysis or the dissipation of an electrochemical potential to move ions against their electrochemical gradient. In a

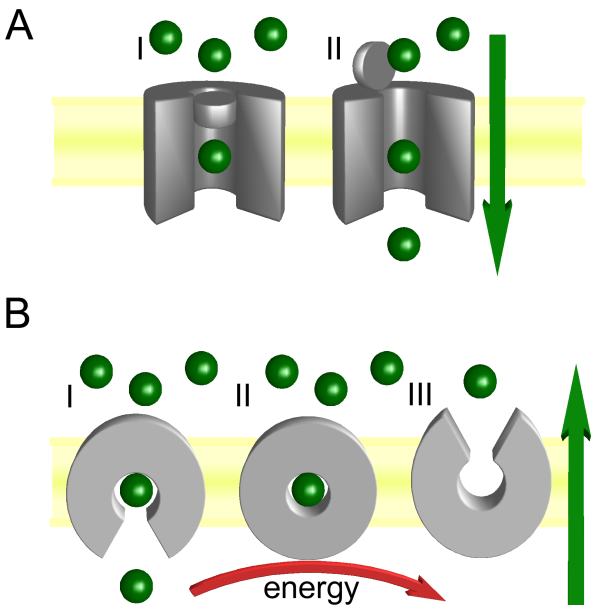

Figure 1: **Channels and Transporters** A schematic comparison of the mechanism of ion channels and ion transporters. Ion channels (A) simply allow passive diffusion of ions. Upon channel opening state I to II selected ions can pass through the pore along their electrochemical gradient, as indicated by the green arrow. Ion transporters (B) undergo a more complex cycle of different states. Substrate has to bind on one side of the membrane and the protein undergoes a structural re-arrangement releasing the substrate on the other side. This process allows accumulation of substrate against its electrochemical gradient requiring the concerted input of energy either from ATP hydrolysis or the dissipation of another ion gradient.

classical perspective the two classes of ion conducting proteins operate via distinct mechanisms. Ion channels are thought of as ion selective pores in the membrane that allow the passive diffusion of ions across the membrane. They are regulated by the opening and closing of gates that are able to plug the pore rendering the channel closed. This gating mechanism is in the simplest view a two-state process switching the channel on and off like depicted in Figure 1A. In ion transporters on the other hand one of the main features is the coupling of ion translocation to a secondary driving force like the hydrolysis of ATP or the transport of another ion species. This allows to link an energy consuming process, like an ion movement against an electrochemical gradient, to an energetically favorable event, like the downhill movement of an ion along its electrochemical gradient. The process of driving one energy dependent reaction by a second exergonic event requires tight coupling of these reactions to avoid the favorable reaction to independently occur and waste energy. In accordance to this the need for coupling imposes the necessity to have a more elaborate translocation cycle, where the protein passes through several states. The transport cycle is usually accompanied by large conformational changes in the protein granting alternate access of the substrate binding pocket to either side of the membrane (Figure 1B).

Like enzymes both channels and transporters can be characterized by several key properties: 1. Ion selectivity, a measure for the substrate specificity; 2. Ion conductance, an equivalent to the catalytic turnover of the protein; 3. Activation of ion transport,

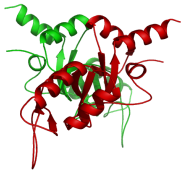

which is called gating in channels, describes the regulation of the enzymatic activity. To meet the requirements of efficient ion movement, high fidelity and tight control of the activity, transport proteins are frequently organized in a modular fashion consisting of catalytic and regulatory domains. The catalytic domain is embedded in the membrane and provides the structural scaffold to form an ion pathway across the hydrophobic interior of the membrane. It makes specific interactions with the respective substrate and is therefore essential to establish selectivity by binding the substrate and conduction by releasing the substrate to the other side of the membrane. Regulatory domains often accompany the catalytic domains and modulate their activity in response to different stimuli like membrane voltage,[4] ligand binding[5,6] or mechanic pressure.[7] These domains tune the activity of the transport protein by a mechanism called gating.

Chloride Transport Of the different ions that function as substrates for channels and transporters the most abundant in biological systems are potassium, sodium, calcium and chloride. Each ion has its own set of proteins that evolved specifically for its transport with high efficiency. Chloride is by far the most prevalent anion in nature. Several distinct families of chloride transporting enzymes are well established by functional characterization: ClC channels and transporters, ligand-gated GABA and glycine receptors, Cystic Fibrosis Conductance Transmembrane Regulator (CFTR), Chloride Cation Co-transporters or the Cl^-/HCO_3^- exchangers. These proteins reside both in the plasma membrane and intracellular organelles and they function in a variety of essential processes like regulation of electrical excitability, transepithelial transport, ion homeostasis and cell volume regulation.[8,9] Their physiological importance is illustrated by several hereditary diseases like Bartter's syndrome, cystic fibrosis, Dent's disease or myotonia.[10] The ClC family of chloride channels and transporters has recently been recognized as unique among ion transport proteins, since the same structural scaffold is used to support passive chloride conduction and the secondary active transport of chloride against protons.[11]

1.2 ClC Chloride Channels and Transporters

1.2.1 History

ClC chloride channels and transporters are ubiquitous in biological systems; they are found in all phylae from bacteria to humans. These proteins are expressed in almost

every living cell and serve a variety of functions. ClC proteins are involved in the stabilization of membrane potentials, transepithelial transport or the acidification of intracellular vesicles.[12] The initial breakthrough in the ClC research field was the description of ClC chloride conduction back in 1980 when protein from the electric ray *Torpedo californica* could be functionally reconstituted and characterized.[13] The name ClC resulted from this period from the term Cl^- Channel. It took until 1990 when expression cloning revealed the sequence of ClC-0, the voltage-gated chloride channel from *Torpedo marmorata*.[14] This quickly led to the identification of nine homologs in human allowing for characterization by heterologous expression techniques.[15–20] Another significant advance in the understanding of ClC function came from the high resolution structures of two bacterial homologs.[21] The crystal structures allowed for the first time to visualize the complex topology of the membrane embedded catalytic domain and the architecture of the ion translocation pore of this protein family.[22]

1.2.2 The ClC Family

The nine homologs found in humans can be grouped based on sequence homology into three subfamilies (α, β, γ).[23] ClC-0, the channel from the electroplax organ of the electric ray, is included in this enumeration due to its high sequence homology and thorough characterization that makes it a paradigm for ClC channel function. The α-subfamily is comprised of the voltage-gated chloride channels ClC-1, ClC-2, ClC-Ka and ClC-Kb that are expressed in the plasma membrane. The members of the two other branches are predominantly located in intracellular vesicles making the electrophysiological characterization difficult. ClC-4 and ClC-5 from the β-subfamily can under certain conditions be trafficked to the plasma membrane and could therefore be studied in heterologous expression.[19,24] These proteins have been recently shown to function as secondary active chloride proton antiporters.[25,26] The homologs ClC-6 and ClC-7 of the γ-subfamily on the other hand are exclusively residing in intracellular compartments and have so far eluded functional characterization. It is to this point unclear if all the intracellular ClC proteins function as transporters although some hints exist on the level of the primary sequence.[27] Consistently it has been shown that the homologous protein in *E.coli* that serves as a structural model for the entire protein family is acting as an antiporter.[28] Some family members require additional β-subunits to exert their proper function as in the case of ClC-Ka, ClC-Kb or ClC-7.[29,30] It is unclear however, whether this is due to a modulation of the conductance properties or sorting and trafficking effects.[31] Although

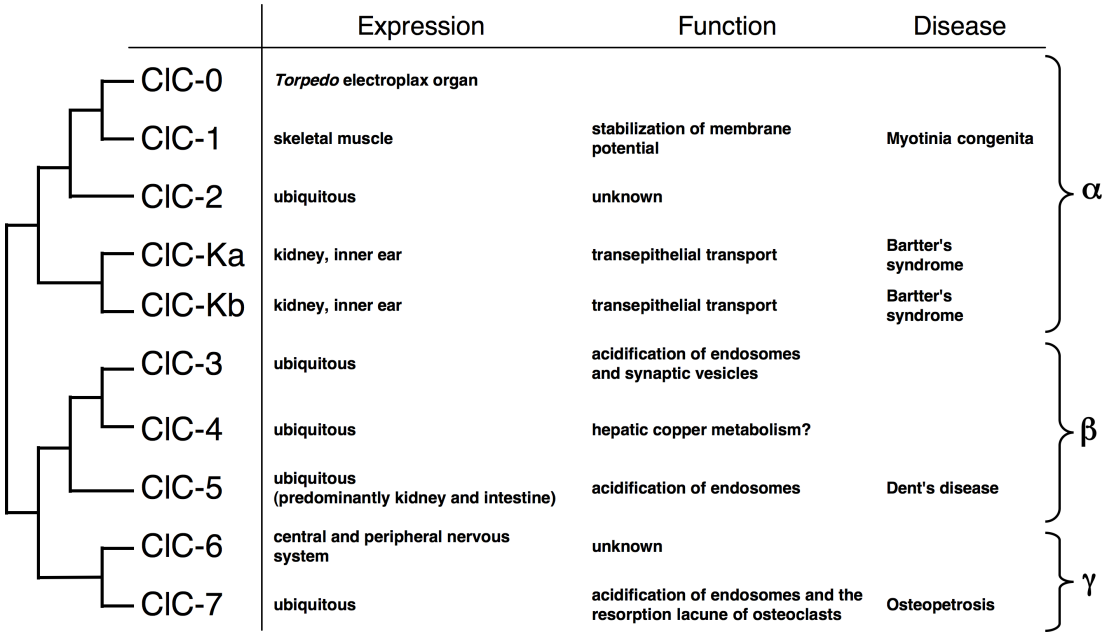

Figure 2: **Dendrogram of Mammalian ClC Proteins**
Based on sequence homology the nine ClC family members from human can be devided into three subfamilies. The well characterized ClC from *Torpedo* can be grouped to the α-subfamily. The columns state important features of each family member, like tissue distribution, presumed function and associated human diseases.

not all of the family members have been studied on the molecular level, a lot of insight into their physiological roles could be derived from mouse knock-out models that allowed in many cases subsequent linking to human hereditary diseases.[32]

1.2.3 Physiological Function, Expression and Disease

The nine ClC homologs found in humans are involved in a variety of different cellular processes, a property that is reflected by differing expression patterns and cellular localization.[33] For most of the family members some physiological function could be pinpointed due to the combined use of mouse models and by linking the observed phenotypes to the inactivation of ClCs in human disease. In the following a concise overview will be given of the different ClC proteins found in human and their proposed function, expression patterns and resulting pathologies.

α-Subfamily ClC-1 is a voltage-gated chloride channel, expressed almost exclusively in skeletal muscle and the closest homolog to ClC-0 from the Torpedo electric organ.

The resting conductance of skeletal muscle is dominated by chloride currents mediated by ClC-1 instead of potassium currents.[34] Thereby ClC-1 is responsible for the stabilization of the resting potential as well as for the repolarization of the membrane after action potentials.[15] Mutation in ClC-1, which cause a reduction of the conductance or an altered voltage dependence, lead to myotonia congenita in human patients.[35] This symptom is marked by an impairment of muscle relaxation after voluntary contraction impressively demonstrated by the example of the animal model of the myotonic or fainting goat strain.[36]

ClC-2 is a chloride channel with an ubiquitous expression pattern.[16] The channel is regulated by a variety of different stimuli like hyperpolarization, cell swelling or extracellular pH, thus making it a candidate for various functions. The speculative involvement in epilepsy[37] could not be confirmed by the analysis of ClC-2 knock-out mice, which in contrast display testicular and retinal degeneration.[38] In summary the precise role of this channel remains uncertain as well as its involvement in human disease.

The two paralogs ClC-Ka and ClC-Kb are highly homologous (94 % sequence identity) and are expressed specifically in the kidney and the inner ear with only slightly differing expression patterns.[17] Both channels are involved in transepithelial salt transport and impairment in any of the two leads to the renal salt wasting disorder Bartter's disease.[39] These were the first ClC proteins that were recognized to require a β-subunit, in this case Barttin, to exert their physiological function.[29]

β-Subfamily ClC-3 is the first ClC in the closely related group of ClC-3,-4 and -5 that reside mainly in intracellular compartments.[40] This protein is widely expressed and is difficult to study due to its subcellular localization in endosomal and lysosomal compartments and synaptic vesicles. Despite a severe phenotype of ClC-3 knock-out mice showing degeneration of the hippocampus and the retina no corresponding disease in humans could be identified.[40]

The secondary active transporter ClC-4 is broadly expressed and is predominantly found in intracellular membranes.[41] Similar to the afterwards discussed ClC-5 this protein can reach the plasma membrane to a certain degree when expressed heterologously.[42] The physiological relevance of the currents measured at the plasma membrane is puzzling since both proteins exhibit a strong rectification, conducting only at membrane potentials larger than +20 mV, a situation unlikely to be reached under physiological conditions in the plasma membrane or intracellular membranes. Hence, the physiological role of ClC-4 remains unclear, although it has been proposed to be involved in hepatic copper

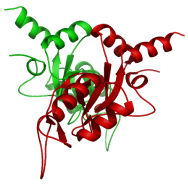

metabolism.[43]

The transporter ClC-5 is expressed in most tissues while being most abundant in kidney and intestine,[19] where it was found to be involved in endocytosis.[44] On the subcellular level, it is found predominantly in endosomes, where it co-localizes with the vesicular H^+-ATPase.[45] In these vesicles ClC-5 is presumed to dissipate the electric potential created by the ATPase during acidification of the endosomes.[45] The detailed mechanism however is obscured by the recent findings that show chloride to proton exchange activity of the protein.[25,26] Malfunction of ClC-5 leads to Dent's disease, an x-chromosome-linked disorder associated with proteinuria and kidney stones.[46]

γ-Subfamily The intracellular protein ClC-6 and ClC-7 constitute another branch in the ClC family with about 45 % sequence identity. ClC-6 is almost exclusively expressed in the central and peripheral nervous system, where it is found in late endosomes.[20] The analysis of mice with disrupted ClC-6 revealed a reduced pain sensitivity and hints at a lysosomal storage disease.[47] Although the later phenotype resembles neuronal ceroid lipofuscinosis, a disease found in humans, a correlation of ClC-6 defects in patients remains to be shown.

ClC-7 is another intracellularly located protein that is ubiquitously expressed and localizes to late endosomes and lysosomes.[20] It is by far the most predominant ClC protein present in lysosomes, additionally it is also found in the ruffled border of osteoclasts.[48] These specialized membrane domains are facing the resorbtion lacuna of this bone-degrading cell type and resemble an extracellular lysosome in its composition. ClC-7 co-localizes with the V-type H^+-ATPase, much like ClC-5, and is therefore thought to be involved in the efficient acidification of the vesicle and lacuna. Mutations in ClC-7 underly several variants of osteopetrosis, a human disorder resulting from impaired bone resorption, and are implied in lysosomal storage disease and neurodegeneration.[48,49] Similar to the ClC-K channels it has been shown that ClC-7 directly interacts with a β-subunit, however, the functional implications of this protein Ostm-1 are still unclear.[30] It is obvious from the different examples that ClCs play a diverse role in a variety of physiological processes. Nevertheless, many of the detailed functions are to this date only poorly understood and the key to comprehend their physiological function in the organism lies in the behavior of these proteins on the molecular level.

1.2.4 Molecular Architecture

Despite their functional diversity all ClCs share a common architecture resulting in a conserved scaffold and a number of mutual features. On the level of quaternary structure ClCs have been shown to assemble into dimers.[50] Moreover, they are thought to only function as homodimers although, currents from functional concatemers of different ClCs have been described.[51] Each of the two subunits harbors a single ion pathway that is able to conduct ions independently, thereby giving the protein a double-barreled architecture.[21,52] The tertiary structure of the ClC family is complex and consists of a catalytic domain that is comprised of 18 α-helices, 17 of which are embedded in the membrane. Only some of these transmembrane α-helices span the membrane completely and most are severely tilted with respect to the face of the bilayer. These features made the topology assignment of the catalytic domain by biochemical methods extremely difficult and a conclusive picture only resulted from the determination of the high resolution structures of two bacterial homologs.[21] The resulting topology of the membrane-embedded pore domain of a single ClC subunit is shown in Figure 3. The catalytic pore domain consists of two anti-parallel halves of 8 transmembrane helices. The structure revealed that the residues, which coordinate the chloride ions during their passage through the membrane are spread throughout the primary sequence of the protein.[21] These sequence motifs, which are highlighted red in Figure 3, are conserved among ClC channels and transporters and they create specific binding sites for chloride in the translocation pore. Both termini of the ClC subunit are located in the cytoplasm and in addition to the catalytic domain all eukaryotic ClCs possess an intracellular domain that is located at the C-terminus of the protein. A common feature of these cytoplasmic domains, which will be discussed later in greater detail, is the presence of two CBS subdomains named after their initial description in the enzyme cystathionine-β-synthase.[53] The domains are included in Figure 3 outlining the typical CBS fold and additional sequence features. The location of these intracellular domains is interesting since they are attached to the last transmembrane helix R that takes part in the ion coordination in the center of the membrane, therefore implying a regulatory function. The conservation of the overall topology among ClCs and the ion translocation pathway results in the presence of characteristic signature motifs for the pore lining residues. The direct interaction of these sequence stretches with the permeant ions are responsible for the observed ion conduction properties of the protein.[22]

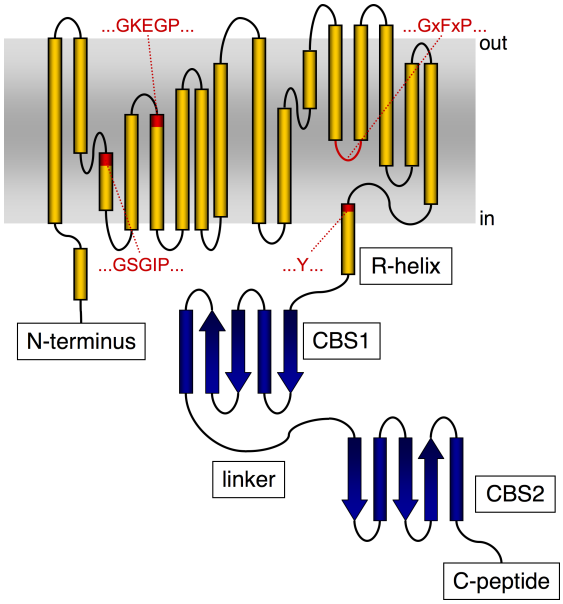

Figure 3: **Topology of Eukaryotic ClC Proteins**
A schematic view of the ClC subunit including secondary structure elements. The membrane embedded pore domain is shown in yellow with the parts contributing to the ion selectivity filter highlighted in red. The last transmembrane helix (R) is labeled and the two cytoplasmic CBS subdomains are shown in blue featuring their characteristic topology. The variable sequence stretches between the CBS subdomains and at the C-terminus are labeled.

1.2.5 Principles of Ion Conduction

The general requirements to assure efficient transport of ions across the membrane with high specificity include the molecular recognition of the ion by interacting with the specific parts of the protein. This will compensate for the loss of the hydration shell of the ion in the pore and allows the protein to select the proper substrate among related ion species. On the other hand it is crucial for this interaction not to be too tight to prevent the rapid flow of ions. Ensuring high selectivity while simultaneously allowing high conductance is the major challenge in ion transport.[54]

Pore Properties In order to meet these demands ClCs have evolved three binding sites for chloride in the middle of the membrane, by which they bridge two aqueous cavities approaching from both sides towards the pore.[21,22] These sites have been termed S_{ext}, S_{cen} and S_{in} based on their location along the ion translocation pathway. The pore is lined by four amino acid stretches that contribute to the ion coordination from distant parts of the primary sequence. These motifs are conserved among the family: GSGIP in the D helix, GKEGP in the F helix, GxFxP in the N helix and finally a Y in the last transmembrane helix R. Interestingly all of these residues are located at the N-terminus of their respective helices. The partial positive charge of the helix dipole might therefore contribute to the favorable environment for anion binding.

The previously mentioned key properties of channels and transporters, namely selec-

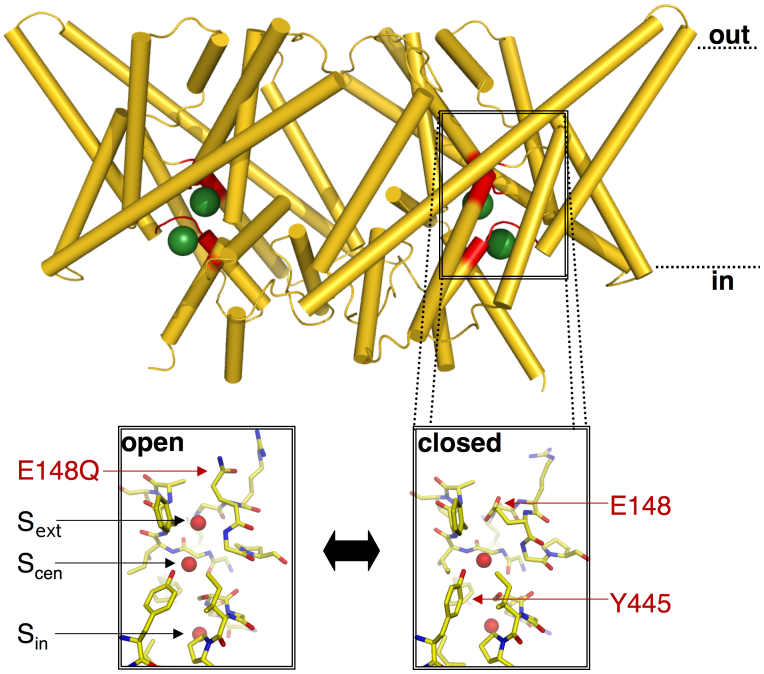

Figure 4: **ClC Selectivity Filter**
A side view of the ecClC dimer with the selectivity filter highlighted in red and two chloride ions included in green. In bottom panels two close up representations of the filter with the chloride coordinating residues depicted as sticks and the ions as red spheres. The closed conformation shows the wildtype protein with the residue E148 blocking the pore by occupying the external chloride binding site. The presumed open conformation is represented by the E148Q mutant that allows an additional chloride ion to bind in the filter by an outward motion of the glutamine side chain. In the close-up view of the selectivity filter the chloride binding sites, the glutamate associated with the individual gating as well as the Tyrosine residue located on the R-helix are labeled.

tivity, gating and conductance, can now be attributed to the molecular architecture of the pore. The selectivity describes the fidelity with which the protein can distinguish between different ionic species. Although this is less of an issue for chloride since it is by far the most common anion under physiological conditions, it is nevertheless observed that all ClC favor chloride over all other anions.

The mechanism of gating is usually a term to describe the controlled opening and closing of ion channels, either allowing passive diffusion through the pore or prohibiting it. The equivalent mechanism in ion transporters, which can be performed by homologous residues as will be described later, would correspond to activation or inactivation of the transport cycle. The conductance is the quantitative measure of the rate of ion translocation through the protein. In the case of the ClC family this property is not very uniform

and is ranging from 10 pS in ClC-0[55] and 1 pS in ClC-1[56,57] in the channels to only about an approximate 2000 per second for the ecClC from *E.coli*.[58] To illustrate this enormous difference, one would have the chloride flux of about $6 \cdot 10^7$ per second through ClC-0 at a membrane voltage of -100 mV, as shown in Fiugre 1.2.5.

Assigning Structure to Function A joined discussion of the mechanistic features of ClC channels and transporters appears difficult when considering these vastly differing transport properties. Most of the functional work has been conducted on the muscle-type channels, like ClC-0 and ClC-1, while the only structural information on the catalytic domain originates from the crystal structures of two prokaryotic transporters, ecClC and stClC. However, it has been shown that the conclusions drawn from the crystal structures apply to a large extend also to ClC channels.[59] Regardless of whether they allow passive diffusion of chloride or coupled exchange for protons all ClCs share several common features. They exhibit a strict selectivity for small monovalent anions, while cations, taken aside protons in the transporters, do not permeate and iodide blocks the pore. In contrast to cation channels the ClCs do not possess a high interanionic selectivity, although the preference was always found to be $Cl^- > Br^- > NO3^-$.[23]
The plasma membrane channels ClC-1, -2 and -0 are the most thoroughly described family members with respect to their electrophysiological behavior. Particularly ClC-0 has been extensively studied as it is expressed in high amounts in the electric organ of *Torpedo* and has a high single channel conductance. This gave the possibility to record currents from a single protein dimer in artificial lipid membranes.[55] Next to the voltage dependence of the currents through the channel some fundamental characteristics of the protein structure became apparent. The equally spaced conductance states with their binomial distribution argued for a protein with two identical and independent pores.[52] Another feature is the existence of multiple gating mechanisms: 1. individual gating acting on each pore separately 2. common gating affecting both pores simultaneously. Due to their kinetics in ClC-0 they have been also termed fast and slow gating, respectively.[60,61]

Two Kinds of Gating The individual gating behavior is influenced by several factors like changes in the external and internal chloride concentration, the external pH or the membrane potential.[62] The individual gating is strongly voltage dependent, the more positive the membrane potential the higher is the open probability in ClC-0 and also

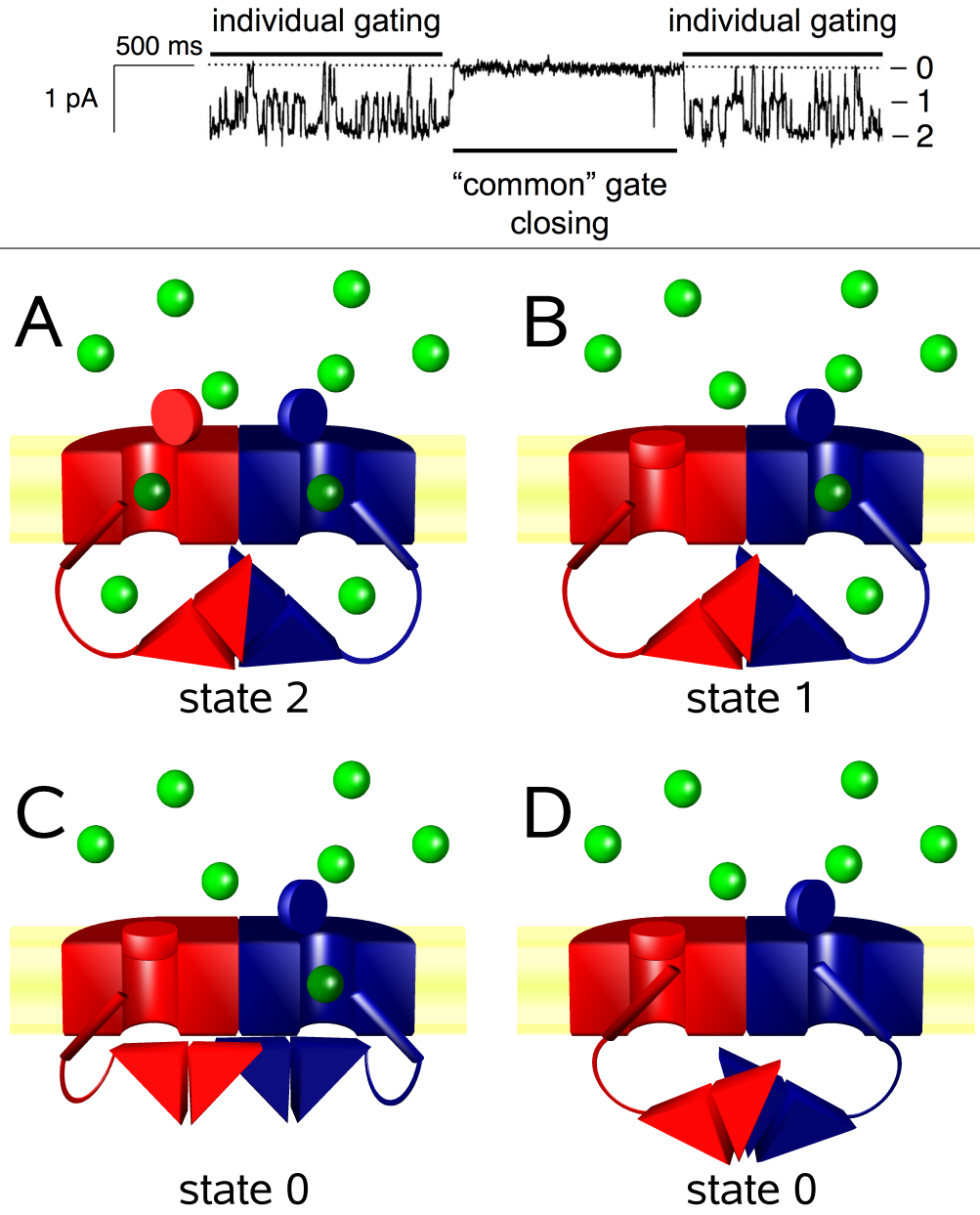

Figure 5: **Gating in ClC-0**
The upper panel shows a single channel recording of ClC-0. Three conductance states can be observed: closed (0), one pore open (1) and two pores open (2). Bursts of activity with rapid fluctuations controlled by the individual gates are observed. The appearance of these bursts is interrupted by the temporary closing of both pores by the common gate, which is seen to have slower kinetics. The panels A-D schematically depict some of the conformations in the protein during these gating processes. The two subunits are colored in blue and red with each chain forming an independent pore, each with an individual gate symbolized by lids. Chloride ions are shown in green. A cylinder represents the last transmembrane helix R that coordinates a chloride ion in the filter and has the C-terminal domains attached that assemble in the cytoplasm. The panels (A) and (B) depict the two of the three possible states observed during the burst-like activity, which is dominated by individual gate opening and closing. Panels (C) and (D) are two possible mechanisms of common gate closing that acts on both pores in a concerted manner. In (C) the cytoplasmic domains directly prohibit access to the pore while in (D) rearrangements in the domains lead to a displacement of the R-helix, which in turn shuts down chloride flux.

ClC-1.[62] This voltage dependence of channel opening involves an extracellular chloride binding site outside of the selectivity filter and is thought to arise from the movement of the permeant ion across the electric field.[63] This mechanism is profoundly different from voltage-gated potassium channels, where the gating charge is located on the protein in form of several positively charged residues in the S4 voltage sensor segment.[64,65] The structural determinant of the indiviual gating process has been identified to be a single glutamate residue (see Figure 4).[22] This residue can either occupy the outer binding site for chloride in the selectivity filter, thereby prohibiting ion flow, or it may swing out from this site allowing chloride to diffuse through the filter. This distinct gating mechanism is located entirely within each subunit resulting in two pores that act independently of each other.

The common gating mechanism on the other hand, acting in a concerted manner on the two individual pores, is by far less well understood. Mutations in the dimer interface of the catalytic domains[57,66] as well as in the cytoplasmic domains have been described to influence the common gate.[67] The evidence towards an involvement of the intracellular segments of the ClC in this regulatory process is discussed in more details in the following section. The common gate is influenced by chloride concentration,[68,69] temperature,[70] pH and the membrane potential.[71] In ClC-0 membrane depolarization favors common gate closing.

Regulation in the ClC Transporters Since the plasma membrane channels have been studied in more details than the transporters, it is unclear how the mechanisms of individual and common gating translate into the functional mechanism of the latter. Eukaryotic family members that have been confirmed to function as secondary active transporters are the two vesicular proteins ClC-4 and ClC-5.[25,26] In addition to these two human homologs, ecClC, of which the structure has been determined at high resolution, was the first ClC to have been recognized as a chloride proton antiporter.[28] This process is so far only poorly understood, although several residues have been identified to be critical for the transport cycle. It has been shown that the glutamate residue involved in the individual gating of the channels is essential for the coupling of chloride to proton flux in the transporters.[28] When this residue is mutated the protein turns into a constitutively open chloride conductor. Similar to this amino acid position at the outer chloride binding site another glutamate residue towards the inside of the membrane has been identified with comparable importance for the coupling.[27] In contrast to the outer glutamate, however, this inner glutamate residue is crucial only for proton transport,

while not being part of the chloride pathway. Thus it has been speculated that the chloride and proton translocation pathways, although conjoint at the extracellular face of the membrane, diverge towards the intracellular side.[27]
In addition, the coupling of the two substrates appears to be dependent on a tyrosine residue coordinating chloride in the central site of the selectivity filter.[72] While for the wildtype ecClC a transport stoichiometry of 1 proton per 2 chloride has been determined,[73] alterations in this conserved residue result in various degrees of slippage making the protein more chloride selective.[72] Until now no complete picture of the transport cycle in ClC proteins has emerged, which is partly due to the fact that the proton pathway in ecClC cannot be visualized crystallographically and the current resolution of the structures is not high enough to identify all water molecules that are likely to be involved in the coupling. It is intriguing, however, that it seems difficult to strictly divide ClC mechanistically into channels and transporters, since it becomes apparent that the channels bear some transporter-related features and vice versa.

1.2.6 Cytoplasmic Domains

The modular domain architecture found in ClC proteins resembles the domain organization in a variety of other channel families that consist of a membrane bound catalytic domain and a soluble regulatory module. All eukaryotic ClCs and a number of prokaryotic homologs feature this characteristic composition and have at the C-terminus large intracellular extensions. The only ClC of known atomic structure, however, the ClC from *E.coli* does not have these cytoplasmic components. In the eukaryotic proteins they have been shown to be critical for proper protein function.[74,75] This is emphasized by a number of mutations in the cytoplasmic domains of various family members that lead to diseases like myotonia, Dent's disease or osteopetrosis.[76] The intracellular extensions vary among the different homologs in length from about 155 to 398 amino acids. As mentioned earlier a mutual feature is the presence of two CBS subdomains that are conserved within the family. In contrast to the conserved subdomains, the interdispersed linker and the so-called C-peptide following CBS2 are of variable length and sequence composition.

CBS Subdomains CBS domains were initially described in the enzyme cystathionine-β-synthase,[53] but they are also found in a variety of functionally unrelated proteins like metabolic enzymes, kinases, channels and transporters.[77] The fold of these conserved protein subdomains consists of three beta strands and two alpha helices in a $\beta 1 - \alpha 1 -$

$\beta 2 - \beta 3 - \alpha 2$ arrangement. CBS domains are usually found as pairs in tandem repeats that are associating in an pseudo two-fold arrangement via the beta sheets 2 and 3 of the two subdomains. While the beta strands are tightly interacting, the four alpha helices are positioned on the periphery of the structure leaving a cleft in between the subdomains.[77] In a number of cases two pairs of CBS domains have been seen to dimerize. In these structures the CBS pairs from bacterial proteins are interacting via the alpha helices in two possible arrangements either head-to-head (PDB accession 1VR9) or head-to-tail[78](Figure 6). The functional purpose of the CBS subdomains in the context of their different catalytic proteins is to this point not fully resolved, although a study has been suggesting that they function as energy sensing modules.[79] In this work it was shown that isolated CBS domain tandems from various proteins are able to bind adenosine nucleotides. This finding led to the hypothesis of CBS domains as sensors of the metabolic energy state of the cell and regulators of the activity of their catalytic domains.

The Functional Importance of the Cytoplasmic Domains In the context of ClC channels and transporters the function of CBS subdomains is still poorly understood, although recent results give first leads towards their purpose. The majority of studies have employed mutational analysis in combination with biochemical and electrophysiological methods to address the functional importance of the cytoplasmic domains in ClCs.[67,74,80] While even minor changes in these domains can lead to drastic effects in protein function, the precise role in regulation is still uncertain. Initial approaches using large deletions in the domains resulted in a failure of the proteins to reach the plasma membrane, whereas in some cases it was possible to reconstitute functional protein upon co-expression of the complementary protein fragments.[74,75] These results suggested an involvement of the intracellular domains in folding and trafficking of ClCs. Indeed, in the cases of the human kidney transporter ClC-5[81] and the homolog from yeast scClC,[80] studies correlate trafficking effects with alterations in the domains. In addition to these effects, the cytoplasmic domains are also involved in modulation of the conductance properties, which is impressively demonstrated by a single amino acid exchange in ClC-1 causing a shift in the open probability of the channel that leads to myotonia.[36] This and other naturally occurring mutations result in an altered current phenotype of ClC-1 by changing the voltage-dependence of the common gate. A number of additional residues have been identified to be critical for the mechanism of the common gate.[66,70,82] In this respect the location of the intracellular domains is intriguing, since they are following the last transmembrane helix R that is directly involved in coordinating a chloride ion in the cen-

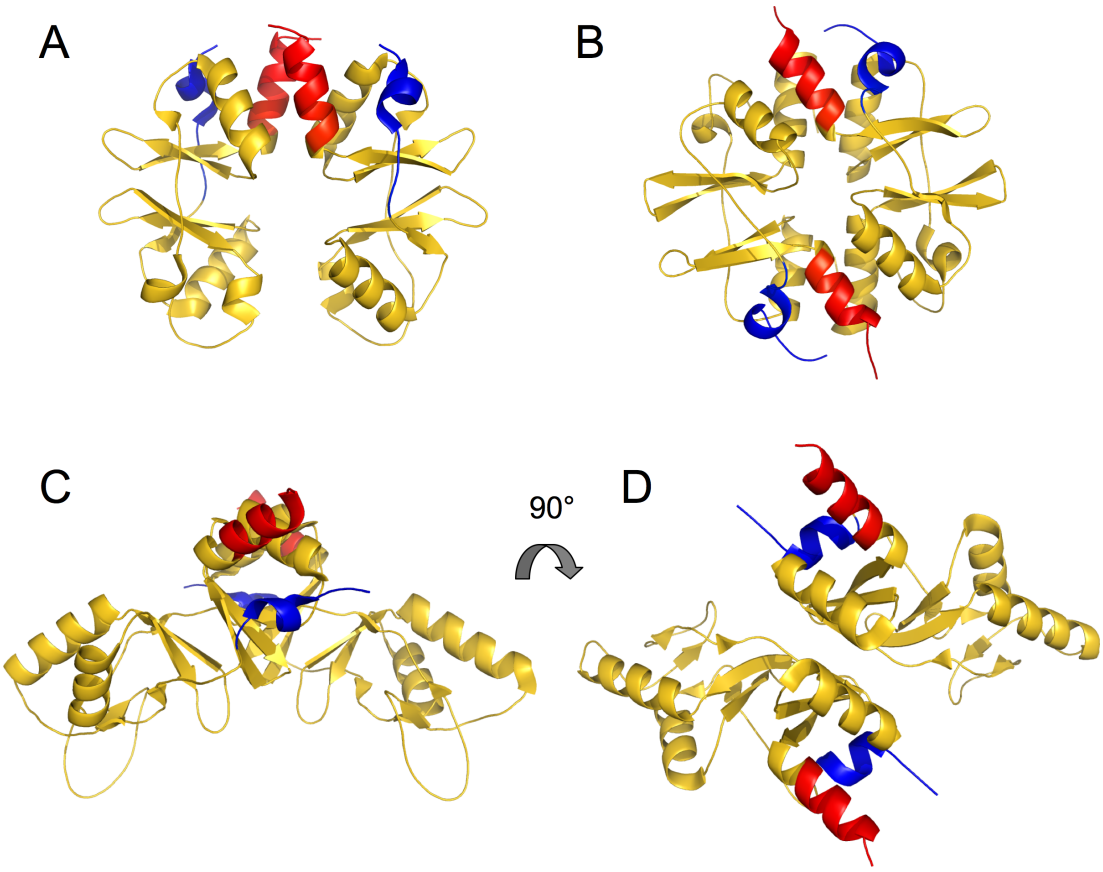

Figure 6: **CBS Protein Dimerization**
Examples of the different modes of dimerization observed in CBS domain containing proteins. The protein chains are shown as ribbons with the N-terminus colored in blue and the C-terminus colored in red. The conventional head-to-head (A) and the head-to-tail (B) configuration are indicated by two structures of CBS proteins from *Thermotoga maritima* PDB accessions 1VR9 and 1O50 respectively. The novel mode of dimerization discovered in ClC proteins is exemplified by the cytoplasmic domain structure from the human ClC-5 (PDB accession 2J9L) and is shown from the side (C) and the top (D) after a 90° rotation.

tral site of the selectivity filter. The conserved tyrosine located on the R-helix has been already discussed as being crucial for the coupling of proton to chloride flux in the transporters of the ClC family.[72] It appears likely that the cytoplasmic domains may exert a regulatory effect on the protein by altering the position of the R-helix. There is indeed evidence of large movements in the intracellular domains of ClC-0 that are associated with the common gating of the channel from a study employing the "Förster resonance energy transfer" combined with electrophysiological measurements.[83] The mechanism of how this rearrangement of the cytoplasmic domains alters the conductance properties will require the structural analysis of these domains and their interaction with the catalytic domain.

Structural Insights and Ligand Recognition Concerning the structural aspects of the intracellular domains in ClC proteins, the first insight came from the crystal structure of the C-terminal domains of ClC-0 presented in section 2.1.2. The CBS tandem of CBS1 and CBS2 is forming a tightly interacting protein core similar to CBS motifs from other proteins. Although not observed in the crystal, it was shown that two cytoplasmic domains form a dimer in solution. Thus, the mode of this assembly of four CBS subdomains remained uncertain. Interestingly a large part of the sequence of the linker connecting the two CBS subdomains and the stretch after CBS2 was not resolved in the structure. In a subsequent study described in section 2.1.3 these segments were found to be disordered in solution. The functional importance of these natively disordered sequence segments that are present in ClC family members of the α-subfamily remains to be elucidated. In a subsequent structural study on the cytoplasmic domains of ClC-5 presented in section 2.2.2 several novel aspects of structure and function of these components were revealed. The crystal structure showed the molecular interaction of specific residues with the bound adenosine nucleotides and binding assays could confirm the reports of ligand binding.[79,84] In addition, this interaction could be correlated with functional effects on the transport behavior of the protein when studied in electrophysiological experiments. This regulatory effect of nucleotide binding is an emerging facet of ClC function[42] with recent results in ClC-1 showing an alteration of the open probability of the channel upon changed ATP concentration.[85–87] In addition, the crystal structure of the ClC-5 domains contained a novel interaction of two CBS tandems profoundly different from the previously observed head-to-head and head-to-tail configurations. This mode of cytoplasmic domain dimerization in ClC proteins was later recognized to be conserved in ClC-Ka and ClC-0 by cross-linking studies.[88]

In summary these initial insights into the domain organization and the novel feature of ligand regulation in ClC protein provide valuable leads for the future detailed study of ClC function.

Chapter 2

Results

2.1 The Cytoplasmic Domain of ClC-0 from *Torpedo marmorata*

2.1.1 Introduction

The voltage-gated chloride channel from the electroplax organ of electric rays (ClC-0) is a close homolog of ClC-1 from human skeletal muscle with 44 % sequence identity. The electroplax organ consists of stacks of specialized muscle fibers arranged in series that can generate extremely high voltage. Acetylcholine receptors, sodium channels and also ClC-0 are highly abundant in these noncontractile muscle cells. Since its discovery in the 1980's ClC-0 has become the prototypical ClC channel, studied to establish important features like the homodimeric structure and the double-barreled architecture of the family.[52,55] Its function has been well characterized by reconstitution into planar lipid bilayers and single channel recordings of a conductance of about 10 pS per pore (see Introduction Figure 1.2.5).[55] Initial work focused on the determination of the pore properties of the channel, while soon the importance of the cytoplasmic domains for its proper function was recognized. These domains have a length of about 285 amino acids in ClC-0 following the last transmembrane helix. For these C-terminally located segments the sequence identity with ClC-1 is only about 13 % arising from pronounced differences in the interdispersed sequences between the CBS subdomains and after CBS2. Comparison of the two CBS subdomains with their counterparts in ClC-1 yields about 50 % sequence identity suggesting a strong structural conservation. Limited insight into the function of the cytoplasmic domains in ClC-0 was achieved by mutational analy-

sis.[76] It was shown that truncation of the domains resulted in non-functional protein. On the other hand it was possible to reconstitute functional protein by splitting the channel in the linker connecting CBS1 and CBS2 when both constructs were expressed simultaneously,[74] an observation that was also made in ClC-1.[75] Biochemical attempts to uncover the domain organization led to somewhat contradictory results leaving it unclear whether the CBS subdomains within one subunit are in contact. Furthermore it needed to be resolved whether the cytoplasmic domains from two neighboring subunits are interacting[76] or not.[89] Homology modeling of the ClC CBS subdomains onto known CBS structures failed to conclusively rationalize the functional effects of various point mutations on the channel.[76] The available biochemical and functional information on the cytoplasmic domains in ClCs clearly marks their importance for the physiological function of the channels, however, the missing structural perspective complicates a correlation of structure to function.

2.1.2 Crystal Structure of the Cytoplasmic Domain of the Chloride Channel ClC-0

Aim of the Study At this point the main objective for this study was the determination of the first high resolution structure of the isolated intracellular domains of a ClC family member in order to establish a structural framework for these components. Investigation of the cytoplasmic domains of ClC-0 would reveal the structural organization of the CBS tandem from one subunit potentially giving insight into the oligomeric state of the cytoplasmic components.

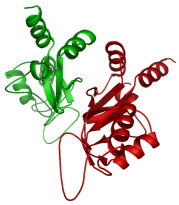

Structure *14*, 299–307, February 2006 DOI 10.1016/j.str.2005.10.008

Crystal Structure of the Cytoplasmic Domain of the Chloride Channel ClC-0

Sebastian Meyer[1] and Raimund Dutzler[1,*]
[1] Department of Biochemistry
University of Zürich
Winterthurer Strasse 190
CH-8057 Zürich
Switzerland

Summary

Ion channels are frequently organized in a modular fashion and consist of a membrane-embedded pore domain and a soluble regulatory domain. A similar organization is found for the ClC family of Cl^- channels and transporters. Here, we describe the crystal structure of the cytoplasmic domain of ClC-0, the voltage-dependent Cl^- channel from *T. marmorata*. The structure contains a folded core of two tightly interacting cystathionine β-synthetase (CBS) subdomains. The two subdomains are connected by a 96 residue mobile linker that is disordered in the crystals. As revealed by analytical ultracentrifugation, the domains form dimers, thereby most likely extending the 2-fold symmetry of the transmembrane pore. The structure provides insight into the organization of the cytoplasmic domains within the ClC family and establishes a framework for guiding future investigations on regulatory mechanisms.

Introduction

Ion channel proteins catalyze the flow of ions across cellular membranes, a mechanism that underlies many physiologically important processes. To achieve this, channels usually combine two important properties: selective ion conduction at high rates, and the ability to regulate the conduction in a process called gating (Hille, 2001). These proteins are therefore frequently organized in a modular fashion and consist of a transmembrane catalytic domain, which allows the diffusion of ions through an aqueous pore, and an additional regulatory domain that controls the opening and closing of the pore in response to external stimuli (Jiang et al., 2002). With the exception of voltage-sensing domains, most regulatory domains resemble soluble proteins facing either the cytoplasm or the extracellular solution (MacKinnon, 2004). These soluble domains are commonly found to specifically bind ligands, and thereby to activate or inhibit ion permeation by opening and closing of the pore (Hille, 2001).

An important class of ion channel proteins that exhibits this modular organization is the ClC family. The ClC channels constitute a large protein family of chloride (Cl^-) channels and transporters that is ubiquitously expressed from bacteria to man (Jentsch et al., 2002). Nine isoforms of the family are expressed in human and serve as key players in various physiological processes. Mutations in those isoforms have been identified to cause familial diseases such as myotonias, nephropathies, and osteopetrosis (Jentsch et al., 2005). The ClC proteins are unique, as they are not related to any other class of ion transport proteins. Within this family the members are closely related in sequence and architecture. All ClC proteins contain a conserved membrane-inserted catalytic pore domain, which is, in many cases, followed by a large cytoplasmic domain (Figure 1A). The X-ray structure of the prokaryotic ClC homolog from *E. coli* (EcClC) provides a structural framework for the membrane-inserted domain (Dutzler et al., 2002, 2003). The ClC proteins are homodimers of two identical subunits, and each subunit contains an ion translocation pore. The topology of the pore domain is complex (Figure 1A). Two roughly repeated halves span the membrane in opposite directions and thereby contribute residues from different parts of the protein to form a selectivity filter for chloride ions in the center of the membrane. This selectivity filter harbors closely spaced ion binding sites that bridge the intra- and extracellular solution. Although EcClC shares the conserved membrane-embedded pore domain with other ClC family members, it lacks the cytosolic domain frequently found at their C terminus. This domain is present in all eukaryotic and some prokaryotic ClC proteins, regardless of whether they function as chloride-dependent ion channels or as secondary chloride transporters (Estevez and Jentsch, 2002). Up until now, there was no structural information of this regulatory domain available.

In vertebrates, the length of the cytoplasmic domain is variable and ranges from 160 to 315 amino acids. A common feature in all family members is the presence of two CBS subdomains, CBS1 and CBS2, each about 50 residues long (Estevez and Jentsch, 2002). These small, compact protein domains consist of a three-stranded β sheet and two α helices and were originally discovered in the enzyme cystathionine-β-synthetase (Bateman, 1997). The large size difference in the ClC C terminus between different family members results from a variable linker region (linker) between the two CBS domains and the sequence that follows CBS2 (C-peptide). The topological organization of the ClC subunit is schematically depicted in Figure 1A. The domains share the closest homology within the different branches of the ClC family. One important branch includes the chloride channels ClC-0, ClC-1, and ClC-2 and the kidney channels ClC-Ka and ClC-Kb (Jentsch et al., 2002). All family members of this branch reside in the plasma membrane of various tissues and function as gated chloride channels. Figure 1B shows a sequence alignment of the two closely related channels: ClC-0 from the torpedo electric ray, and ClC-1, a human channel that is expressed in skeletal muscle cells. The strong conservation within the CBS domains is evident from the alignment, although there are large differences in the linker and the C-peptide, both being significantly longer in ClC-1.

The role of the cytoplasmic domains for ClC function is still obscure, but several experiments suggest that

*Correspondence: dutzler@bioc.unizh.ch

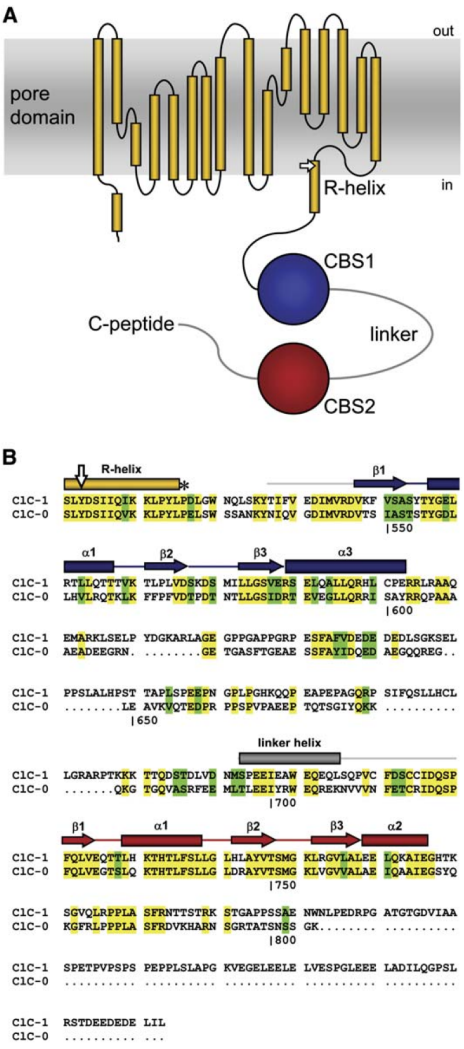

Figure 1. Subunit Organization and Sequence Alignment

(A) Schematic overview of the ClC-0 subunit. The construction principle is general for eukaryotic ClC family members. The α helices of the transmembrane pore domain are shown as yellow cylinders, and the approximate position of the membrane is shown as a gray box. The last, partly membrane-embedded α helix of the pore domain is labeled (R helix); the arrow points at the position of the residue involved in ion binding. The cytoplasmic domain is shown attached to the pore, and the two CBS subdomains are depicted as blue and red spheres, respectively.

(B) Sequence alignment of the cytoplasmic domains of ClC-0 and ClC-1. Identical residues are highlighted in yellow, and similar residues are highlighted in green. Secondary structure and numbering (ClC-0) are indicated above and below the sequences, respectively. The R –helix, with the Cl^--coordinating tyrosin residue (arrow) preceding the domains, is included in the alignment. The first residue of the crystallized construct is highlighted (*). Amino acid sequences are ClC-0 *T. marmorata* (GenBank: X56758) and ClC-1 *H. sapiens* (GenBank: M97820).

they are vital for proper functioning of the proteins (Bennetts et al., 2005; Denton et al., 2003; Estevez and Jentsch, 2002). The ClC family members show a complex functional behavior, and this is underlined by the fact that a very similar protein architecture encodes both coupled Cl^- transporters and gated Cl^- channels. The Cl^- channels ClC-0 and ClC-1 are the best-characterized members of the ClC family. Two modes of gating have been described for these proteins: gating of the individual pore of each subunit, and a common gating mechanism that opens and closes both pores at once (Accardi and Pusch, 2000; Chen, 2005; Miller, 1982). While the gating of the individual pore occurs at the selectivity filter, the molecular mechanism underlying common gating is so far not known. Its large temperature dependence suggests substantial conformational changes, and mutational studies indicate an involvement of the cytoplasmic domain (Estevez et al., 2004; Fong et al., 1998; Pusch et al., 1997). In that respect, the location of the domain in relation to the selectivity filter is intriguing. It directly follows the last helix of the pore domain, which itself contributes a coordinating side chain to a specific ion binding site in the selectivity filter (Figure 1A). This peculiar architecture immediately hints at a possible interaction with the selectivity filter, thus providing a possible mechanism by which the domains can modulate the channel's opening and closing (Dutzler et al., 2002).

In the absence of a structure, it is difficult to achieve detailed insight into the molecular mechanisms underlying gating and into the role of the cytoplasmic domains for channel function. Here, we report the structure of the cytoplasmic domain of the Cl^- channel ClC-0 from *Torpedo maromorata* (Jentsch et al., 1990). The two CBS subdomains are found to interact tightly in a well-folded core. A 96 residue long mobile linker connecting the two subdomains, in contrast, is disordered in the crystals. As revealed by analytical ultracentrifugation, the domains form dimers in solution, thereby most likely extending the 2-fold symmetry of the transmembrane pore. To our knowledge, the structure describes for the first time the architecture of the soluble part of any member of the ClC family and thus makes an important contribution to the understanding of ClC function.

Results

Domain Architecture

To gain insight into the structural organization of the cytoplasmic domains of ClC channels, we have determined the structure of the domain of ClC-0 at 3.1 Å resolution by X-ray crystallography (Table 1; Figures S1A and S2A; see the Supplemental Data available with this article online). The construct containing residues 525–805 was expressed in *E. coli* as a soluble hexahistidine fusion protein. Limited proteolysis after purification not only removed the hexahistidine tag, but it also removed the residues of the C-peptide following CBS2. As confirmed by mass spectrometry, the crystallized construct consisted of the residues from 525 to 774 and included the N terminus that follows the R helix, both CBS subdomains, and the connecting linker region (Figure 1). The crystal structure was determined by multiple isomorphous replacement, including the anomalous scattering contribution of a Pt and a Hg heavy metal derivative for phasing. The crystals were of space group $P2_13$, with two copies of the ClC-0 domain in the asymmetric unit. Unexpectedly, there is no 2-fold relationship between

Table 1. Data Collection and Model Refinement Statistics

	Native	Native2	Hg	Pt
Data Collection				
Space group	$P2_13$	$P2_13$	$P2_13$	$P2_13$
Cell dimensions				
a = b = c (Å)	126.7	126.0	126.5	125.2
Wavelength (Å)	0.919	0.919	1.008	1.072
Resolution (Å)	50–3.1	50–3.4	50–3.7	50–4.1
R_{sym}	5.3 (50.7)	7.5 (46.8)	11.7 (51.6)	11.9 (49.0)
$I/\sigma I$	23.3 (3.3)	17.3 (4.4)	14.8 (4.6)	12.7 (3.5)
Completeness (%)	99.7	99.7	99.8	98.7
Mosaicity (°)	0.38	0.27	0.53	0.63
Refinement				
Resolution (Å)	20–3.1			
Number of reflections	12,254			
R_{work}/R_{free}	27.3/30.9			
Number of atoms	2,472			
Average B factor	91.0			
Rmsd bond length (Å)	0.01			
Rmsd bond angle (Å)	1.5			

Values for the highest-resolution shell are given in parentheses. Native2 was used as the native data set for calculating initial phases. $R_{sym} = \Sigma|I_i - \langle I_i \rangle|/\Sigma|I_i|$, where I_i is the scaled intensity of the i^{th} measurement and $\langle I_i \rangle$ is the mean intensity for that reflection. $R_{work} = \Sigma||F_o| - |F_c||/\Sigma|F_o|$, where F_o and F_c are the observed and calculated structure factor amplitudes, respectively. R_{free} was calculated by using a randomly selected 5% sample of the reflection data omitted from refinement.

interacting proteins found in the crystals, which would be anticipated from the symmetry of the transmembrane domain. The well-ordered core structures of the two proteins in the asymmetric unit are very similar, and there are no large differences apparent at this resolution.

Figure 2 shows the topology and the structure of the ClC-0 domain. The two CBS subdomains (CBS1, CBS2) are well defined in the electron density. As anticipated, they share the typical topology with other CBS domain-containing proteins (Miller et al., 2004; Zhang et al., 1999). As with those proteins, the two triangular-shaped subdomains are related by pseudo 2-fold symmetry and interact via the β sheet formed by β strands 2 and 3 (Figures 2B and 2C). The N terminus (after residue 536) preceding CBS1 forms a well-ordered loop that specifically interacts with residues on the surface of CBS2 (Figure 2C). As it is commonly observed in other proteins with the same fold, this interaction positions the N and C termini of the protein in close proximity. On the opposite side of the protein, 25 residues of the linker region prior to CBS2 are found to be well ordered in the electron density. Those residues form an α helix followed by an extended loop, which resembles the N terminus in its interaction with CBS1 (Figure 2C). Additional weak electron density is found for residues at the N terminus that appear to interact in extended conformation with symmetry-related proteins in the crystal, and for several additional residues of the linker region (Figure S1B). The remainder of the linker between CBS1 and CBS2 lacks electron density and is therefore most likely unstructured. The fact that a large fraction of the protein is disordered is reflected in the high average B factor and the somewhat elevated R factors of the otherwise well-refined structure (Table 1).

The absence of well-ordered electron density in the linker motivated us to investigate its amino acid composition. Within the ClC family, this region shows large variation in length and only poor sequence conservation. When analyzing the ClC-0 domain with algorithms predicting the propensity of a sequence to form a well-ordered structure, we found a strong correlation between order in the crystal and the probability of being structured (Figure 2D) (Ward et al., 2004). The region of the CBS subdomains and the end of the linker have strong electron density and are predicted to be ordered. The unstructured part of the linker lacks electron density, and the C-peptide is found to be susceptible to proteolysis. Both regions show a high propensity for disorder (Figure 2D). A similar propensity distribution is found for ClC-1. This indicates that the absence of well-ordered electron density in the linker region is not an artifact of crystallization, but rather reflects the intrinsic flexibility of the domains.

Oligomeric State in Solution

In the high-resolution structures of ion channel proteins and of their soluble domains, we generally observe two properties: the soluble domains are involved in mutual tight interactions and mirror both the symmetry and oligomeric states of the transmembrane channel domain (Brejc et al., 2001; Jiang et al., 2002; Nishida and MacKinnon, 2002; Zagotta et al., 2003). Neither of these two features were found in the ClC-0 domain crystals, in which the proteins appear to be monomeric, in contrast to the homodimeric architecture of the transmembrane ClC pore domain. We were therefore particularly interested to investigate whether the oligomeric state of the domains in the crystal corresponds to their state in solution and to their organization when attached to the channel.

The first hints of the domain size in solution came from gel filtration, which showed that the protein eluted with an apparent molecular weight of a dimer (~60 kDa). To quantitatively determine the oligomeric state of our construct in solution, we studied its sedimentation properties with analytical ultracentrifugation. The distribution of sedimentation coefficients obtained from sedimentation velocity experiments clearly shows a predominant peak with a maximum of 2.17 ± 0.02 S (SD averaged over six experiments) (Figure 3A). The corrected sedimentation coefficient ($S^0_{20,w}$) of 3.56 S corresponds well with the dimeric form of the domain. A second minor peak with about half the sedimentation coefficient most certainly represents a single subunit, possibly due to a slow monomer-dimer equilibrium (Figure 3A). The molecular weight of the domain was subsequently determined in a sedimentation equilibrium experiment (Figure 3B). Fitting the data to a single-species model ($S^0_{20,w}$ value of 3.50 S; rms deviation of fit, 0.00606 ± 0.00026) results in a molecular weight of 55.3 kDa, which is in good agreement with the 55.5 kDa calculated for the dimer. The sedimentation data clearly show that the domains are dimers in solution, rather than monomers, as seen in the crystal. It is likely that the protein dissociated into monomers at the high salt concentration present during crystallization.

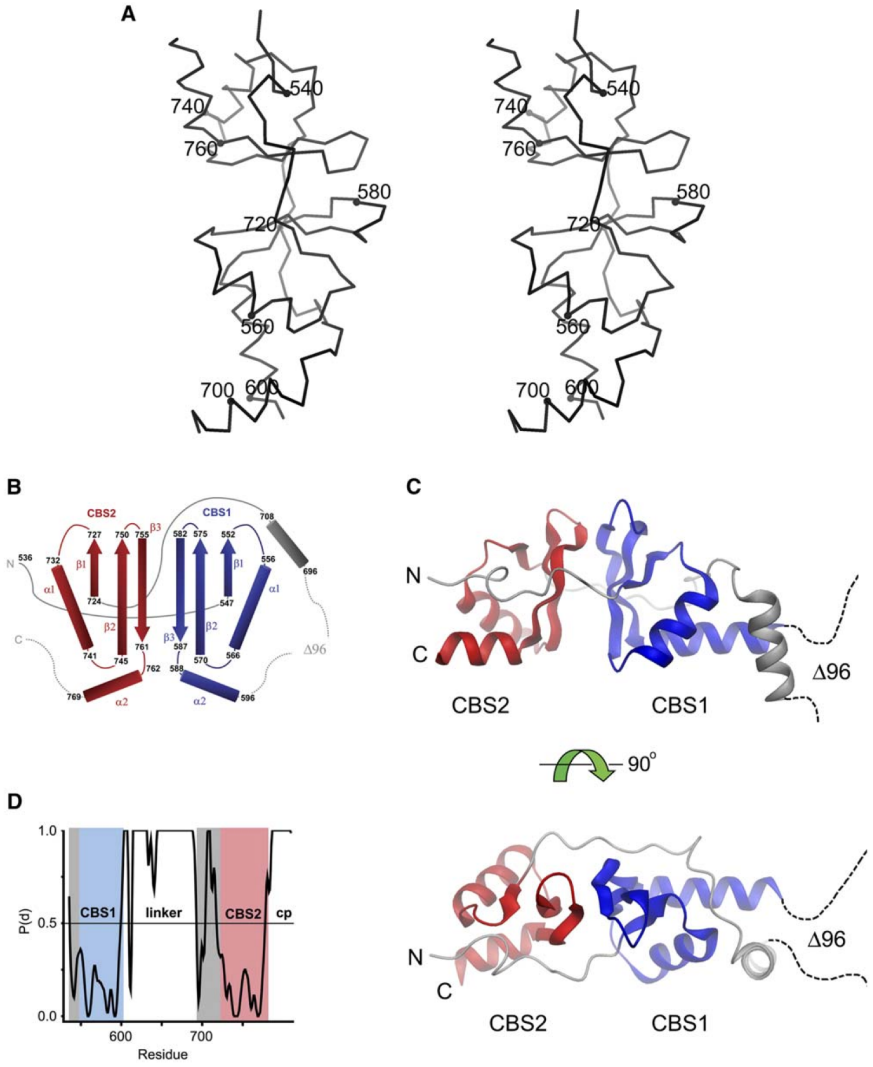

Figure 2. Topology and Structure of the ClC-0 Domain

(A) Stereoview of a C-α trace of the ClC-0 domain. Selected residues are labeled according to their position in the ClC-0 sequence.

(B) Cartoon of the secondary structure. The two CBS subdomains are colored in blue and red, respectively, additional ordered parts of the structure are shown in gray, and disordered regions are marked by dashed lines. The residue numbers (ClC-0) at the beginning and end of the secondary structure elements are shown.

(C) Ribbon representation of the ClC-0 domain in two orientations. Colors are according to (A). The relationship between the two views is indicated. This figure and Figure 4 were prepared with DINO (http://www.dino3d.org).

(D) Propensity of the ClC-0 domain sequence to form an ordered structure. P(d) describes the propensity for disorder; residues with values above P(d) = 0.5 are likely to be unstructured. The segments corresponding to the subdomains are labeled.

Quaternary Structure

The oligomeric state of the cytoplasmic domains in solution suggests that the domains also tightly interact when attached to the transmembrane pore. Although the crystal structure does not reveal the interactions in the dimer, a possible mode of dimerization is found in the crystal structure of TM0935, a CBS domain-containing protein from *T. maritima* (Figure 4A) (Miller et al., 2004). Two intimately interacting subunits of this homologous protein are related by 2-fold symmetry. The extended dimer interface involves helices α1 and α2 of the four CBS subdomains in the crystal and buries more than 2000 Å^2 of the monomer surface. A dimer of two ClC-0 domains, which was generated by superposition with the protein from *T. maritima*, is shown in Figure 4A. The respective subunits of the two proteins superimpose with an rms deviation of 4.2 Å. The model shows good packing in the subunit-subunit interface without major clashes between protein residues. Despite the similarity of the two structures, it has to be pointed out that the two equivalent surfaces involved in dimerization differ in their distribution of hydrophobic and charged residues (Figure 4B).

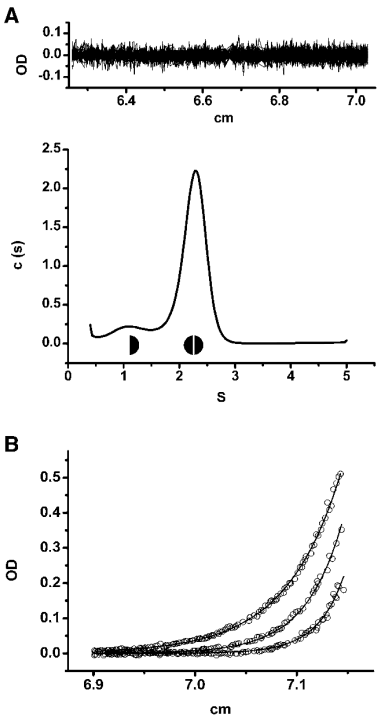

Figure 3. Analytical Ultracentrifugation Data of the ClC-0 Domain

(A) Distribution of the sedimentation coefficient (c[s]) as calculated from sedimentation velocity experiments (bottom) and the corresponding residuals (top). The x axis (top cm) corresponds to the distance from the rotation axis. The predominant peak (black circle) has a maximum at an experimental sedimentation coefficient of 2.17 ± 0.02 S (SD) that is consistent with a dimer. A second minor peak at about half the value, consistent with a single subunit, is indicated (black semicircle).

(B) Fit from sedimentation equilibrium experiments. Three representative absorbance readings correspond to rotor speeds of 19 (left), 23 (center), and 27 krpm (right), respectively; the x axis corresponds to the distance from the rotation axis. The data were fitted with a single species model with an average rms deviation of 0.00606, yielding a molecular mass of 55 kDa.

While the dimer interface in the *T. maritima* protein is found to be predominantly hydrophobic, the equivalent surface in ClC-0 contains several charged side chains. If, despite the difference in the contact surface, the ClC-0 domains share the same mode of interaction, the entire channel could be assembled as shown in Figure 4C. The model emphasizes the size relationship between the transmembrane pore and the cytoplasmic domain. The surface of the domain in contact with the channel, however, remains ambiguous. A remarkable feature of the domain structure is the spatial proximity of the N and C termini. The position of the N terminus with respect to the pore is constrained by its attachment to the R helix. Consequently, CBS2 and the C terminus have to be closer to the pore region, while CBS1 is more remote (Figure 4C). This arrangement is interesting with regard to the influence of CBS2 and the C terminus on channel function (Estevez et al., 2004; Hebeisen and Fahlke, 2005).

Discussion

We have solved the structure of the cytoplasmic domain of the voltage-dependent Cl^- channel ClC-0 from the electric ray *T. marmorata*. About two-thirds of the protein forms a well-folded core structure, and its two CBS subdomains interact tightly. In contrast to the folded core, the linker between the two CBS domains and the residues at the very C terminus, which constitute about one-third of the protein, are highly mobile and do not fold into a defined structure. In aqueous solution, the ClC-0 domains form dimers, which most likely extend the 2-fold symmetry of the transmembrane pore domain. The structure, which is conserved within the family, provides insight into the architecture of the water-soluble part of ClC channels and transporters. However, even with this first structure in hand, our understanding of how the cytoplasmic domains contribute to proper ClC function is far from complete. In the following paragraphs, we will discuss the currently available functional data in light of the structure.

After the first sequences of the ClC family became available, the region at the C terminus immediately came into focus for functional characterization (Jentsch et al., 1990). Several mutations in the domains have been identified in familial diseases, and the role of the cytoplasmic domains in ClC function has been studied by a combination of mutagenesis and electrophysiology (Jentsch et al., 2002). Maduke et al. (1998) used a split channel approach to investigate the role of the CBS domains for ClC-0 channel function. While channels lacking the domains were not functional when expressed in *Xenopus* oocytes, constructs in general showed wild-type-like behavior if the channel was split at a residue in the linker region between CBS1 and CBS2. A similar phenotype was also observed for the homologous muscle channel ClC-1 (Estevez et al., 2004; Hebeisen et al., 2004; Schmidt-Rose and Jentsch, 1997). Interestingly, channel function was not affected by the removal of residues that were part of the disordered linker region. In contrast, no functional channels were obtained if the truncation was made in the structurally well-defined part of the linker region preceding CBS2 or within the CBS subdomains (Estevez et al., 2004). These observations are well explained by the structure, which shows a strong interaction between the two CBS subdomains. They also imply that the structured C-terminal part of the linker is necessary for assembly, while the largest part of the disordered region is not interacting with the folded core.

Mutations in the cytoplasmic domains have been shown to interfere with gating in ClC-0 and ClC-1, particularly the common gating. This regulatory process affects both subunits in concert and is still not well understood. The structure of the domains and their arrangement with respect to the transmembrane pore give several leads for interpretation of the available biochemical data. In general, most mutations that change gating are located within CBS2 and the C-peptide that follows CBS2 (Estevez et al., 2004). This is in agreement with the higher sequence conservation of CBS2 within the ClC family when compared to CBS1. The proximity of CBS2 and the C-peptide to the pore region (Figure 4C) points toward a possible interaction during the gating process. Several residues affecting gating in ClC-1 are

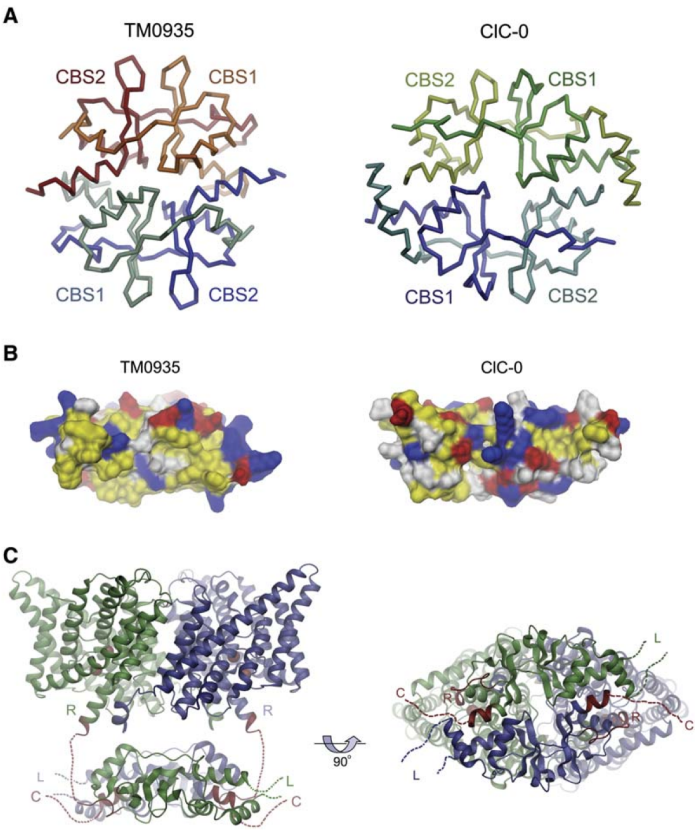

Figure 4. Model of the ClC-0 Domain in Its Context in the Channel

(A) Proposed quaternary structure of the domain. The dimeric crystal structure of the related protein TM0935 (*T. maritima*) viewed along the 2-fold axis (left) and a model of the ClC-0 dimer obtained from a least square fit of the two CBS subdomains onto the respective subunit of TM0935 (right) are shown as a Cα-trace. The subunits are colored in red and blue for TM0935 and in green and blue for ClC-0, and the two halves of each subunit are shown in different shades of the same color.

(B) View on the dimer interface of a single subunit of TM0935 (left) and of the ClC-0 domain (right). The surface was calculated with MSMS (Sanner et al., 1996). Residues at the surface are colored according to their physicochemical properties (acidic residues are in red, basic residues are in blue, hydrophobic residues are in yellow, and all other residues are in white).

(C) Model of the ClC-0 domains relative to the transmembrane pore. The views are from within the membrane—the extracellular side is on top, and the cytoplasm is on the bottom (left)—and from the cytoplasm (right). The structure of the EcClC dimer (PDB code: 1OTS) serves as model for the pore domain. Both EcClC and the dimeric ClC-0 domain are shown as ribbon models. The two subunits are colored in blue and green. The C terminus of the EcClC subunit and the N and C termini of the ClC-0 domain are colored in red. The residues connecting the pore (R) and the cytoplasmic domain and the disordered C terminus are depicted by dashed, red lines. The disordered linker between two CBS subdomains is indicated by a dashed line in the respective color of the subunit. Ions bound to the selectivity filter within each subunit are shown as red spheres.

located at the surface in a cleft between α helices 1 and 2 of CBS2 (Estevez et al., 2004). Interestingly, a cluster of residues in the same region of the more distantly related ClC-7 is found to be mutated in the bone remodeling disease osteopetrosis (Estevez and Jentsch, 2002). It is possibly not a coincidence that the mutations are in proximity to both the N and C termini of the domain. Interaction with the termini or the pore domain may thus prove to be important for regulatory processes.

Next to CBS2, residues of the C-peptide appear to play an important role in the gating process. A naturally occurring mutation of ClC-1 in the myotonic goat (A885P) concerns a residue that is located only 10 residues after CBS2 (Beck et al., 1996). This mutation and the corresponding mutation in ClC-0 both have a large effect on gating by shifting the voltage dependence of opening toward more positive voltages (Beck et al., 1996; Maduke et al., 1998). Moreover, several truncations of the C terminus of ClC-1 after CBS2 show large shifts in the open probability of the channels (Hebeisen and Fahlke, 2005; Hryciw et al., 1998). The influence of the C-peptide on gating remains puzzling. In ClC-0, the C-peptide following CBS2 includes a region of 33 amino acids (Figure 1B). In ClC-1, the same region, which is conserved to ClC-0 at its beginning, extends to 112 amino acids (Figure 1B). The C-peptides in both channels have an unusual amino acid composition and are predicted to be disordered (Figure 2D). The protein in our crystals did not include this region since it was found to be susceptible to proteolysis, and since other constructs that included the C-peptide failed to crystallize. The position of the C-peptide in the domain structure is found close to the proposed dimer interface; thus, a change in the sequence close to CBS2 could interfere with dimerization (Figures 4A and 4C). At present, we do not understand the mechanism by which the disordered C terminus affects gating. It is conceivable that the residues interact with the pore region, and that during gating the access of the C-peptide to the pore is modulated.

Soluble domains are frequently found in different ion channel families to regulate ion permeation in response to ligand binding. Recent studies suggest that the CBS domains of certain ClC family members bind ATP and thereby regulate ion permeation and transport (Bennetts et al., 2005; Scott et al., 2004; Vanoye and George, 2002). The measured binding affinity for the nucleotide is relatively low (~1 mM). In an attempt to investigate the interaction of ligands with the ClC-0 domain, we studied ATP binding with radiolabeled nucleotides in equilibrium dialysis experiments, and we crystallized the domain in the presence of 10 mM ATP (data not shown). Both attempts failed to show binding, which could either

mean that the construct we used does not bind the ligand in the absence of the transmembrane domain, or, alternatively, that ClC-0 is not regulated by ATP. More experiments will be needed to clarify the interaction of ligands with the cytoplasmic domains of ClC channels and transporters.

In the ClC-0 domain, 96 residues of the linker region between the two CBS domains are found to be disordered in the crystal. The role of this linker for ClC function is currently unknown. Interestingly, disordered regions are frequently found in the sequences of eukaryotic proteins, while they are much less frequent in their homologs from prokaryotic organisms (Ward et al., 2004). It was proposed that these highly mobile loops are involved in the regulation of protein function by providing binding sites for kinases or other regulatory proteins (Dyson and Wright, 2005). Indeed, several studies suggested a regulation of ClC family members by kinases (Denton et al., 2005; Rosenbohm et al., 1999). It will be interesting to gain insight into the role of these disordered linker regions with respect to channel function from future studies.

It remains to be shown whether and how the cytoplasmic domains of ClC channels receive signals from the intracellular environment and how such signals are transmitted from the domains to the transmembrane pore to influence gating. A similar mechanism might also modulate function in the secondary active H^+/Cl^- transporters within the family in a yet unknown way. The model shown in Figure 4C offers some hypotheses. The soluble domains are close to the transmembrane pore. A conformational change in the domains could thus trigger a rearrangement in the ion conduction path. Two possible ways to transduce a conformational change could be imagined: either via the N terminus of the domain, which is bound to a helix that contributes a residue to the selectivity filter, or through the C terminus in a way similar to inactivation processes seen in voltage-dependent K^+ channels (Dutzler et al., 2002; Zhou et al., 2001). In order to gain further insight into the mechanism, we will need to see a structure of a channel with C-terminal domains attached.

The structure of the C-terminal domain of ClC-0 has closed a gap in our understanding of the structural organization of the ClC channels and transporters by outlining the molecular architecture of the soluble part of these physiologically important ion transport proteins. In combination with the multitude of biochemical data, the structure offers initial insight into the regulatory processes these domains confer. Although it will ultimately be necessary to reveal the relation of the domains with respect to the transmembrane pore, the structure of the isolated domain from ClC-0 already presents an important step in the elucidation of the molecular mechanisms of ClC function, and it provides a framework for guiding further experiments.

Experimental Procedures

Cloning and Expression

Residues 525–805 of ClC-0 from *Torpedo marmorata* (Jentsch et al., 1990) were cloned into the pET28-b+ expression vector (Novagen) with a C-terminal thrombin cleavage site and a hexa-histidine tag. Transformed *E. coli* BL21 (DE3) cells were grown at 37°C in LB medium containing 50 mg/l kanamycin to an OD_{600} of 1.5. Expression was induced by the addition of 0.5 mM isopropyl-D-thiogalactopyranoside (IPTG) and proceeded overnight at 20°C. Harvested cells were lysed by sonication in 50 mM Tris-HCl (pH 7.5), 400 mM NaCl, 5 mM $MgCl_2$, 5 mM β-mercapto-ethanol, 200 mg/l lysozyme, 20 mg/l DNase, leupeptin, pepstatin, and 1 mM phenylmethyl sulphonyl fluoride. The lysate was cleared by centrifugation and loaded onto a Ni-affinity column (Chelating Sepharose, Pharmacia Biotech). The column was washed with buffer containing 15 mM imidazole, and the pure protein was eluted with 300 mM imidazole. The protein was dialyzed into gel-filtration buffer and digested with thrombin until protease cleavage was complete. After concentrating, the protein was run on a Superdex 200 column in 10 mM Tris-HCl (pH 7.5), 400 mM NaCl, 5 mM $MgCl_2$, 5 mM β-mercapto-ethanol. Pooled peak fractions were concentrated to a protein concentration of 20–30 mg/ml.

Crystal Preparation

ClC-0 domain crystals were grown in sitting drops at 4°C by equilibrating a 1:1 mixture of protein and reservoir solution against the reservoir. The reservoir solution contained 3.25–3.5 M sodium formate. The crystal for the best native data set was grown in the same conditions with additional 10 mM $MgCl_2$. Crystals were of space group $P2_13$ ($a = b = c = 126$ Å, $\alpha = \beta = \gamma = 90°$), with two copies of the domain in the asymmetric unit. Heavy metal derivatives were obtained by soaking native crystals for 20 hr in mother-liquor containing either 1 mM methyl mercury chloride or 1 mM Pt(II)-terpyridine chloride (Aldrich). Crystals were prepared for cryocrystallography by successive transfer into higher concentrations of sodium formate up to a final concentration of 4.2 M and were subsequently flash frozen in liquid propane and stored in liquid nitrogen. For the analysis of the protein after crystallization, a crystal was washed twice in mother liquor and submitted to MALDI-TOF mass spectrometry.

Structure Determination and Modeling

Data were collected on frozen crystals on a Mar CCD detector on the microdiffractometer at the X06SA beamline at the Swiss Light Source (SLS) of the Paul Scherrer Institute (PSI). For collecting anomalous differences, the wavelength was set to 1.008 Å and to 1.072 Å for the Hg and the Pt derivatives, respectively. The data were indexed and integrated with DENZO and SCALEPACK (Otwinowski and Minor, 1997) and were further processed with CCP4 programs (CCP4, 1994). Heavy metal positions for the first derivative were determined by a Patterson search with RSPS (CCP4, 1994), and, for the second derivative, positions were determined by difference Fourier methods (CCP4, 1994). Heavy atom positions were refined, and phases were calculated by using SHARP (de La Fortelle and Bricogne, 1997). Initial phases were improved by solvent flattening with SOLOMON (Abrahams and Leslie, 1996), and by 2-fold noncrystallographic symmetry (NCS) averaging with DM (Cowtan, 1994). A model containing residues 536–602 and 696–770 was built into the electron density with the program O (Jones et al., 1991). Refinement was carried out by several cycles of simulated annealing in CNS (Brunger et al., 1998) alternated with inspection and manual rebuilding with O. Two-fold NCS constraints were used in the initial stages of the refinement. In later stages, the strict constraints between the two copies in the asymmetry unit were loosened, and restraint individual B factors were refined. R_{free} (calculated from 5% of the reflections omitted during refinement) was monitored throughout. Residual weak electron density in a $2F_o - F_c$ map allowed for tracing of the backbone of several additional residues of the N terminus and the linker region of the molecule (Figure S1B). Including those residues, which are found to interact with symmetry-related molecules, in the model had little influence on the statistics. The final model contains 2472 atoms with good geometry and no outliers in the Ramachandran plot. The slightly elevated R factors for this resolution ($R = 27.3/R_{free} = 30.9$) and the high B factors are probably due to the large fraction of the molecule that is found to be poorly ordered in the crystals.

The dimer of the ClC-0 domain was generated by fitting the subunit to each chain of the dimeric CBS domain-containing protein from *T. maritima* (TM0935, PDB code: 1o50) by using the program O. A total of 81 C-α atoms were found to superimpose with a rms deviation of 4.22 Å. Analysis of the sequence with respect to its

propensity to form structure was performed with the program DRIPPRED (http://www.sbc.su.se/~maccallr/disorder/).

Analytical Ultracentrifugation

Experiments were performed with a Beckman XL-I analytical ultracentrifuge with an An 50-Ti rotor at 4ºC. For the sedimentation velocity experiments, 12 mm epon double-sector cells were filled with 400 μl 150 mM NaCl, 10 mM Tris (pH 7.5), 5 mM $MgCl_2$, 5 mM β-mercapto-ethanol, and protein sample. Sedimentation velocity experiments were performed at protein concentrations of 18, 35, and 75 μM. Data were acquired at 280 nm in continuous scan mode in 0.003 cm intervals at a rotor speed of 42,000 rpm. The data analysis was performed with the c(S) module of Sedfit (Schuck, 2000; Schuck et al., 2002). The buffer parameters, partial-specific volume of the protein, and the corrected $S^0_{20,w}$ were calculated by using Sednterp (Laue et al., 1992). Sedimentation equilibrium experiments were conducted at protein concentrations of 18 and 75 μM at rotor speeds of 19,000, 23,000, and 27,000 rpm, 4ºC. Data were modeled with the program Sedphat (Vistica et al., 2004).

Supplemental Data

Supplemental Data including stereoviews of the electron density and of the asymmetric unit are available at http://www.structure.org/cgi/content/full/14/2/299/DC1/.

Acknowledgments

X-ray data were collected at the Swiss Light Source (SLS) of the Paul Scherrer Institute (PSI). We are grateful to Thomas Jentsch for providing the ClC-0 clone, Sergiy Chesnov and Peter Hunziker for their help with mass spectrometry, Thomas Schalch for his help with analytical ultracentrifugation, the staff of the X06SA beamline for their support during data collection, Sara Savaresi, and other members of the Dutzler lab for help at all stages of the project. This work was supported by the Swiss National Science Foundation (SNSF) and the National Center for Competence in Research Structural Biology program. S.M. is affiliated with the Molecular Life Sciences Ph.D. Program of the University/Eidgenössisch Technische Hochschule Zürich. The authors declare that they have no competing financial interests.

Received: September 14, 2005
Revised: October 26, 2005
Accepted: October 27, 2005
Published: February 10, 2006

References

Abrahams, J.P., and Leslie, A.G. (1996). Methods used in the structure determination of bovine mitochondrial F1 ATPase. Acta Crystallogr. D Biol. Crystallogr. *52*, 30–42.

Accardi, A., and Pusch, M. (2000). Fast and slow gating relaxations in the muscle chloride channel CLC-1. J. Gen. Physiol. *116*, 433–444.

Bateman, A. (1997). The structure of a domain common to archaebacteria and the homocystinuria disease protein. Trends Biochem. Sci. *22*, 12–13.

Beck, C.L., Fahlke, C., and George, A.L., Jr. (1996). Molecular basis for decreased muscle chloride conductance in the myotonic goat. Proc. Natl. Acad. Sci. USA *93*, 11248–11252.

Bennetts, B., Rychkov, G.Y., Ng, H.L., Morton, C.J., Stapleton, D., Parker, M.W., and Cromer, B.A. (2005). Cytoplasmic ATP-sensing domains regulate gating of skeletal muscle ClC-1 chloride channels. J. Biol. Chem. *280*, 32452–32458.

Brejc, K., van Dijk, W.J., Klaassen, R.V., Schuurmans, M., van Der Oost, J., Smit, A.B., and Sixma, T.K. (2001). Crystal structure of an ACh-binding protein reveals the ligand-binding domain of nicotinic receptors. Nature *411*, 269–276.

Brunger, A.T., Adams, P.D., Clore, G.M., DeLano, W.L., Gros, P., Grosse-Kunstleve, R.W., Jiang, J.S., Kuszewski, J., Nilges, M., Pannu, N.S., et al. (1998). Crystallography & NMR system: a new software suite for macromolecular structure determination. Acta Crystallogr. D Biol. Crystallogr. *54*, 905–921.

CCP4 (Collaborative Computational Project, Number 4). (1994). The CCP4 suite: programs for X-ray crystallography. Acta Crystallogr. D Biol. Crystallgr. *50*, 760–763.

Chen, T.Y. (2005). Structure and function of CLC channels. Annu. Rev. Physiol. *67*, 809–839.

Cowtan, K. (1994). An automated procedure for phase improvement by density modification. Joint CCP4 and ESF-EACBM Newsletter on Protein Crystallography *31*, 34–38.

de La Fortelle, E., and Bricogne, G. (1997). Methods in Enzymology. In Methods in Enzymology, C.W. Carter and R.M. Sweet, eds. (New York: Academic Press), pp. 492–494.

Denton, J., Nehrke, K., Rutledge, E., Morrison, R., and Strange, K. (2003). Alternative splicing of N- and C-termini of a *C. elegans* ClC channel alters gating and sensitivity to external Cl− and H+. J. Physiol. *555*, 97–114.

Denton, J., Nehrke, K., Yin, X., Morrison, R., and Strange, K. (2005). GCK-3, a newly identified Ste20 kinase, binds to and regulates the activity of a cell cycle-dependent ClC anion channel. J. Gen. Physiol. *125*, 113–125.

Dutzler, R., Campbell, E.B., Cadene, M., Chait, B.T., and MacKinnon, R. (2002). X-ray structure of a ClC chloride channel at 3.0 Å reveals the molecular basis of anion selectivity. Nature *415*, 287–294.

Dutzler, R., Campbell, E.B., and MacKinnon, R. (2003). Gating the selectivity filter in ClC chloride channels. Science *300*, 108–112.

Dyson, H.J., and Wright, P.E. (2005). Intrinsically unstructured proteins and their functions. Nat. Rev. Mol. Cell Biol. *6*, 197–208.

Estevez, R., and Jentsch, T.J. (2002). CLC chloride channels: correlating structure with function. Curr. Opin. Struct. Biol. *12*, 531–539.

Estevez, R., Pusch, M., Ferrer-Costa, C., Orozco, M., and Jentsch, T.J. (2004). Functional and structural conservation of CBS domains from CLC chloride channels. J. Physiol. *557*, 363–378.

Fong, P., Rehfeldt, A., and Jentsch, T.J. (1998). Determinants of slow gating in ClC-0, the voltage-gated chloride channel of *Torpedo marmorata*. Am. J. Physiol. *274*, C966–C973.

Hebeisen, S., and Fahlke, C. (2005). Carboxy-terminal truncations modify the outer pore vestibule of muscle chloride channels. Biophys. J. *89*, 1710–1720.

Hebeisen, S., Biela, A., Giese, B., Muller-Newen, G., Hidalgo, P., and Fahlke, C. (2004). The role of the carboxyl terminus in ClC chloride channel function. J. Biol. Chem. *279*, 13140–13147.

Hille, B. (2001). Ion Channels of Excitable Membranes, Third Edition (Sunderland, MA: Sinauer Associates, Inc.).

Hryciw, D.H., Rychkov, G.Y., Hughes, B.P., and Bretag, A.H. (1998). Relevance of the D13 region to the function of the skeletal muscle chloride channel, ClC-1. J. Biol. Chem. *273*, 4304–4307.

Jentsch, T.J., Steinmeyer, K., and Schwarz, G. (1990). Primary structure of *Torpedo marmorata* chloride channel isolated by expression cloning in *Xenopus* oocytes. Nature *348*, 510–514.

Jentsch, T.J., Stein, V., Weinreich, F., and Zdebik, A.A. (2002). Molecular structure and physiological function of chloride channels. Physiol. Rev. *82*, 503–568.

Jentsch, T.J., Poet, M., Fuhrmann, J.C., and Zdebik, A.A. (2005). Physiological functions of CLC Cl− channels gleaned from human genetic disease and mouse models. Annu. Rev. Physiol. *67*, 779–807.

Jiang, Y., Lee, A., Chen, J., Cadene, M., Chait, B.T., and MacKinnon, R. (2002). Crystal structure and mechanism of a calcium-gated potassium channel. Nature *417*, 515–522.

Jones, T.A., Zou, J.Y., Cowan, S.W., and Kjeldgaard, M. (1991). Improved methods for building protein models in electron density maps and the location of errors in these models. Acta Crystallogr. A *47*, 110–119.

Laue, T., Shah, B., Ridgeway, T., and Pelletier, S. (1992). Computer aided interpretation of analytical sedimentation data for proteins. In Analytical Ultracentrifugation in Biochemistry and Polymer Science, S. Harding, A. Rowe, and J. Horton, eds. (Cambridge, UK: The Royal Society of Chemistry), pp. 90–125.

MacKinnon, R. (2004). Potassium channels and the atomic basis of selective ion conduction (Nobel Lecture). Angew. Chem. Int. Ed. Engl. *43*, 4265–4277.

Maduke, M., Williams, C., and Miller, C. (1998). Formation of CLC-0 chloride channels from separated transmembrane and cytoplasmic domains. Biochemistry *37*, 1315–1321.

Miller, C. (1982). Open-state substructure of single chloride channels from Torpedo electroplax. Philos. Trans. R. Soc. Lond. B Biol. Sci. *299*, 401–411.

Miller, M.D., Schwarzenbacher, R., von Delft, F., Abdubek, P., Amb-ing, E., Biorac, T., Brinen, L.S., Canaves, J.M., Cambell, J., Chiu, H.J., et al. (2004). Crystal structure of a tandem cystathionine-β-synthase (CBS) domain protein (TM0935) from *Thermotoga maritima* at 1.87 Å resolution. Proteins *57*, 213–217.

Nishida, M., and MacKinnon, R. (2002). Structural basis of inward rectification: cytoplasmic pore of the G protein-gated inward rectifier GIRK1 at 1.8 Å resolution. Cell *111*, 957–965.

Otwinowski, Z., and Minor, W. (1997). Processing of X-ray diffraction data collected in oscillation mode. Methods Enzymol. *267*, 307–326.

Pusch, M., Ludewig, U., and Jentsch, T.J. (1997). Temperature dependence of fast and slow gating relaxations of ClC-0 chloride channels. J. Gen. Physiol. *109*, 105–116.

Rosenbohm, A., Rudel, R., and Fahlke, C. (1999). Regulation of the human skeletal muscle chloride channel hClC-1 by protein kinase C. J. Physiol. *514*, 677–685.

Sanner, M.F., Olson, A.J., and Spehner, J.C. (1996). Reduced surface: an efficient way to compute molecular surfaces. Biopolymers *38*, 305–320.

Schmidt-Rose, T., and Jentsch, T.J. (1997). Reconstitution of functional voltage-gated chloride channels from complementary fragments of CLC-1. J. Biol. Chem. *272*, 20515–20521.

Schuck, P. (2000). Size-distribution analysis of macromolecules by sedimentation velocity ultracentrifugation and lamm equation modeling. Biophys. J. *78*, 1606–1619.

Schuck, P., Perugini, M.A., Gonzales, N.R., Howlett, G.J., and Schubert, D. (2002). Size-distribution analysis of proteins by analytical ultracentrifugation: strategies and application to model systems. Biophys. J. *82*, 1096–1111.

Scott, J.W., Hawley, S.A., Green, K.A., Anis, M., Stewart, G., Scullion, G.A., Norman, D.G., and Hardie, D.G. (2004). CBS domains form energy-sensing modules whose binding of adenosine ligands is disrupted by disease mutations. J. Clin. Invest. *113*, 274–284.

Vanoye, C.G., and George, A.L., Jr. (2002). Functional characterization of recombinant human ClC-4 chloride channels in cultured mammalian cells. J. Physiol. *539*, 373–383.

Vistica, J., Dam, J., Balbo, A., Yikilmaz, E., Mariuzza, R.A., Rouault, T.A., and Schuck, P. (2004). Sedimentation equilibrium analysis of protein interactions with global implicit mass conservation constraints and systematic noise decomposition. Anal. Biochem. *326*, 234–256.

Ward, J.J., Sodhi, J.S., McGuffin, L.J., Buxton, B.F., and Jones, D.T. (2004). Prediction and functional analysis of native disorder in proteins from the three kingdoms of life. J. Mol. Biol. *337*, 635–645.

Zagotta, W.N., Olivier, N.B., Black, K.D., Young, E.C., Olson, R., and Gouaux, E. (2003). Structural basis for modulation and agonist specificity of HCN pacemaker channels. Nature *425*, 200–205.

Zhang, R., Evans, G., Rotella, F.J., Westbrook, E.M., Beno, D., Huberman, E., Joachimiak, A., and Collart, F.R. (1999). Characteristics and crystal structure of bacterial inosine-5′-monophosphate dehydrogenase. Biochemistry *38*, 4691–4700.

Zhou, M., Morais-Cabral, J.H., Mann, S., and MacKinnon, R. (2001). Potassium channel receptor site for the inactivation gate and quaternary amine inhibitors. Nature *411*, 657–661.

Accession Numbers

Coordinates and structure factors have been deposited with the Protein Data Bank with accession code 2D4Z.

2.1.3 Supplementary Material

Supplementary Figures Figure S1 is an example of the $2F_o$-F_c electron density map giving an impression of the quality of model building at the resolution of 3.1 Å. Figure S2 shows the asymmetric unit in the crystal including parts of the disordered linker and C-peptide that could only be included as a poly-glycine chain in the model. These elongated chains disobey the non-crystallographic symmetry in the asymmetric unit and are most likely in a non-native conformation.

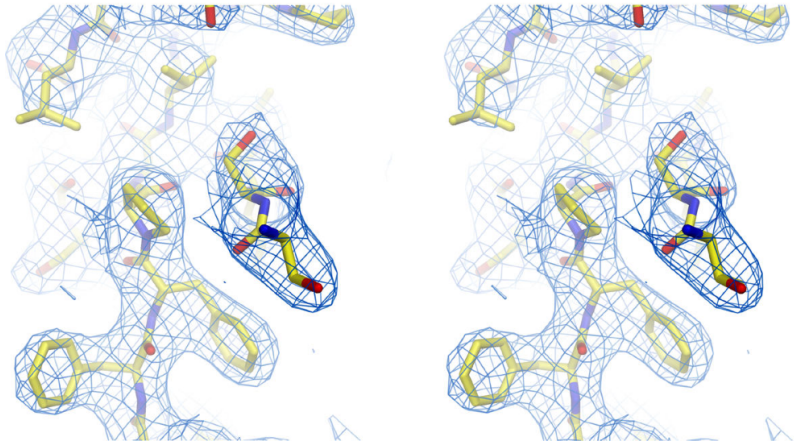

Figure S1: **Electron Density Map of the ClC-0 Domain**
Stereo view of a representative section of a $2F_o$-F_c electron density map around the β-strands 1 to 3 of CBS1 is shown superimposed on the model. The density is contoured at 1.0 σ.

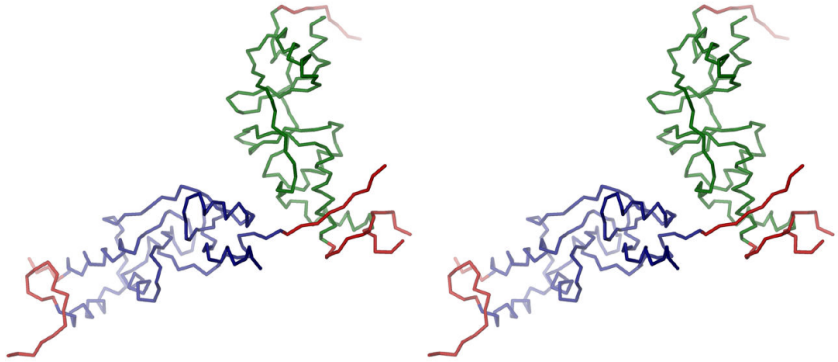

Figure S2: **View of the Asymmetric Unit**
Stereo view of a C-α trace of the asymmetric unit. The well defined core structures of the two copies of the ClC-0 domain in the asymmetric unit are colored in green and blue, respectively. Residues modeled into residual weak electron density at the N-terminus and the linker are shown in red.

2.1.4 The Cytoplasmic Domain of the Chloride Channel ClC-0: Structural and Dynamic Characterization of Flexible Regions

Aim of the Study The structure of the cytoplasmic domains from ClC-0 laid the foundation for the structural understanding of these components in ClCs, however the lack of electron density for substantial parts of the protein was a suprising finding. Based on the observations made in the crystal structure this following work characterizes the flexible regions of the C-terminus of the channel by nuclear magnetic resonance (NMR) techniques. These regions had been recognized previously to contain regulatory motifs that could lead to functional regulation of the protein upon phosphorylation[90,91] or alternative splicing.[82] The absence of electron density for large parts of the CBS subdomain linker and the pronounced protease susceptibility of the C-peptide was a striking and unexpected feature of this initial structural study. Although the primary sequence analysis of the cytoplasmic domains of members from the α-subfamily suggested that these segments are natively disordered this hypothesis still required experimental proof. By the use of nuclear magnetic resonance methods the linker region between CBS1 and CBS2 as well as the C-peptide following CBS2 could be analyzed in solution ideally answering the question whether these regions are completely disordered or retain some secondary structure but are flexibly attached to the protein core.

doi:10.1016/j.jmb.2007.04.020 *J. Mol. Biol.* (2007) **369**, 1163–1169

JMB

Available online at www.sciencedirect.com

ScienceDirect

ELSEVIER

COMMUNICATION

The Cytoplasmic Domain of the Chloride Channel ClC-0: Structural and Dynamic Characterization of Flexible Regions

Simon Alioth[1], Sebastian Meyer[2], Raimund Dutzler[2] and Konstantin Pervushin[1]*

[1]*Laboratorium für Physikalische Chemie ETH Zürich, CH-8093 Zürich, Switzerland*

[2]*Department of Biochemistry University of Zürich Winterthurer Strasse 190 CH-8057 Zürich, Switzerland*

**Corresponding author*

Eukaryotic members of the ClC family of chloride channels and transporters are composed of a transmembrane ion transport domain followed by a cytoplasmic domain, which is believed to be involved in the modulation of ClC function. In some family members this putative regulatory domain contains next to a well-folded structured part, long sequence stretches with low sequence complexity. These regions, a 96 residue long linker connecting two structured sub-domains, and 35 residues on the C teminus of the domain were found disordered in a recent crystal structure of this domain in ClC-0. Both regions have a large influence on the modulation of channel function in closely related family members. Here we describe a NMR study to characterize the structural and dynamic properties of these putatively unstructured stretches. Our study reveals that the two regions indeed show large conformational flexibility with dynamics on the nanosecond time-scale. However, small islands of secondary structure are found interdispersed between the unfolded regions. This study characterizes for the first time the biophysical properties of these protein segments, which may become important for the understanding of novel regulatory mechanisms within the ClC family.

Keywords: ClC channels and transporters; NMR spectroscopy; natively disordered regions; ion transport; protein dynamics

Up to 30% of the sequences encoding for eukaryotic proteins do not fold into a defined tightly packed conformation. Those unstructured regions show a distinct distribution of amino acids that is easily recognized on the level of primary sequence. Natively disordered sequences either constitute entire proteins, or sections of a protein where they are interdispersed between well folded parts of the polypeptide chain.[1,2] In many cases these flexible protein segments are believed to play an important role in the interaction with other molecules in regulatory processes.

Such natively unfolded sequence stretches are also found in the ClC proteins, a large family of chloride channels and transporters, which is ubiquitously expressed from bacteria to mammals.[3,4] While the bacterial sequences are compact and usually lack these long regions of low sequence complexity, their eukaryotic counterparts have large sequence segments, which presumably do not fold into defined structures, inserted between structured parts of the protein. The members of the ClC family share a common molecular architecture, which consists of a transmembrane pore domain that is in many cases followed by a cytoplasmic putative regulatory domain.[5] These domains are found in all eukaryotic family members and contain two structured cys-

Present address: K. Pervushin, School of Biological Sciences, Nanyang Technological University, 60 Nanyang Drive, 637551 Singapore, Singapore.

Abbreviations used: ClC, chloride channel; CBS, cystathionine β-synthase; TROSY, transverse relaxation optimized spectroscopy; HSQC, heteronuclear single quantum coherence; NOE, nuclear Overhauser enhancement; NOESY, NOE spectroscopy; RDC, residual dipolar coupling.

E-mail address of the corresponding author: kpervushin@ntu.edu.sg

tathionine β-synthase (CBS) sub-domains. Embedded between the two CBS sub-domains and following the second sub-domain are sequences varying considerably in length between the nine family members of ClC proteins found in mammals (Figure 1(a)). The two sequence stretches were named linker and C-peptide in a previous study.[4] Both regions are extended in the closely related chloride channels ClC-0, ClC-1 and ClC-2 and show a high probability of being disordered, as predicted by different sequence analysis programs.[6–8] We currently do not understand the role of these two potentially disordered regions; however, several observations suggest that they play an important role in channel regulation and in the interaction with regulatory proteins.[9] (i) Both the linker and C-peptide of a particular ClC family member are conserved between species. (ii) Point mutations and splice variants affecting the C-peptide in related channels exhibit pronounced differences in channel gating that in certain cases result in familial diseases.[10,11] (iii) Residues in the linker region contain recognition sequences for interacting proteins as kinases, which have been linked to channel regulation in response to phosphorylation.[12,13]

Here, we present an NMR study that characterizes the structural and dynamic properties of the cytoplasmic domain of the chloride channel ClC-0

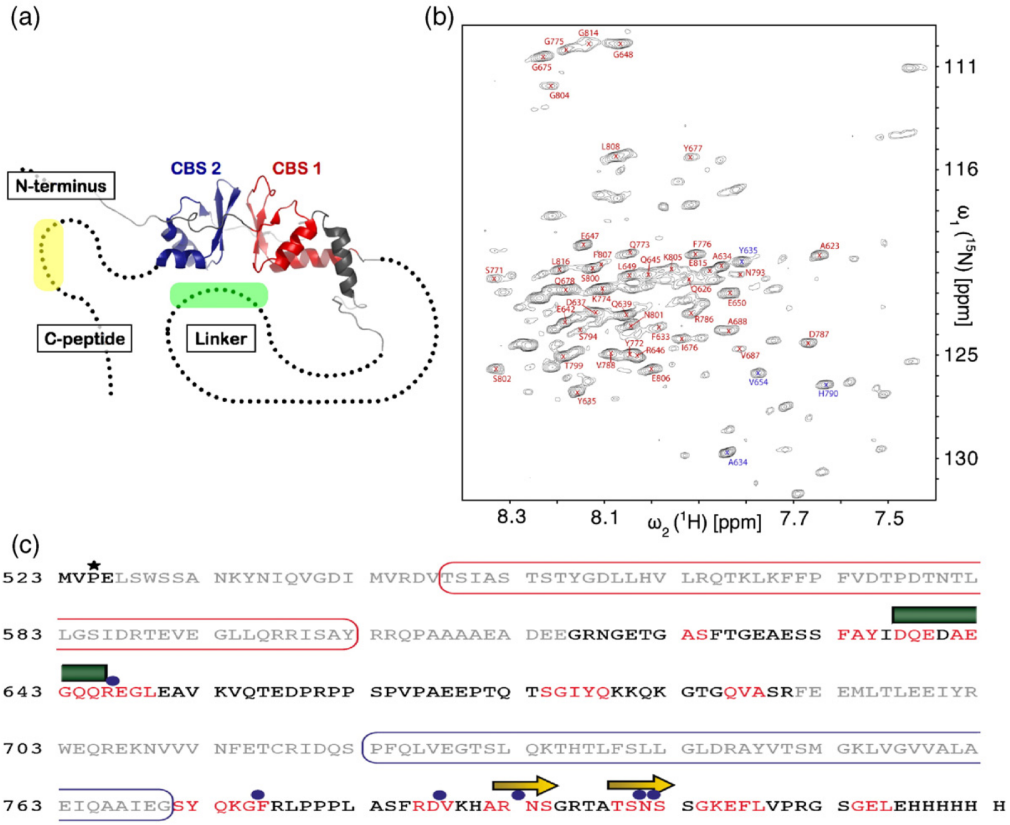

Figure 1. Structural organization and assignment of the ClC-0 domain. (a) Crystal structure of the cytoplasmic domain of the chloride channel ClC-0[4] (PDB accession code 2D4Z). The two CBS sub-domains are shown in red and blue, respectively. Parts with missing electron density in the X-ray structure are depicted as dots. The green (α-helix) and yellow (β-strand) boxes indicate the approximate position of the secondary structure elements obtained from the chemical shift index (CSI) analysis. (b) TROSY spectrum of the ClC-0 cytoplasmic domain recorded on a Bruker Avance 900 MHz spectrometer with a 1 mM $^{2}H,^{15}N$-labeled sample at 7 °C. The assigned resonances are indicated with the amino acid numbering corresponding to the full length ClC-0 protein. Resonances labeled in red are assignments with high spin link probability, whereas the assignment of the resonances labeled in blue is ambiguous. Data for these amino acids were therefore excluded from the study. (c) Amino acid sequence of the ClC-0 cytoplasmic domain including a hexa-histidine tag. An asterisk (*) indicates the start of the domain in the full length ClC-0. The green box marks the position of the α-helix and the yellow arrows the β-strands; the blue dots represent the position of inter-residue NOEs between two adjacent amino acids. Amino acids labeled in red were assigned using the automated assignment program AutoLink[23] and the program CARA.[24] For the automated assignment only the sequence of the flexible part (black or red) of the protein was entered into the program. The assignment was achieved with TROSY-HNCA[25,26] and [$^{1}H,^{1}H,^{15}N$]-NOESY[27] (200 ms mixing time) data. Only spin systems with a spin link probability higher than 0.9 were linked.

from the electric ray, which is homologous to the mammalian muscle channel ClC-1.[3] We put special emphasis on the 96 amino acid long linker and the 35 amino acid long C-peptide, which putatively lack tertiary structure. The study was motivated by a crystal structure of the domain in which large parts of the linker region were not visible in the electron density and where the C-peptide was found to be susceptible to proteolysis.[4] Both linker and C-peptide share considerable homology with ClC-1, although they are somewhat shorter in ClC-0.[4] Our study reveals that both regions are indeed disordered, with local stretches of secondary structure scattered within protein segments that otherwise exhibit large conformational flexibility.

Experimental setup

Here we have used a 302 residue long construct, which encompasses the entire cytoplasmic domain of ClC-0 followed by a 12 amino acid long spacer and a hexa-histidine tag. The protein was stable in solution and did not show any aggregation during the course of the experiment. The construct contains the entire region of the crystal structure, including the unresolved parts of the linker (residue 616 to 690), of the C-peptide (residue 671 to the C terminus) and four residues of the N terminus (Figure 1(a) and (c)). The hexa histidine tag was not removed to prevent proteolysis of the flexible C-peptide.[4] The lack of structural information is presumably due to a substantial flexibility of these sequence stretches, since even at low contour there was no hint of a defined conformation. Determining the timescale of these motions gives insight into the structural organization of these regions: if the segments are mobile on the fast timescale (ns) they most probably lack a defined secondary and higher-order structure. Although in this case the sequence might still have finite structural propensities that in certain cases result in an ordering upon binding of interacting molecules. Conversely, if the dynamics proceed in the millisecond timescale, the regions might be structured after all but undergo a conformational exchange between defined states. Due to the collective nature of such dynamic properties, they typically involve movement of entire secondary structure elements with respect to each other.[14] Despite the fact that the later scenario occasionally manifests itself in weak electron density of the alternate conformations, in most cases both possibilities would indiscriminately result in a loss of defined electron density. In contrast both scenarios can be clearly distinguished in an NMR experiment.

Overall characterization of conformational flexibility

For initial NMR spectroscopic characterization a 2D [^{1}H/^{15}N]-transverse relaxation optimized spectroscopy (TROSY) spectrum[15] was measured (Figure 1(b)). The spectrum shows about 140 strong resonance peaks, most of which originate from flexible parts of the protein that were not observed in the crystal structure for the following reasons: (i) ^{1}H and ^{15}N chemical shifts of cross-peaks readily observed in TROSY and heteronuclear single quantum coherence (HSQC) spectra correspond to random coil values typically found in unstructured or unfolded proteins. Figure 1(b) shows that all resonances in the ^{1}H dimension are dispersed within only 1.2 ppm around 8 ppm, a range typical for unstructured proteins. (ii) In a CRIPT experiment, which allows for the characterization of large proteins, additional well dispersed cross-peaks from structured parts of the protein with the corresponding chemical shifts typical for folded proteins were observed (data not shown). (iii) The observed number of cross-peaks is in good agreement with the 147 expected resonances from the flexible part. In summary, these first experiments already indicate a substantial conformational flexibility within the ClC-0 domain.

Backbone resonance assignment and residual dipolar coupling

The triple resonance experiments TROSY-HNCA and ^{15}N-resolved [^{1}H,^{1}H]-nuclear Overhauser enhancement spectroscopy (NOESY) were used for the sequential assignment of the flexible parts of the protein domain. Both experiments allowed the measurement of 120 and 97 non-overlapping correlation strips, respectively. One hundred and twelve out of the 120 correlation strips in the TROSY-HNCA contain two cross-peaks to intra-residual and sequential $^{13}C^{\alpha}$ spins, which was crucial for the assignment of the protein fragments with this limited amount of data. Almost all observed spin systems could be mapped to stretches of the mobile parts of the protein (Figure 1(b) and (c)). The presence of multiple Gly (12), Ser (9) and Thr (2) residues in the sequence facilitated mapping of the connected spin system to the protein sequence due to their characteristic chemical shifts. The data allowed the assignment of 25 residues of the linker and 24 residues of the C-peptide. An additional TROSY-HNCACB experiment was of limited use in the backbone assignment due to low signal intensities.

When comparing the $^{13}C^{\alpha}$ chemical shifts from the assignment to the chemical shift index of random coil proteins,[16] the analysis shows correspondence for the bulk of protein residues with systematic deviation from the random coil values for three short stretches of amino acids (Figure 2(c)). These three stretches of amino acids show distinct chemical shift values usually observed in secondary structure elements. Those regions of local secondary structure include a ten amino acid long α-helix (residue 637 to 646) in the linker between CBS domain 1 and 2 and two short β-strands (residue 692 to 694 and 799 to 802) in the C-peptide of the protein (Figures 1(b) and 2(c)). Strong inter-residue NOEs between adjacent amino acids observed in the [^{1}H/^{1}H/^{15}N]-NOESY spectrum (200 ms mixing time) support the presence of residual structure

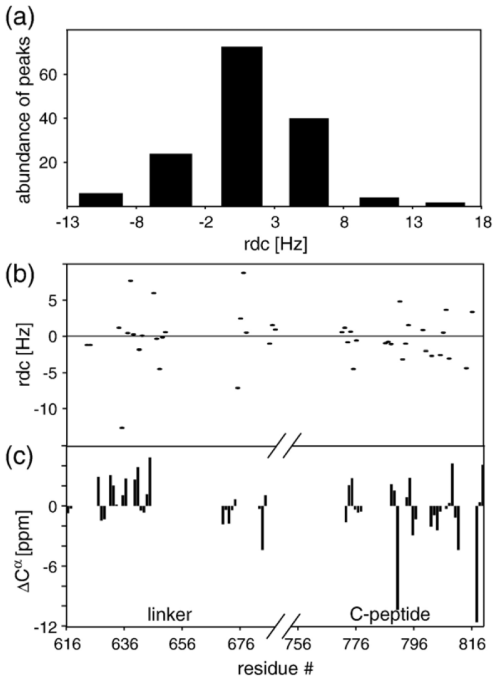

Figure 2. Residual dipolar couplings and chemical shift analysis. (a) RDC distribution obtained from 140 couplings. RDC data were obtained using a $^{2}H,^{15}N$ labeled sample aligned with 1 mM of Pf1 phage.[17,28] (b) RDC values for the assigned residues. The couplings were measured using TROSY and ^{15}N-anti-TROSY spectra[29] measured with and without Pf1 phage at 600 MHz and 7 °C. (c) C^{α} chemical shift deviation from random coil chemical shifts. Large positive values indicate α-helices, whereas negative values indicate a tendency for β-strand formation. Certain residues of the C-peptide show a high β-strand propensity, whereas in the linker a high α-helix propensity is prevailing. The secondary structure propensities are mapped to the sequence in Figure 1(c).

obtained from $^{13}C^{\alpha}$ chemical shifts (Figures 1(c) and 2(c)), although the expected sequential NOEs between adjacent amide groups frequently seen for an α-helix could not be measured. These NOEs were mainly found at the C terminus of the protein, close to the region with high β-strand propensity. The observed NOEs only indicate the presence of local secondary structure, while the characteristic NOE patterns observed for higher-order structure are absent (Figure 1(c)). The sequential NOEs found in the C-peptide are consistent with a pattern frequently seen in β-turns and it is therefore possible that those regions might transiently adopt a similar conformation. This possible scenario is also reflected in the non-uniform generalized order parameters (see the next section).

Additional evidence for local structure within the dynamic regions of the protein was obtained from the distribution of residual dipolar coupling values (RDC). RDCs were measured by partial alignment of the protein in the magnetic field using bacteriophage Pf1.[17] The distribution of measured RDCs is non-uniform, and ranges between −13 and 18 Hz, indicating a variable orientation of amide moieties relative to the global molecular frame (Figure 2(a) and (b)). RDCs measured for completely unstructured proteins are in contrast uniformly distributed over the protein sequence and typically display positive values,[18,19] due to the fact that most of the ^{1}H-^{15}N vectors are, on average, oriented in the same direction.

All three observations, the propensity for secondary structure in parts of the linker and the C-peptide, the presence of inter-residue NOEs, and the non-uniform RDC distribution are indicative for islands of local structural order scattered within the flexible protein segments.

Backbone dynamics

The assignment for a large fraction of the residues in the flexible part of the protein allows for the detailed investigation of backbone dynamics for both, linker and C-peptide. The dynamic properties of individual residues were characterized by measuring standard ^{15}N-relaxation experiments. Generalized order parameters (S^2), rotational correlation times (τ_e) and conformational exchange-induced line broadening (R_{ex}) were calculated from the relaxation rates and hetronuclear steady-state NOE based on the Lipari & Szabo model-free analysis.[20] The order parameters S^2 reflect spatial restriction of ^{1}H-^{15}N bonds on the picosecond-to-nanosecond time scale, and range from close to 0 (unstructured proteins) to nearly 1 (fully structured proteins). As shown in Figure 3, the S^2 values for the protein are non-uniformly distributed, ranging between 0.2 and 0.5, which is typical for flexible protein regions. The S^2 values characteristic for well-folded proteins, in contrast, are found in the range between 0.8 and 0.9. The non-uniform distribution of the S^2 values, however, is indicative for residual structural elements. The presence of residual structure is also reflected in the $[^{1}H,^{15}N]$-NOEs ratios, most of which range between −0.2 and 0.5, due to a variable degree of structural restrictions. Typical random coil elements in proteins in comparison have heteronuclear NOE ratios, which are either negative or close to zero.

Model-free analysis requires an estimation of the rotational correlation time as an input. For globular structured proteins, this parameter is usually estimated using residues from the most structured part of the protein with low intra-molecular mobility. In the case of the ClC-0 domain we lack access to those reference residues due to exceptionally broad lines of the resonances stemming from the folded regions. The rotation correlation time of 30 ns used for calculating the order parameters S^2 was instead derived from the translation diffusion rates of the protein measured at 7 °C with pulse field gradient NMR methods.[21] The corresponding diffusion constant of 4.8×10^{-7} cm^2s^{-1} is in good agreement with

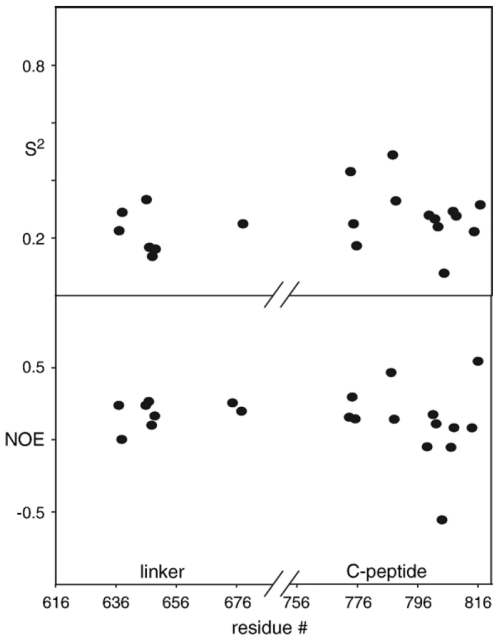

Figure 3. Generalized order parameter S^2 and heteronuclear NOEs. Generalized order parameters were obtained from backbone ^{15}N relaxation data using the program Modelfree 4.15.[30,31] An isotropic model was used with the assumed correlation time of τ_c=30 ns. The correlation time was estimated from translational diffusion measurements obtained with pulse field gradient NMR methods.[21] The molecular mass was calculated from the diffusion constant at 7 °C according to Dingley *et al.*[32,33] using the shape of the dimeric structure modeled from the monomeric crystal structure of the ClC-O domain. Relaxation data could be successfully modeled using the two parameters, S^2 and τ_e. Relaxation experiments were acquired using standard TROSY-based pulse sequences[34] at 7 °C on a Bruker Avance 600 MHz spectrometer. Estimates for R_1 and R_2 values were obtained using a non-linear least-squares fitting of a two-parameter mono-exponential function to the measured peak intensities. τ_e values obtained from the model-free analysis range between 200 ps and 600 ps with and average value of 349 ps. Model-free analysis is reported for 20 residues that had an error estimate for the three input relaxation rates (T_1, T_2 and HNOE) of less than 10%. The fitting errors for S^2 were between 0.005 and 0.052 with an average error of 0.008.

the geometry and size of the dimeric structure of the protein with a molecular mass of 66 kDa as determined by analytical ultracentrifugation.[4] The resulting Lipari & Szabo model satisfactorily explained the experimental values of ^{15}N T_1, T_2 as well as the NOEs.

Since no additional line broadening terms due to conformational dynamics in the microsecond to millisecond time scale were needed to fit the relaxation data, we conclude that this type of dynamics, if present at all, does not significantly contribute to the observed line widths. Most probably the transient inter-conversion in the ensemble of conformations suggested by the low-order parameters proceeds in the nanosecond or lower microsecond time scale, which is only partially detectable by ^{15}N relaxation analysis. However, the presence of motions in the flexible stretches of the ClC-0 domain that are faster than the rotational correlation time or slower than the chemical shifts time scale and therefore escape the detection due to the insensitivity of ^{15}N relaxation cannot be excluded. In a similar case, dynamical behavior in the picosecond to nanosecond time range that extends to the microsecond range was revealed by the Lipari & Szabo analysis of ^{15}N relaxation data from the trimeric chorismate mutase from *Bacillus subtilis*.[22]

The measurement of the backbone dynamics support the general picture of the disordered parts of the ClC-0 domain obtained from the previous experiments, with both regions being very flexible on a fast (ns) timescale with residual structural elements in some parts of the protein chain, which cause a deviation from random coil behavior.

Conclusions

Here we have characterized the disordered regions of the cytoplasmic domain of the Cl^- channel ClC-0 by NMR spectroscopy. The experiments revealed that the two large sections of the protein, the linker and the C-peptide, which were unstructured in a recent crystal structure, show large conformational heterogeneity and fast dynamics on a nanosecond time scale. Scattered within the flexible protein segments, it was possible to assign regions with high structural propensities. The stretches of local secondary structure within disordered regions have been described for other proteins where they serve as nucleation points for folding upon interaction with other proteins.[1] It is currently not clear whether they have a similar purpose in the ClC family. Although, the role of the two disordered protein regions in the cytoplasmic domains is currently still not understood, mutations were shown to have significant effects on channel function and on the interaction with regulatory proteins. It has been shown for instance that the disordered regions for the ClC-2 cytoplasmic domain are responsible for kinase-dependent activation of the channel.[12] It appears that natively disordered protein regions turn out to play an important role in the functional regulation of the ClC proteins, a family of important Cl^- transport molecules whose physiological mechanisms are still only poorly understood.

Acknowledgements

The work was supported by grants funded *via* ETH Zurich and the Swiss National Science

Foundation (to K.P.) and by a grant from the Swiss National Science Foundation (to R.D.).

Supplementary Data

Supplementary data associated with this article can be found, in the online version, at doi:10.1016/j.jmb.2007.04.020

References

1. Dyson, H. J. & Wright, P. E. (2005). Intrinsically unstructured proteins and their functions. *Nature Rev. Mol. Cell Biol.* **6**, 197–208.
2. Fink, A. L. (2005). Natively unfolded proteins. *Curr. Opin. Struct. Biol.* **15**, 35–41.
3. Jentsch, T. J., Neagoe, I. & Scheel, O. (2005). ClC chloride channels and transporters. *Curr. Opin. Neurobiol.* **15**, 319–325.
4. Meyer, S. & Dutzler, R. (2006). Crystal structure of the cytoplasmic domain of the chloride channel ClC-0. *Structure*, **14**, 299–307.
5. Dutzler, R. (2006). The ClC family of chloride channels and transporters. *Curr. Opin. Struct. Biol.* **16**, 439–446.
6. Duffield, M. D., Rychkov, G. Y., Bretag, A. H. & Roberts, M. L. (2005). Zinc inhibits human ClC-1 muscle chloride channel by interacting with its common gating mechanism. *J. Physiol.* **568**, 5–12.
7. Ward, J. J., Sodhi, J. S., McGuffin, L. J., Buxton, B. F. & Jones, D. T. (2004). Prediction and functional analysis of native disorder in proteins from the three kingdoms of life. *J. Mol. Biol.* **337**, 635–645.
8. Yang, Z. R., Thomson, R., McNeil, P. & Esnouf, R. M. (2005). RONN: the bio-basis function neural network technique applied to the detection of natively disordered regions in proteins. *Bioinformatics*, **21**, 3369–3376.
9. Schwake, M., Friedrich, T. & Jentsch, T. J. (2001). An internalization signal in ClC-5, an endosomal Cl-channel mutated in dent's disease. *J. Biol. Chem.* **276**, 12049–12054.
10. He, L., Denton, J., Nehrke, K. & Strange, K. (2006). Carboxy terminus splice variation alters ClC channel gating and extracellular cysteine reactivity. *Biophys. J.* **90**, 3570–3581.
11. Beck, C. L., Fahlke, C. & George, A. L., Jr (1996). Molecular basis for decreased muscle chloride conductance in the myotonic goat. *Proc. Natl Acad. Sci. USA*, **93**, 11248–11252.
12. Cuppoletti, J., Tewari, K. P., Sherry, A. M., Ferrante, C. J. & Malinowska, D. H. (2004). Sites of protein kinase A activation of the human ClC-2 Cl(-) channel. *J. Biol. Chem.* **279**, 21849–21856.
13. Denton, J., Nehrke, K., Yin, X., Morrison, R. & Strange, K. (2005). GCK-3, a newly identified Ste20 kinase, binds to and regulates the activity of a cell cycle-dependent ClC anion channel. *J. Gen. Physiol.* **125**, 113–125.
14. Buck-Koehntop, B. A., Mascioni, A., Buffy, J. J. & Veglia, G. (2005). Structure, dynamics, and membrane topology of stannin: a mediator of neuronal cell apoptosis induced by trimethyltin chloride. *J. Mol. Biol.* **354**, 652–665.
15. Pervushin, K., Riek, R., Wider, G. & Wuthrich, K. (1997). Attenuated T-2 relaxation by mutual cancellation of dipole-dipole coupling and chemical shift anisotropy indicates an avenue to NMR structures of very large biological macromolecules in solution. *Proc. Natl Acad. Sci. USA*, **94**, 12366–12371.
16. Gronwald, W., Willard, L., Jellard, T., Boyko, R. E., Rajarathnam, K., Wishart, D. S. *et al.* (1998). CAMRA: Chemical shift based computer aided protein NMR assignments. *J. Biomol. NMR*, **12**, 395–405.
17. Hansen, M. R., Mueller, L. & Pardi, A. (1998). Tunable alignment of macromolecules by filamentous phage yields dipolar coupling interactions. *Nature Struct. Biol.* **5**, 1065–1074.
18. Alexandrescu, A. T. & Kammerer, R. A. (2003). Structure and disorder in the ribonuclease S-peptide probed by NMR residual dipolar couplings. *Protein Sci.* **12**, 2132–2140.
19. Sallum, C. O., Martel, D. M., Fournier, R. S., Matousek, W. M. & Alexandrescu, A. T. (2005). Sensitivity of NMR residual dipolar couplings to perturbations in folded and denatured staphylococcal nuclease. *Biochemistry*, **44**, 6392–6403.
20. Lipari, G. & Szabo, A. (1982). Model-free approach to the interpretation of nuclear magnetic-resonance relaxation in macromolecules. 1. Theory and range of validity. *J. Am. Chem. Soc.* **104**, 4546–4559.
21. Orekhov, V. Y., Korzhnev, D. M., Pervushin, K. V., Hoffmann, E. & Arseniev, A. S. (1999). Sampling of protein dynamics in nanosecond time scale by N-15 NMR relaxation and self-diffusion measurements. *J. Biomol. Struct. Dynam.* **17**, 157–174.
22. Eletsky, A., Kienhofer, A., Hilvert, D. & Pervushin, K. (2005). Investigation of ligand binding and protein dynamics in Bacillus subtilis chorismate mutase by transverse relaxation optimized spectroscopy-nuclear magnetic resonance. *Biochemistry*, **44**, 6788–6799.
23. Masse, J. E. & Keller, R. (2005). AutoLink: automated sequential resonance assignment of biopolymers from NMR data by relative-hypothesis-prioritization-based simulated logic. *J. Magn. Reson.* **174**, 133–151.
24. Keller, R. (2004). *The Computer Aided Resonance Assignment Tutorial.* CANTINA Verlag, Goldau.
25. Salzmann, M., Pervushin, K., Wider, G., Senn, H. & Wuthrich, K. (1998). TROSY in triple-resonance experiments: new perspectives for sequential NMR assignment of large proteins. *Proc. Natl Acad. Sci. USA*, **95**, 13585–13590.
26. Salzmann, M., Wider, G., Pervushin, K., Senn, H. & Wuthrich, K. (1999). TROSY-type triple-resonance experiments for sequential NMR assignments of large proteins. *J. Am. Chem. Soc.* **121**, 844–848.
27. Talluri, S. & Wagner, G. (1996). An optimized 3D NOESY-HSQC. *J. Mag. Reson. ser.* **112**, 200–205.
28. Hansen, M. R., Mueller, L. & Pardi, A. (1998). Tunable alignment of macromolecules by filamentous phage yields dipolar coupling interactions. *Nat. Struct. Biol.* **5**, 1065–1074.
29. Pervushin, K., Wider, G. & Wuthrich, K. (1998). Single transition-to-single transition polarization transfer (ST2-PT) in [N-15,H-1]-TROSY. *J. Biomol. NMR*, **12**, 345–348.
30. Mandel, A. M., Akke, M. & Palmer, A. G. (1995). Backbone dynamics of *Escherichia-coli* ribonuclease Hi - correlations with structure and function in an active enzyme. *J. Mol. Biol.* **246**, 144–163.
31. Palmer, A. G., Rance, M. & Wright, P. E. (1991). Intramolecular motions of a zinc finger DNA-binding domain from Xfin characterized by proton-detected

natural abundance C-12 heteronuclear NMR-spectroscopy. *J. Am. Chem. Soc.* **113**, 4371–4380.
32. Dingley, A. J., Mackay, J. P., Shaw, G. L., Hambly, B. D. & King, G. F. (1997). Measuring macromolecular diffusion using heteronuclear multiple-quantum pulsed-field-gradient NMR. *J. Biomol. NMR*, **10**, 1–8.
33. Dingley, A. J., Mackay, J. P., Chapman, B. E., Morris, M. B., Kuchel, P. W., Hambly, B. D. & King, G. F. (1995). Measuring protein self-association using pulsed-field-gradient NMR-spectroscopy - application to myosin light-chain-2. *J. Biomol. NMR*, **6**, 321–328.
34. Zhu, G., Xia, Y. L., Nicholson, L. K. & Sze, K. H. (2000). Protein dynamics measurements by TROSY-based NMR experiments. *J. Mag. Reson.* **143**, 423–426.

Edited by A. G. Palmer 3rd

(Received 4 September 2006; received in revised form 19 March 2007; accepted 6 April 2007)
Available online 14 April 2007

2.1.5 Supplementary Material

Materials and Methods

NMR Spectroscopy NMR spectra were including two dimensional (2D) [^{1}H,^{15}N]-TROSY,[92] and 3D [^{1}H,^{15}N] TROSY-HNCA[93,94] and [^{1}H,^{1}H,^{15}N]-NOESY[95] (Figure S1) were recorded at 7 °C on a Bruker Avance 600 MHz spectrometer equipped with a cryogenic Z-gradient TXI probe and a Bruker Avance 900 MHz spectrometer. [^{1}H,^{15}N]-TROSY were acquired with 1024 complex points in the direct dimension (^{1}H) and 150 complex points in the indirect dimension (^{15}N) using 32 scans with a ^{2}H,^{15}N labeled protein sample. The TROSY-HNCA (Figure S1A) was recorded with 2048 points in the direct dimension (^{1}H), 128 points in the 15N dimension and 80 points in ^{13}C dimension using 8 scans with a ^{2}H,^{15}N,^{13}C-labeled sample. The ^{15}N-resolved [^{1}H,^{1}H] NOESY (Figure 1 B) was measured using the ^{2}H,^{15}N labeled sample with 1024 points in the direct dimension (^{1}H), 82 points in the ^{15}N dimension and 256 points in ^{1}H dimension and a mixing time of 200 ms. Relaxation experiments were acquired using standard TROSY based pulse sequences[96] at 7 °C on 600 MHz spectrometer. The relaxation delays used were 50, 125, 200, 275, 350, 425, 500, 575, 650, 725, 1000 and 1200 ms for longitudinal relaxation rate constant measurements (R1) and 0.5, 3,10, 18, 30, 45, 60, 81, 99 and 120 ms for spin-spin relaxation rate constant measurements (R2). Estimates for R1 and R2 values (Figure 3) were obtained using a non-linear least squares fitting of a two-parameter monoexponential function to the measured peak intensities. Generalized order parameters were obtained from backbone ^{15}N relaxation data using the program Modelfree 4.15.[97,98] An isotropic model was used with the assumed correlation time of τ_c = 30 ns. The correlation time was estimated from translational diffusion measurements, measured with pulse field gradient NMR methods, according to.[99] The molecular weight was calculated from the diffusion constant at 7 °C according to[100,101] using the shape of the dimeric structure modeled from the monomeric crystal structure of the ClC-O domain. Relaxation data could be successfully modeled using two parameters, S2 and τ_e. RDC data were obtained using ^{2}H,^{15}N labeled sample aligned with approximately 1 mM of Pf1 phages (Asla Biotech).[102,103] The couplings were measured using TROSY and ^{15}N-anti-TROSY spectra measured with and without Pf1 pages, recorded with 1024 points in the direct ^{1}H dimension and 300 points in the indirect ^{15}N dimension with 64 scans at 600 MHz. All spectra were transformed with XWIN-NMR (Brucker), the analysis of the spectral data was done with the software CARA.[104] For the assignment the automated

assignment program AutoLink[105] was used. The ^{1}H chemical shifts were referenced to 2,2 dimethyl-2-silapentane-5-sulfonate sodium salt (DSS).[106] The ^{13}C and ^{15}N chemical shifts were referenced indirectly using ^{13}C/^{1}H and ^{15}N/^{1}H gyro magnetic ratios.

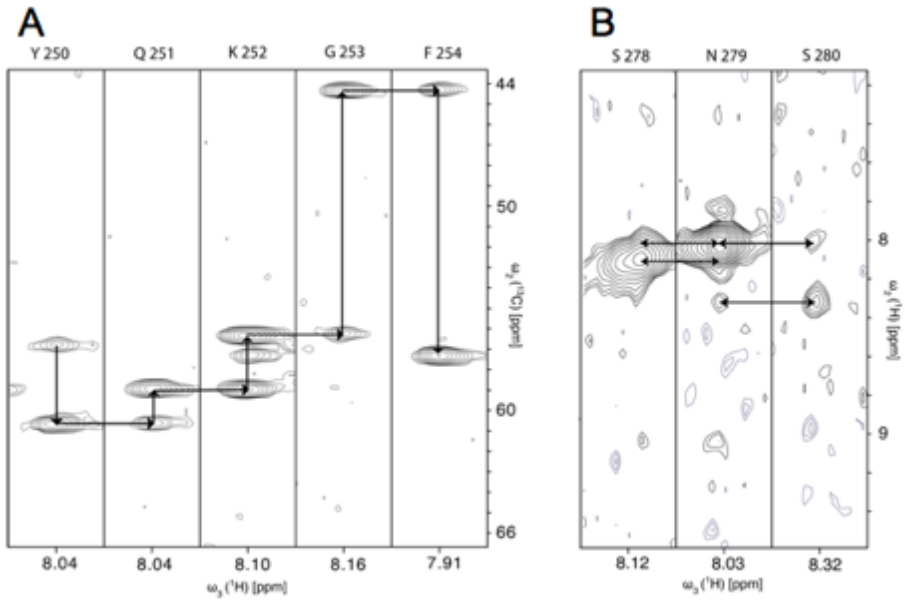

Figure S1: **NMR Spectra**
(A) 3D [^{1}H,^{15}N] TROSY-HNCA recorded with 2048 points in the direct dimension (^{1}H), 128 points in the 15^{N} dimension and 80 points in ^{13}C dimension using 8 scans with a ^{2}H,^{15}N,^{13}C-labeled sample. The sequential connectivity used for resonance assignment is indicated. (B) ^{15}N-resolved [^{1}H,^{1}H] NOESY was measured using the ^{2}H,^{15}N labeled sample with 1024 points in the direct dimension (^{1}H), 82 points in the ^{15}N dimension and 256 points in ^{1}H dimension and a mixing time of 200 ms. The intra-residue NOEs are indicated for this short sequence fragments.

Protein Expression and Purification The construct of the ClC-0 cytoplasmic domain contains the residues 525-805 of ClC-0 from *Torpedo marmorata* in the pET28-b(+) expression vector (Novagen). Transformed *E. coli* BL21(DE3) cells were grown at 37 °C in Silantes OD2 medium (^{2}H, ^{15}N labeled #105202 or ^{2}H, ^{13}C, ^{15}N labeled #107202) with 50 mg/l kanamycin to an OD_{600} of 1.0. Expression was induced by addition of 0.5 mM of isopropyl-D-thiogalactopyranoside (IPTG) and proceeded overnight at 20 °C. Harvested cells were lysed by sonication in 50 mM Tris-HCl (pH 7.5), 150 mM NaCl, 5 mM MgCl2, 5 mM β-mercapto-ethanol, 200 mg/l lysozyme, 20 mg/l DNase, leupeptin, pepstatin and 1 mM phenylmethyl sulphonyl fluoride. The lysate was cleared by centrifugation and loaded onto a Ni-affinity column (Chelating Sepharose, Pharma-

cia Biotech). The column was washed with buffer containing 15 mM imidazole and the pure protein eluted with 300 mM imidazole. The protein was dialysed in buffer without imidazole and concentrated to a concentration of 400 μM for subsequent measurements. The measurements were performed in 10 mM Tris (pH 7.5), 150 mM NaCl, 5 mM $MgCl_2$ and 5 mM β-mercapto-ethanol. The protein was found to be stable in solution at 7 °C during the course of the experiment.

2.2 The Cytoplasmic Domain of Human ClC-5

2.2.1 Introduction

The structure of the cytoplasmic domains of ClC-0 showed the structural arrangement of the CBS tandem in ClC proteins that is likely to be conserved in the family. The structure, however, does not account for a number of aspects associated with the intracellular domains like the interaction with adenosine nucleotides or the dimeric assembly of the C-termini from two subunits.

Compared to this, the cytoplasmic domains of chloride transporter ClC-5 vary in parts considerably from the previously described regions in ClC-0. Although the conservation of the CBS subdomains is substantial, the extended linker region and C-peptide are considerably shorter in ClC-5. The importance of the intracellular domains is also in this case illustrated by a number of mutations in this region that lead to Dent's disease.[46] Unique in the ClC family, the linker between the two CBS subdomains in ClC-5 contains a PY motif that has been shown to be important for regulating the surface expression of the transporter via ubiquitination.[81]

ClC-5 is expressed mainly in the proximal tubule of the kidney.[19] The malfunction of this protein in humans is associated with Dent's disease, a recessive X-linked nephrolithiasis.[44] On the subcellular level ClC-5 resides in endosomal membranes but has been described to reach the plasma membrane upon heterologous expression.[19] Whether ClC-5 also shuttles to the plasma membrane under physiological conditions is not clear. When studied on the plasma membrane of heterologously expressing *Xenopus* oocytes the transporter exhibits strong outward rectifying currents. Similar to the ClC homolog from *E.coli*, ClC-5 was found to transport protons by exchanging them for chloride ions as a secondary active chloride proton antiporter.[25,26] The contribution of chloride and protons to the overall charge movement is estimated to be equal, suggesting a significance of this process *in vivo*.[26] The recent advances in the elucidation of ClC-5 function on the molecular level have rather obscured the picture of the physiological role of this protein in the kidney. On one hand, the symptom of low molecular weight proteinuria in Dent's disease patients suggests a role of ClC-5 in endocytosis.[45] On the other hand, it has been shown that the knock out of ClC-5 in mice leads to a reduced acidification of vesicles in the endosomal/lysosomal pathway.[44] In this process ClC-5 had been thought to act as a shunt for chloride ions preventing the building up of large electric potentials by the V-type ATPase across the vesicular membrane. Thus, this function appears not to be consistent with the recently discovered transporter function and the strong rectification

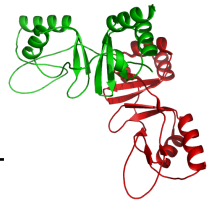

of the observed plasma membrane currents.

2.2.2 Nucleotide Recognition by the Cytoplasmic Domain of the Human Chloride Transporter ClC-5

Aim of the Study The structure of the cytoplasmic domain of ClC-0 left a number of open questions that could potentially be addressed by the structural and biochemical analysis of the cytoplasmic domains of ClC-5. The dimer assembly of the C-terminal domains from the two subunits was to be confirmed via analytical ultracentrifugation and possibly resolved by native contacts in the crystal. The interaction of the domains with adenosine ligands was to be assessed using binding assays, co-crystallization and electrophysiolological experiments.

nature structural & molecular biology

Nucleotide recognition by the cytoplasmic domain of the human chloride transporter ClC-5

Sebastian Meyer[1], Sara Savaresi[1], Ian C Forster[2] & Raimund Dutzler[1]

The ubiquitous CBS domains, which are found as part of cytoplasmic domains in the ClC family of chloride channels and transporters, have previously been identified as building blocks for regulatory nucleotide-binding sites. Here we report the structures of the cytoplasmic domain of the human transporter ClC-5 in complex with ATP and ADP. The nucleotides bind to a specific site in the protein. As determined by equilibrium dialysis, the affinities for ATP, ADP and AMP are in the high micromolar range. Point mutations that interfere with nucleotide binding change the transport behavior of a ClC-5 mutant expressed in *Xenopus laevis* oocytes. Our results establish the structural and energetic basis for the interaction of ClC-5 with nucleotides and provide a framework for future investigations.

The ClC proteins constitute a large and physiologically important family of Cl^- transport proteins. They are ubiquitously expressed and function as either Cl^--selective ion channels or secondary active Cl^- transporters[1]. The overall architecture of the family is conserved and consists of a transmembrane catalytic domain followed by a cytoplasmic putative regulatory domain[2]. The proteins are homodimers, with each subunit containing an independent ion-translocation path[3]. The transmembrane region harbors specific Cl^--binding sites that are located in the center of the membrane and are arranged to connect the two aqueous vestibules approaching the binding sites from the extra- and intracellular solution[4]. The cytoplasmic component of the protein contains two CBS subdomains, which are present in all eukaryotic family members. These small protein motifs were named after the enzyme cystathionine β-synthetase and are frequently found as building blocks for regulatory nucleotide-binding domains in kinases and enzymes[5,6]. In this structural organization, the location of the cytoplasmic domains with respect to the ion-translocation path is noteworthy, as they are connected to a helix (the R-helix) that contributes a residue to one of the specific ion-binding sites, suggesting that they are important in the regulation of ion transport[3].

Several studies have reported a regulation of certain ClC family members by nucleotide binding to their cytoplasmic domains[7–10]. The most detailed studies have so far been carried out on the voltage-dependent chloride channel ClC-1, where the presence of ATP has been shown to stabilize the closed state of the channel by shifting channel opening to more positive voltages[8]. The only experimental information on the structure of the cytoplasmic domains of ClC family members known so far has been revealed from the crystal structure of the domain of ClC-0, a chloride channel from the *Torpedo marmorata* electric ray and close homolog of the muscle channel ClC-1 (ref. 11). In this structure, the two CBS subdomains (named CBS1 and CBS2) in one polypeptide chain interact tightly to form a well-ordered structural core. However, neither cocrystallization experiments in the presence of ATP nor binding assays using radioactively labeled ATP have shown any evidence of specific interactions of the protein with nucleotides.

As ClC-0 appears to lack nucleotide dependence, we have investigated the nucleotide-binding properties of the human transporter ClC-5 to gain insight into the mechanism of nucleotide regulation of ClC function. We have determined the structures of the cytoplasmic domain of ClC-5 in complex with ATP and ADP by X-ray crystallography. The structures show a single nucleotide bound in a deep cleft of the protein in the interface between the two CBS subdomains. In ligand-binding experiments using equilibrium dialysis, we have determined the binding affinities of the domains for the nucleotides ATP, ADP and AMP. All three ligands bind with K_ds of about 100 μM. Mutations of certain residues interacting with the nucleotide abolish binding. The transport behavior of these mutants, as measured by electrophysiology, was unchanged. This may be due to the fact that human ClC-5 is not in its fully activated state when expressed in *Xenopus* oocytes, while the regulatory effects might be revealed only in the activated protein[12]. Indeed, when we tested the same mutations in the background of a mutant that does not transport H^+ but conducts Cl^- ions in a broad voltage range, we found that the failure to bind nucleotides correlates with a marked decrease of ion flow at negative voltages, suggesting a regulatory influence of nucleotide binding on ion transport.

RESULTS

The structure of the ClC-5 ligand-binding domain

To gain insight into nucleotide binding to the regulatory domains of ClC proteins, we expressed the cytoplasmic component of the human

[1]Department of Biochemistry and [2]Institute of Physiology, University of Zurich, Winterthurer Strasse 190, CH-8057 Zurich, Switzerland. Correspondence should be addressed to R.D. (dutzler@bioc.unizh.ch).

Received 26 July; accepted 6 December; published online 31 December 2006; corrected after print 19 January 2007; doi:10.1038/nsmb1188

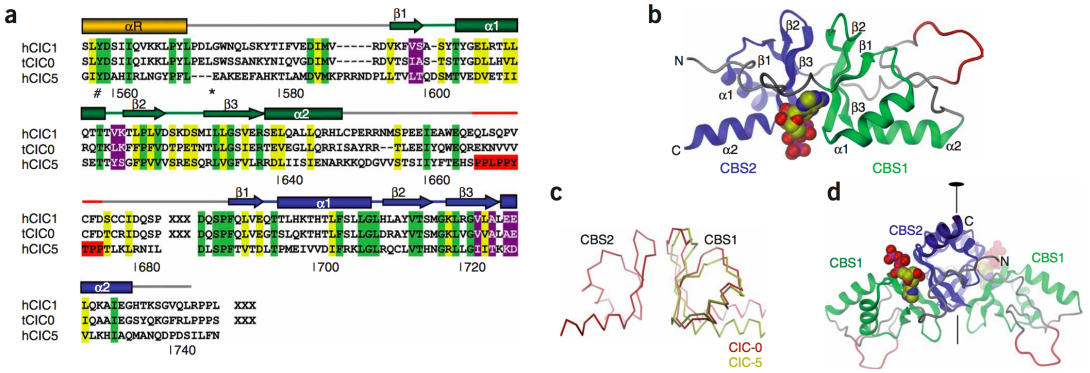

Figure 1 Structure of the ClC-5 domain. (**a**) Structure-based sequence alignment of the cytoplasmic domains of the Cl^- channels ClC-1 and ClC-0 and the Cl^- transporter ClC-5. Identical residues are highlighted in green, similar residues in yellow, residues involved in ATP binding in violet and the recognition sequence for ubiquitin ligase (ClC-5) in red. Secondary structure and numbering (ClC-5) are indicated above and below the sequences, respectively. The R-helix with the Cl^--coordinating tyrosine residue (#) preceding the domains is included in the alignment. The linker sequence between the two CBS domains and the C terminus in ClC-0 and ClC-1 have been omitted (XXX). The first residue of the crystallized construct is highlighted (*). h, *H. sapiens*; t, *T. marmorata*; hClC-5, GenBank 116734718; tClC-0, GenBank X56758; hClC-1, GenBank M97820. (**b**) Ribbon representation of the ClC-0 domain. The two CBS subdomains are colored in green and blue, respectively; residues of the ubiquitin ligase recognition sequence are colored in red. The bound ATP molecule is shown as CPK model. (**c**) Relative arrangement of CBS domains in ClC-5 (yellow) and ClC-0 (red). For the ClC-0 arrangement, the two CBS subdomains of ClC-5 were superimposed on their respective counterparts in ClC-0. (**d**) Dimeric organization of two cytoplasmic domains of ClC-5 (colored as in **a**), as observed in the crystal structure. The ATP molecule is shown as CPK model. Two-fold axis of symmetry is indicated. All structure images were prepared with DINO (http://www.dino3d.org).

transporter ClC-5. The construct encompasses residues 571 to 746, from the start of the domain to the C terminus of the native protein, and contains a protease recognition site and a His_6 tag, which was cleaved during purification. Sedimentation velocity experiments of the purified protein show a monomer-dimer equilibrium that is not perturbed by the addition of 5 mM ATP (**Supplementary Fig. 1** online). As for ClC-0 (ref. 11), the sedimentation properties hint at a weak but specific interaction between protein chains, most probably reflecting the dimeric organization of the domains when attached to the channel. The domains are highly conserved within the sub-branch including ClC3, ClC-4 and ClC-5 (with 63% sequence identity) and are more distantly related to other family members, such as the channels ClC-0 and ClC-1 (with a sequence similarity of 50% and 42% for the two CBS subdomains, respectively) (**Fig. 1a**). The largest difference between the ClC-5 and the ClC-0 domain is found in the linker region and in the C-peptide that follows the CBS subdomains; both are shorter in ClC-5. Our construct allowed us to grow crystals in the presence of ATP that diffract to 2.3-Å resolution. In contrast, no well-diffracting crystals were obtained in the absence of nucleotides. The structure was determined by MAD with data collected from crystals of protein grown in minimal medium containing selenomethionine (SeMet) and crystallized with addition of ATP. The experimental electron density allowed unambiguous tracing of the protein and revealed the presence of an ATP molecule bound to a single site in each protein chain (**Fig. 1b** and **Supplementary Fig. 2** online). In the asymmetric unit, three pairs of two-fold–related protein chains are packed in an approximately three-fold arrangement perpendicular to the two-fold axes. The six copies of the protein are similar in structure but with variation in electron density quality, probably owing to local differences in the crystal packing. **Figure 1b** shows a ribbon representation of the ClC-5 domain. The entire protein is ordered, including the linker region between the CBS subdomains. This linker region contains a recognition motif for the regulatory protein-ubiquitin ligase WWP2 that projects away from the two CBS subdomains in such a way as to be accessible[13] (**Fig. 1b**). Despite the modest conservation between ClC-5 and ClC-0, the core structures encompassing the two CBS subdomains are similar (~1 Å r.m.s. deviation between subdomain counterparts). The relative orientations of the subdomains, however, differs somewhat (**Fig. 1c**), resulting in a rigid body rotation of about 15° (with backbone atom movements up to 8 Å).

As ClC proteins are homodimers related by two-fold symmetry, the dimeric relationship of ClC-5 domains in the asymmetric unit of the crystals is noteworthy (**Fig. 1d**). In this structural arrangement, an extended interface is formed, predominantly between the CBS2 subdomains of both chains. This interaction buries 1,600 $Å^2$ of the protein surface and orients the two protein chains with a mutual inclination of about 120°. Notably, several of the buried residues are conserved among different family members. The largest parts of the two CBS1 subdomains are distant and not involved in interactions with residues of the other chain. This novel two-fold relationship has not yet been observed for a CBS-containing protein and differs from an arrangement proposed for the cytoplasmic domain of ClC-0, which was based on the dimeric structure of a prokaryotic CBS subdomain–containing protein[11]. Both the previously proposed interaction modes and that seen here present possible models for the quaternary organization of the cytoplasmic component of ClC proteins. The intersubunit organization therefore remains ambiguous and will have to be clarified in future studies.

Structural features of nucleotide recognition

ATP binds in a cleft at the interface of the two CBS subdomains, with the base deeply embedded in the binding site and the entire molecule specifically interacting with residues of both halves of the protein (**Fig. 2a**). The adenine base is stabilized in a predominantly

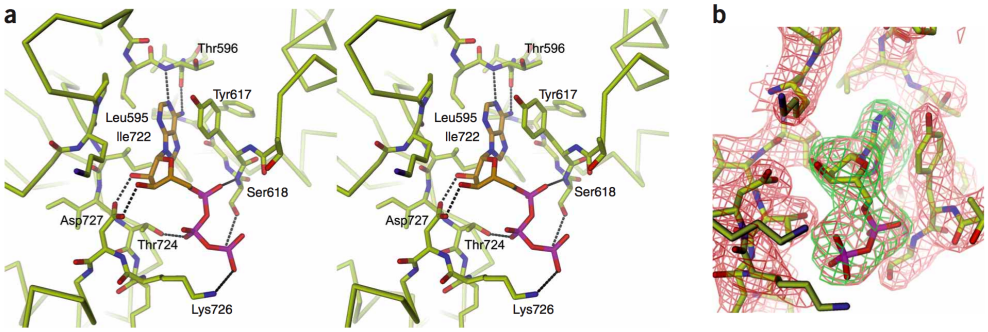

Figure 2 Structure of the nucleotide-binding site. (**a**) Stereo view of the nucleotide-binding site. Protein main chain is shown as Cα trace, colored as in **a**, with selected residues near the bound ATP molecule shown as sticks. Dashed lines denote hydrogen bonds between protein and nucleotide. Selected protein residues in contact with ATP are labeled. (**b**) Electron density of the ClC-5 domain–ADP complex. $2F_o - F_c$ omit map (calculated with phases from the refined protein without nucleotides) is shown contoured at 1 σ and colored in brown; $F_o - F_c$ difference density (calculated with the same set of phases) is contoured at 3 σ and colored in green. ADP and selected residues of protein are shown as sticks.

hydrophobic binding pocket via stacking interactions with a tyrosine residue on one face and by contacting aliphatic side chains of an isoleucine and a leucine residue on its other face. A pair of hydrogen bonds of the 6′-amino group and the 1′-aza group with the protein backbone ensures specificity for adenine over the structurally related guanine base. The two free hydroxyl groups of the ribose moiety are hydrogen-bonded to the side chain carboxyl of an aspartate residue, and all three phosphates are interacting with protein residues: the α-phosphate with the protein backbone, the β-phosphate with the hydroxyl of a threonine residue and the γ-phosphate with the side chains of a lysine and a serine residue. As the three phosphate groups of the ATP molecule are partly exposed to solvent and located at the periphery of the binding site, it appears likely that the related nucleotides ADP and AMP bind in very similar modes. Indeed, a bound nucleotide was also seen in the crystal form of the domain grown in the presence of ADP. The nucleotide there is bound in a virtually identical conformation, without appreciable changes in the protein structure (**Fig. 2b**). In a comparison of the equivalent residues involved in nucleotide binding between ClC proteins, a strong conservation within the sub-branch including ClC-3, ClC-4 and ClC-5 is apparent, whereas there is only moderate conservation with more distantly related family members (**Fig. 1a**).

The energetics of nucleotide binding

To investigate the energetics and the selectivity of ligand recognition quantitatively, we studied the binding of radioactively labeled adenine nucleotides by equilibrium dialysis. The three structurally related nucleotides ATP, ADP and AMP were found to bind the ClC-5 domain in a Mg^{2+}-independent manner, with binding constants around 100 μM (**Fig. 3a–c**). In all three cases, the Scatchard plot intercepts at a ratio close to 1, indicating that all of the protein chains bind a single nucleotide molecule. The lack of discrimination among the substrate nucleotides, which was confirmed in competitive binding assays, is comparable to data measured for the CBS domains of the enzyme AMPK and other CBS domain–containing proteins[6] (**Fig. 3d**). The binding is specific for adenosine nucleotides, as neither GTP nor cAMP compete with ATP binding (**Supplementary Fig. 3** online). The data suggests that the bulk of the binding energy is contributed by the adenosine moiety, whereas the β- and γ-phosphate groups have a negligible influence. The structure of the nucleotide complex allowed us to design point mutations with altered nucleotide-binding properties. The point mutation Y617A, which truncates the side chain involved in stacking interactions with the adenine base, and the mutation D727A, which removes the side chain interactions with the two hydroxyl groups of the ribose moiety, both virtually abolish ATP binding (**Fig. 3e**). In contrast, the mutation S618A, which removes the interaction of the side chain with the γ-phosphate, does not alter the binding affinity, consistent with the previous observation that the interactions with the phosphate groups contribute little to binding (**Fig. 3f**). In all three cases, the side chain of the mutated residue is not interacting with other parts of the protein, ensuring that the protein structure is not perturbed by the mutation. Indeed, all three mutants show a similar biochemical behavior to that of the wild-type (WT) protein. The three mutants are therefore valuable tools for the investigation of possible regulatory mechanisms of ClC-5.

The effect of nucleotide binding on ClC-5 function

To study the influence of nucleotide binding on function, we measured ion transport through human ClC-5 expressed in *Xenopus* oocytes by two-electrode voltage-clamp recording. **Figure 4a** shows the current-voltage relationship of ClC-5 with voltages ranging from +100 to –100 mV. The current is outwardly rectifying, which means that ions essentially flow only in one direction at very positive voltages (with Cl^- ions flowing into the cell)[12]. The current is selective for Cl^- over I^- (**Supplementary Fig. 4** online) and decreases in amplitude when pH is decreased. This decrease is expected, because ClC-5 is a H^+-coupled Cl^- exchanger and the driving force for transport is decreased when the pH is lowered (**Fig. 4a**).

By studying the ClC-5 mutants Y617A and E727A, we wanted to investigate how the functional behavior of the transporter changes when nucleotide binding is compromised. Remarkably, the currents of both mutants were indistinguishable from WT currents, as was the current mediated by the mutant S618A (**Fig. 4b,c**). Although our results do not exclude the possibility that ATP binding physiologically does not affect ClC-5 function, it seems more likely that the protein expressed in *Xenopus* oocytes is not fully activated and the functional modulation is hidden in the wide voltage range over which ClC-5 does not conduct ions. As the domains are located near the intracellular entry of the Cl^- transport pathway, the largest effect on transport

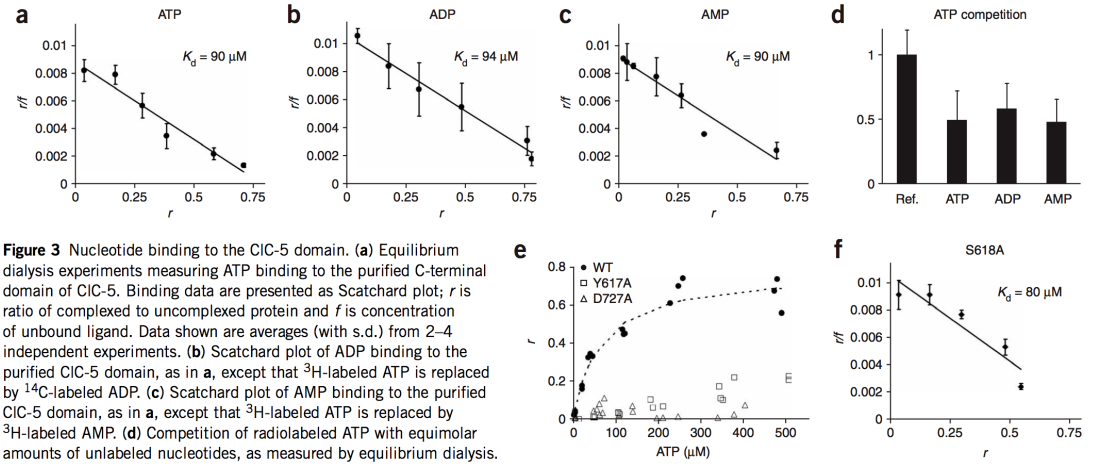

Figure 3 Nucleotide binding to the ClC-5 domain. (**a**) Equilibrium dialysis experiments measuring ATP binding to the purified C-terminal domain of ClC-5. Binding data are presented as Scatchard plot; *r* is ratio of complexed to uncomplexed protein and *f* is concentration of unbound ligand. Data shown are averages (with s.d.) from 2–4 independent experiments. (**b**) Scatchard plot of ADP binding to the purified ClC-5 domain, as in **a**, except that ^{3}H-labeled ATP is replaced by ^{14}C-labeled ADP. (**c**) Scatchard plot of AMP binding to the purified ClC-5 domain, as in **a**, except that ^{3}H-labeled ATP is replaced by ^{3}H-labeled AMP. (**d**) Competition of radiolabeled ATP with equimolar amounts of unlabeled nucleotides, as measured by equilibrium dialysis. Data shown are normalized and compared to a reference (without competing ligand). Averages from three independent experiments are shown with s.d. (**e**) Diminished nucleotide binding to binding site mutants. ATP binding to the mutants D727A and Y617A, compared with the WT ClC-5 domain, as in **a**. Data are plotted as ratio of complexed to uncomplexed protein against concentration of free ligand. Data points represent measurements from individual dialysis chambers. For the WT domain, a fit of the data is shown. (**f**) Scatchard plot of ATP binding to the purified ClC-5 S618A domain, as in **a**.

owing to changes in the domain conformation is expected to be observed when Cl^- ions are entering the binding sites from the cytoplasm. We therefore studied the same mutations in the background of the mutant E211A, which does not transport H^+ but conducts Cl^- ions in a wide voltage range. Equivalent mutants of other family members have been well characterized; the mutation removes gating in the channels and H^+ transport in the transporters without changing the overall structure of the protein, thereby converting both channels and transporters into passive, predominantly open Cl^- conductors[4,14–17]. In the presence of this mutation, we observed large changes in the functional behavior of the transporter. Whereas the ClC-5 mutant E211A shows a nearly linear current-voltage relationship over a broad voltage range, the currents of the nucleotide-binding-deficient double mutants E211A Y617A and E211A D727A markedly decrease at negative voltages, particularly when the direction of the current changes and Cl^- ions flow out of the cell (**Fig. 4d,e**). This phenotype in the current-voltage relationship was observed only for mutants incapable of binding nucleotides, whereas mutants with unchanged nucleotide-binding properties, such as E211A S618A, behaved similarly to the single mutant E211A (**Fig. 4e**). These results strongly suggest that the change is specifically due to the interference with nucleotide binding, and they hint that the ligand induces a conformational change in the protein.

DISCUSSION

A model for regulatory nucleotide-binding sites

The binding of ligands like ATP, ADP and AMP is used by certain proteins for the regulation of catalytic function in response to changes in the local nucleotide concentration[18]. This kind of regulation has also been suggested for members of the ClC family of chloride channels and transporters[7–10]. All eukaryotic ClC proteins contain cytoplasmic components composed of pairs of interacting CBS subdomains, which are also found as building blocks for regulatory nucleotide-binding domains of kinases and enzymes[5]. To gain insight into the structural and energetic basis of nucleotide recognition in the ClC family, we have determined the structure of the cytoplasmic domain of the human transporter ClC-5. This domain has recently been suggested to bind ATP without catalyzing its hydrolysis[10]. Our structure reveals a single molecule of ATP bound to a specific site of the protein, in the interface between the two CBS subdomains. This site is located on the opposite face of the molecule with respect to a previously proposed binding site in ClC-1 and other CBS-containing proteins[8,19]. ATP interacts in an unusual orientation, with the base being deeply buried in a mainly hydrophobic pocket in the protein. The site differs from catalytic ATP-binding sites constructed by conserved P-loop and Walker A and B motifs, which usually bind the nucleotide in a Mg^{2+}-dependent manner, with the phosphate moieties tightly interacting with the protein[20]. Although the specificity for adenosine nucleotides is ensured by hydrogen-bonding to the adenine base, the interaction is nondiscriminatory among ATP, ADP and AMP; all three nucleotides bind to the same site with K_ds of about 100 µM. The similar affinities underline the predominant contribution of the adenosine moiety to the binding affinity. With this structural information in hand, we can now start to explore possible mechanisms for the influence of ligand binding on the function of ClC-5.

Possible mechanisms of regulation

Ligand-dependent regulation of transport in channels and transporters commonly involves the transduction of conformational changes, induced by ligand binding, from the regulatory domains to the transmembrane catalytic domains[21]. The structure of the ClC-5 domain and its interactions in the crystal offer noteworthy insight into possible regulatory mechanisms. The difference in the arrangement of the two CBS subdomains in ClC-0 and ClC-5 (**Fig. 1c**) could represent a structural change upon ligand binding. The mode of dimerization of the cytoplasmic domains in the context of the full-length transporter is still ambiguous. However, it is interesting to compare the arrangement we observed in the crystals, which has proper two-fold symmetry, with a previously postulated arrangement,

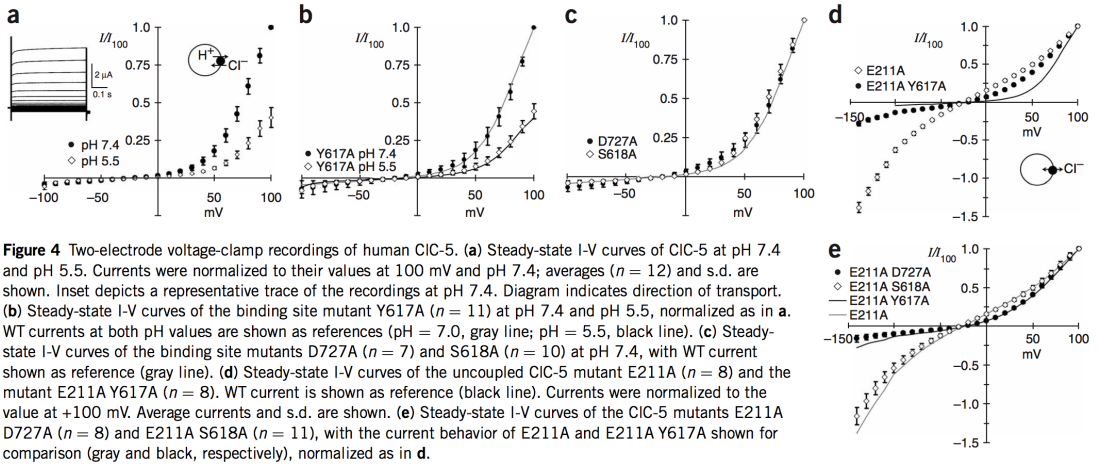

Figure 4 Two-electrode voltage-clamp recordings of human ClC-5. (**a**) Steady-state I-V curves of ClC-5 at pH 7.4 and pH 5.5. Currents were normalized to their values at 100 mV and pH 7.4; averages ($n = 12$) and s.d. are shown. Inset depicts a representative trace of the recordings at pH 7.4. Diagram indicates direction of transport. (**b**) Steady-state I-V curves of the binding site mutant Y617A ($n = 11$) at pH 7.4 and pH 5.5, normalized as in **a**. WT currents at both pH values are shown as references (pH = 7.0, gray line; pH = 5.5, black line). (**c**) Steady-state I-V curves of the binding site mutants D727A ($n = 7$) and S618A ($n = 10$) at pH 7.4, with WT current shown as reference (gray line). (**d**) Steady-state I-V curves of the uncoupled ClC-5 mutant E211A ($n = 8$) and the mutant E211A Y617A ($n = 8$). WT current is shown as reference (black line). Currents were normalized to the value at +100 mV. Average currents and s.d. are shown. (**e**) Steady-state I-V curves of the ClC-5 mutants E211A D727A ($n = 8$) and E211A S618A ($n = 11$), with the current behavior of E211A and E211A Y617A shown for comparison (gray and black, respectively), normalized as in **d**.

with respect to nucleotide binding[11] (**Fig. 5**). In the dimer observed in the crystal structure, the binding sites are distant, whereas they would be in close proximity in the previously postulated assembly, with possible electrostatic interactions between the phosphate groups. In either case, nucleotide binding could be accompanied by conformational changes in the dimeric arrangement, possibly transmitted to the transmembrane transport domain via the R-helix[3] (**Fig. 5c**). Because of the interactions of the two domains in the homodimeric transporter, those conformational changes could affect both subunits and could therefore underlie concerted regulatory mechanisms found in various members of the ClC family[22,23]. Such changes have recently been proposed for the common gating mechanism in ClC-0 (ref. 24). This proposed mechanism is also consistent with the mutant phenotypes we observed in electrical recordings. As shown in the background of a mutant that does not transport H^+ but, unlike WT, conducts Cl^- ions in a broad voltage range, mutations that abolish nucleotide binding greatly change the ion-transport properties of the protein. The change is most pronounced at negative voltages, where Cl^- ions flowing out of the cell would be strongly affected by conformational transitions near the intracellular entrance to the Cl^--binding sites. Although our results hint at possible regulatory mechanisms, to gain deeper insight, structures of full-length ClC proteins with the cytoplasmic domains attached will be required.

Possible signals sensed by the ClC-5 domains

The nature of the regulatory stimulus sensed by ClC-5 in its cellular environment is currently unclear. The relatively low K_d of ~100 μM, which is considerably lower than the ATP concentrations typically found in cells (2–5 mM), implies that the binding sites will be occupied under essentially all metabolic conditions. Notably, the members of the AMPK family are believed to be regulated in response to changes in the intracellular AMP/ATP ratio, which is a sensitive measure of the metabolic state of the cell[6,18]. However, because of its poor discrimination of nucleotides and the low intracellular concentration of AMP, such a regulation mode seems unlikely for ClC-5. As ClC-5 is believed to reside in endosomes, near the V-type ATPase, regulation in response to changes in the ADP/ATP ratio would be a possible scenario. However, the local ADP concentration would have to deviate substantially from that typically found in a resting cell. Notably, an electrophysiological study of the closely related transporter ClC-4 has shown a rundown of current upon ATP

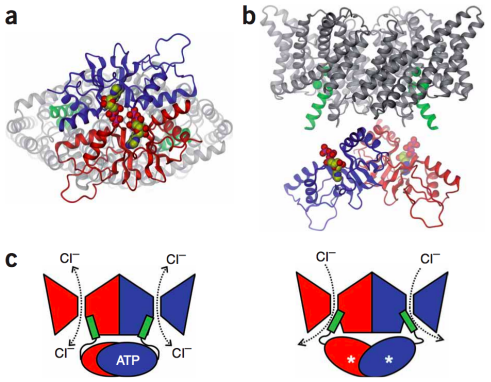

Figure 5 Ligand-binding domains in the context of the full-length transporters. (**a**) Model of the cytoplasmic domains in a hypothetical dimeric arrangement, with the transmembrane domain viewed from the intracellular side. Gray ribbon, structure of *E. coli* ClC dimer (gray ribbon), which serves as a model for the transmembrane domains; green ribbon, R-helix; green spheres, bound ions; blue and red ribbons, the two domains, in arrangement observed in a homologous bacterial protein. ATP molecules are shown as CPK models. (**b**) Alternative model, with domain dimers in the conformation observed in the ClC-5 domain crystal form. View is from within the membrane; coloring scheme is similar to **a**. (**c**) Schematic model of a possible conformational change in ClC-5 induced by ATP binding. Left, model of the ClC-5 mutant E211A. ATP is bound to the cytoplasmic domain, stabilizing a conformation that allows Cl^- ions to flow equally well in both directions. Right, model of a mutant with compromised nucleotide-binding properties. In the absence of bound nucleotides, the cytoplasmic domains induce a conformational change in the ion-binding site via a regulatory helix of the transmembrane domain (R- helix, green) that diminishes Cl^- flow from the cytoplasm. The two subunits are colored in red and blue, respectively.

depletion[7]. This rundown is prevented if the intracellular concentration of ATP is kept at a high level, whereas a high intracellular ADP concentration has a similar effect to that of ATP depletion, decreasing the currents.

It should also be emphasized that we currently cannot exclude the possibility that the binding affinities for nucleotides change in the context of the full-length protein and in the presence of potential interaction partners. Such changes have been reported for other CBS domain–containing molecules and might shift the binding affinity to a range closer to physiological ATP concentrations[6]. In this case, regulation could occur through binding and dissociation of ATP, the most abundant ligand, a scenario that has been suggested to be relevant for the homologous muscle channel ClC-1 (ref. 8).

Ligand binding in the ClC family

It is currently not known which ClC family members carrying cytoplasmic CBS domains are regulated by nucleotides. Although the residues involved in nucleotide binding to the ClC-5 domain are conserved in ClC-3 and ClC-4, there is only poor sequence conservation between this subfamily and the channels ClC-0, ClC-1, ClC-2 and ClC-K. ATP regulation of ClC-1 seems now to be established, but no ATP binding has been observed for the chloride channel ClC-0 from the torpedo electric organ[8,11]. The physiological importance of nucleotide binding to ClC-5 is still unclear, as this channel's function when expressed in *Xenopus* oocytes did not change upon ATP binding. Electrophysiological recordings show that the protein is inactive over a wide voltage range and is activated only at very positive voltages. However, it is conceivable that the protein studied in the plasma membrane of oocytes and other cell lines might lack an important interaction partner, which might prevent its full activation[12]. The physiological role of nucleotide regulation for intracellular ClC transporters will therefore have to be clarified in their natural cellular environment.

Although there have been previous reports on the possible regulation of ClC function by nucleotides, our study now unequivocally clarifies the molecular framework underlying nucleotide recognition in ClC proteins. The elucidation of the detailed regulatory mechanisms will be the next challenging step, with our results serving as a basis for future investigations.

METHODS

Protein expression and purification. For expression in *Escherichia coli*, residues 568–746 of ClC-5 from *Homo sapiens* (GenBank 116734718) were inserted into a pET28 b+ vector (Novagen) with a C-terminal recognition site for *Herpes simplex* 3C protease (Amersham) followed by a His_6 tag. The vector was transformed into *E. coli* BL21 (DE3) cells, which were grown at 37 °C in LB medium containing 50 mg l^{-1} kanamycin to an absorbance at 600 nm (A_{600}) of 1.2. Expression was induced by addition of 0.5 mM IPTG at 20 °C overnight. Cells were harvested and lysed by sonication in 50 mM Tris-HCl (pH 7.5), 150 mM NaCl, 5 mM $MgCl_2$ and 5 mM mercaptoethanol (TBS) with the addition of 200 mg l^{-1} lysozyme, 20 mg l^{-1} DNase, leupeptin, pepstatin and 1 mM phenylmethylsulfonyl fluoride. The lysate was cleared by centrifugation and purified by affinity chromatography on a column loaded with nickel-chelating Sepharose (Pharmacia Biotech). After a wash with buffer containing 15 mM of imidazole, the pure protein was eluted with 300 mM of imidazole. At this point, the protein was cleaved with Prescission protease (Amersham) and dialyzed into TBS. After concentration, the protein was subjected to gel filtration on a Superdex-200 column (Amersham). All purification steps were carried out at 4 °C. For preparation of the SeMet-labeled protein, the bacterial culture was grown in minimal medium containing 50 mg l^{-1} SeMet.

Crystal preparation. Purified protein was concentrated to 7.5–15 mg ml^{-1} and crystals were grown in sitting drops at 4 °C by equilibrating a 1:1 mixture of protein and reservoir solution against the reservoir. The reservoir contained 200 mM $(NH_4)_2SO_4$, 10 mM Tris-HCl (pH 7.4), 15%–20% (w/v) PEG 4,000 and 5 mM of either ATP or ADP. Crystals grew within several days in the space group $P2_12_12$ ($a = 122$ Å, $b = 148$ Å, $c = 80$ Å, $\alpha = \beta = \gamma = 90°$), with six copies of the protein in the asymmetric unit. The crystals were prepared for cryo-crystallography by successive transfer into higher concentrations of ethylene glycol, to a final concentration of 25% (v/v), flash-frozen in liquid propane and stored in liquid nitrogen.

Structure determination. Data were collected on a Mar225 CCD detector (Marresearch) at the X06SA beamline at the Swiss Light Source of the Paul Scherrer Institute. The data were indexed and integrated with DENZO and SCALEPACK and further processed with CCP4 programs[25,26]. The ClC-5 domain–ATP complex structure was determined by SeMet MAD using data sets collected at three wavelengths around the selenium-absorption edge. The selenium sites were identified using SHELX C and D[27,28]. Experimental density was calculated and phases were improved by solvent flattening with SHELX E[29]. The model was built using Coot[30]. Refinement of the model was initially done by simulated annealing in CNS[31] alternated with inspection and manual

Table 1 Data collection and refinement statistics

	Native ATP	SeMet ATP			Native ADP
Data collection					
Space group	$P2_12_12$	$P2_12_12$			$P2_12_12$
Cell dimensions					
a, *b*, *c* (Å)	123.3, 148.6, 80.2	123.4, 148.7, 80.2			126.6, 149.3, 81.0
		Peak	*Inflection*	*Remote*	
Wavelength	0.9649	0.9789	0.9792	0.9649	0.9193
Resolution (Å)	40–2.3	40–2.7	40–2.5	40–2.5	40–3.05
R_{merge}	0.074 (0.408)	0.089 (0.558)	0.066 (0.463)	0.073 (0.487)	0.093 (0.424)
$I / \sigma I$	18.9 (3.3)	14.0 (2.5)	23.0 (2.2)	19.6 (2.5)	17.1 (2.1)
Completeness (%)	97.5 (68.5)	91.0 (86.1)	97.6 (83.5)	98.7 (89.9)	93.7 (64.2)
Redundancy	5.2 (1.8)	6.6 (4.3)	6.5 (3.7)	6.7 (3.1)	7.7 (3.1)
Refinement					
Resolution (Å)	20–2.3				20–3.05
No. reflections	63,482				26,547
R_{work} / R_{free}	26.3 / 29.5				26.3 / 31.5
No. atoms					
Protein	8,003				8,003
Ligand	196				162
Water	267				–
B-factors					
Protein	34.6				63.1
Ligand	61.7				96.5
Water	68.8				–
R.m.s. deviations					
Bond lengths (Å)	0.005				0.006
Bond angles (°)	0.89				0.95

Values in parentheses are for highest-resolution shell.

rebuilding in Coot[31]. R_{free} was calculated using a randomly selected 5% sample of the reflection data omitted from refinement. Six-fold noncrystallographic symmetry constraints were used in the initial stages of refinement. In later stages, the strict constraints were loosened and restraint individual *B*-factors were refined against a native data set at 2.3-Å resolution with CNS and REFMAC[26,31,32] (**Table 1**). The structure contains 8,003 protein atoms, six molecules of ATP, 258 water molecules and nine Cl^- ions with good geometry, and no outliers in the Ramachandran plot. The ClC-5 domain structure in complex with ADP was determined by molecular replacement using the protein part of the ClC-5 ATP complex. Refinement was initiated with several cycles of rigid-body refinement and continued by restraint individual refinement in CNS and REFMAC. The ADP nucleotides were modeled into the well-defined electron density of a $2F_o - F_c$ omit map and of a $F_o - F_c$ difference map and included in a final round of refinement.

Equilibrium dialysis. The binding affinity of radioactive adenosine nucleotides was measured by equilibrium dialysis (**Supplementary Methods** online). Custom microdialysis chambers with 75-µl volume were separated by a dialysis membrane with a 8,000-Da cutoff. One chamber contained 300 µM of purified protein in TBS buffer and radiolabeled nucleotide, whereas the other was filled with TBS and radiolabeled nucleotide. Protein concentration was determined by A_{280} using an extinction coefficient that was calibrated by quantitative amino acid analysis. Amounts of 10–600 µM of various labeled nucleotides ([2.8-^{3}H]ATP or [2-^{3}H]AMP (Amersham), or [8-^{14}C]ADP (Perkin Elmer)) were used. For competition experiments, 300 µM of protein was incubated with 400 µM radiolabeled ATP, in addition to 400 µM of unlabeled ATP, ADP and AMP. Equilibrium was reached after 15 h at 4 °C, and two samples were drawn from every chamber and mixed with 200 µl of scintillation liquid (Amersham). Samples were measured in a 1450 Microbeta Plus liquid scintillation counter (Wallac).

Expression in *Xenopus laevis* oocytes and voltage-clamp studies. A human ClC-5 complementary DNA was cloned into the pTLN vector for expression in *X. laevis*[33]. Mutations were inserted with the QuikChange method (Stratagene) and confirmed by sequencing. After linearization of the plasmid DNA by MluI, capped complementary RNA was transcribed with the mMessage mMachine kit (Ambion) and purified with the RNeasy kit (Qiagen). For expression, 10–25 ng of RNA was injected into defolliculated oocytes. The oocytes were kept at 17 °C in modified Barth's solution as described[14]. Two-electrode voltage clamp measurements were performed 2–3 d after injection at 20 °C using Geneclamp500 (Axon Instruments). Currents were recorded in ND96 solution (96 mM NaCl, 2 mM KCl, 1.8 mM $CaCl_2$, 1 mM MgCl, 5 mM sodium HEPES (pH 7.4)). To produce different pH values, 5 mM HEPES was replaced by 5 mM MES (pH 5.5 and pH 6.5) or 5 mM TAPS (pH 8.5). Oocytes were clamped at –30 mV and a pulse protocol was applied from 100 mV to –100 mV or –140 mV (for mutants in the E211A background), in 10-mV steps. For data reported, the currents measured at 100 mV and pH 7.5 in all cases ranged between 4 and 6 µA for oocytes expressing WT ClC-5 and between 3 and 6 µA for oocytes expressing ClC-5 mutants. The currents were found to be selective for Cl^- over I^-. In contrast, the endogenous currents at 100 mV ranged between 0.5 and 0.8 µA, with selectivity for I^- over Cl^- (**Supplementary Figs. 4–6** online).

Accession Codes. Protein Data Bank: Coordinates and structure factors have been deposited with accession codes 2J9L (ATP complex) and 2JA3 (ADP complex).

Note: Supplementary information is available on the Nature Structural & Molecular Biology website.

ACKNOWLEDGMENTS

X-ray data were collected (MDC Berlin) at the Swiss Light Source of the Paul Scherrer Institute. We thank T. Jentsch (MDC Berlin) for providing the ClC-5 clone, S. Chesnov and P. Hunziker for help with mass spectrometry, B. Blattmann for help with crystal screening, P. Lindner for advice on equilibrium binding assays, E. Hänsenberger for preparation of the *Xenopus* oocytes, the staff of the X06SA beamline for their support during data collection and R. MacKinnon for comments on the manuscript. This work was supported by a grant from the Swiss National Science Foundation and the National Center of Competence in Research in Structural Biology program. S.M. is affiliated with the Molecular Life Sciences PhD Program of the University/ETH Zürich.

AUTHOR CONTRIBUTIONS

S.M. carried out all experiments, S.S. assisted in protein preparation and binding assays, I.C.F. contributed to electrophysiology experiments and R.D. conceived and planned the experiments and interpreted the data. S.M. and R.D. jointly wrote the manuscript.

COMPETING INTERESTS STATEMENT

The authors declare that they have no competing financial interests.

Published online at http://www.nature.com/nsmb/
Reprints and permissions information is available online at http://npg.nature.com/reprintsandpermissions/

1. Jentsch, T.J., Neagoe, I. & Scheel, O. CLC chloride channels and transporters. *Curr. Opin. Neurobiol.* **15**, 319–325 (2005).
2. Dutzler, R. The ClC family of chloride channels and transporters. *Curr. Opin. Struct. Biol.* **16**, 439–446 (2006).
3. Dutzler, R., Campbell, E.B., Cadene, M., Chait, B.T. & MacKinnon, R. X-ray structure of a ClC chloride channel at 3.0 A reveals the molecular basis of anion selectivity. *Nature* **415**, 287–294 (2002).
4. Dutzler, R., Campbell, E.B. & MacKinnon, R. Gating the selectivity filter in ClC chloride channels. *Science* **300**, 108–112 (2003).
5. Ignoul, S. & Eggermont, J. CBS domains: structure, function, and pathology in human proteins. *Am. J. Physiol. Cell Physiol.* **289**, C1369–C1378 (2005).
6. Scott, J.W. *et al.* CBS domains form energy-sensing modules whose binding of adenosine ligands is disrupted by disease mutations. *J. Clin. Invest.* **113**, 274–284 (2004).
7. Vanoye, C.G. & George, A.L., Jr. Functional characterization of recombinant human ClC-4 chloride channels in cultured mammalian cells. *J. Physiol. (Lond.)* **539**, 373–383 (2002).
8. Bennetts, B. *et al.* Cytoplasmic ATP-sensing domains regulate gating of skeletal muscle ClC-1 chloride channels. *J. Biol. Chem.* **280**, 32452–32458 (2005).
9. Niemeyer, M.I. *et al.* Functional evaluation of human ClC-2 chloride channel mutations associated with idiopathic generalized epilepsies. *Physiol. Genomics* **19**, 74–83 (2004).
10. Wellhauser, L. *et al.* Nucleotides bind to the C-terminus of ClC-5. *Biochem. J.* **398**, 289–294 (2006).
11. Meyer, S. & Dutzler, R. Crystal structure of the cytoplasmic domain of the chloride channel ClC-0. *Structure* **14**, 299–307 (2006).
12. Steinmeyer, K., Schwappach, B., Bens, M., Vandewalle, A. & Jentsch, T.J. Cloning and functional expression of rat CLC-5, a chloride channel related to kidney disease. *J. Biol. Chem.* **270**, 31172–31177 (1995).
13. Schwake, M., Friedrich, T. & Jentsch, T.J. An internalization signal in ClC-5, an endosomal Cl-channel mutated in dent's disease. *J. Biol. Chem.* **276**, 12049–12054 (2001).
14. Friedrich, T., Breiderhoff, T. & Jentsch, T.J. Mutational analysis demonstrates that ClC-4 and ClC-5 directly mediate plasma membrane currents. *J. Biol. Chem.* **274**, 896–902 (1999).
15. Accardi, A. & Miller, C. Secondary active transport mediated by a prokaryotic homologue of ClC Cl^- channels. *Nature* **427**, 803–807 (2004).
16. Picollo, A. & Pusch, M. Chloride/proton antiporter activity of mammalian CLC proteins ClC-4 and ClC-5. *Nature* **436**, 420–423 (2005).
17. Scheel, O., Zdebik, A.A., Lourdel, S. & Jentsch, T.J. Voltage-dependent electrogenic chloride/proton exchange by endosomal CLC proteins. *Nature* **436**, 424–427 (2005).
18. Hardie, D.G. & Hawley, S.A. AMP-activated protein kinase: the energy charge hypothesis revisited. *Bioessays* **23**, 1112–1119 (2001).
19. Adams, J. *et al.* Intrasteric control of AMPK via the gamma1 subunit AMP allosteric regulatory site. *Protein Sci.* **13**, 155–165 (2004).
20. Walker, J.E., Saraste, M., Runswick, M.J. & Gay, N.J. Distantly related sequences in the alpha- and beta-subunits of ATP synthase, myosin, kinases and other ATP-requiring enzymes and a common nucleotide binding fold. *EMBO J.* **1**, 945–951 (1982).
21. Jiang, Y. *et al.* Crystal structure and mechanism of a calcium-gated potassium channel. *Nature* **417**, 515–522 (2002).
22. Miller, C. Open-state substructure of single chloride channels from *Torpedo electroplax*. *Phil. Trans. R. Soc. Lond. B* **299**, 401–411 (1982).
23. Fong, P., Rehfeldt, A. & Jentsch, T.J. Determinants of slow gating in ClC-0, the voltage-gated chloride channel of *Torpedo marmorata*. *Am. J. Physiol.* **274**, C966–C973 (1998).
24. Bykova, E.A., Zhang, X.D., Chen, T.Y. & Zheng, J. Large movement in the C terminus of CLC-0 chloride channel during slow gating. *Nat. Struct. Mol. Biol.* **13**, 1115–1119 (2006).
25. Otwinowski, Z. & Minor, W. Processing of X-ray diffraction data collected in oscillation mode. *Methods Enzymol.* **267**, 307–326 (1997).
26. Collaborative Computational Project, Number 4. The CCP4 suite: programs for X-ray crystallography. *Acta Crystallogr. D Biol. Crystallogr.* **50**, 760–763 (1994).

27. Pape, T. & Schneider, T.R. HKL2MAP: a graphical user interface for phasing with SHELX programs. *J. Appl. Cryst.* **37**, 843–844 (2004).
28. Schneider, T.R. & Sheldrick, G.M. Substructure solution with SHELXD. *Acta Crystallogr. D Biol. Crystallogr.* **58**, 1772–1779 (2002).
29. Sheldrick, G.M. Macromolecular phasing with SHELXE. *Z. Kristallographie* **217**, 644–650 (2002).
30. Emsley, P. & Cowtan, K. Coot: model-building tools for molecular graphics. *Acta Crystallogr. D Biol. Crystallogr.* **60**, 2126–2132 (2004).
31. Brunger, A.T. *et al.* Crystallography & NMR system: A new software suite for macromolecular structure determination. *Acta Crystallogr. D Biol. Crystallogr.* **54**, 905–921 (1998).
32. Painter, J. & Merritt, E.A. Optimal description of a protein structure in terms of multiple groups undergoing TLS motion. *Acta Crystallogr. D Biol. Crystallogr.* **62**, 439–450 (2006).
33. Lorenz, C., Pusch, M. & Jentsch, T.J. Heteromultimeric CLC chloride channels with novel properties. *Proc. Natl. Acad. Sci. USA* **93**, 13362–13366 (1996).

2.2.3 Supplementary Material

Equilibrium dialysis

Methods The binding affinity of radioactive adenosine nucleotides was measured by equilibrium dialysis. Custom microdialysis chambers with 75 μl volume separated by a dialysis membrane with a cutoff of 8000∼Da were used. One chamber contained 300 μM of purified protein in TBS* buffer (150 mM NaCl, 50 mM Tris pH 7.5, 5 mM $MgCl_2$, 5 mM β-mercapto ethanol) and radiolabeled nucleotide, the other was filled with TBS* and radiolabeled nucleotide. For each side of the chamber 55 μl of solution were applied. Applied nucleotide concentration ranged from 10 to 600 μM ([2.8-^{3}H] ATP, [2-^{3}H] AMP (Amersham) or [8-^{14}C] ADP (Perkin Elmer)) to test binding of nucleotides over relevant concentrations. Bound and free nucleotide concentrations were measured independently after equilibration. As experimentally determined equilibrium was reached after 15 h at 4 °C. The non-specific binding of protein to the chamber and the dialysis membrane (about 20 %) was measured and taken into account. The non-specific interaction of nucleotides with the protein can be assessed from experiments with the mutant D727A, which shows negligible binding. For measurements two samples of 20 μl were drawn from every chamber and mixed with 200 μl of scintillation liquid (Amersham). Samples were measured in a 1450 Microbeta Plus liquid scintillation counter (Wallac) in opaque 96-well plates with clear bottom (Wallac). The counts of the samples were in the range between 200 and 20000 cpm. The concentration of free and bound ATP was determined by calibrating the cpm values with a standard curve of the radiolabeled ATP stock solution. The same experimental setup was used for competition experiments. Experiments were carried out with addition of 400 μM of radiolabeled ATP and equivalent amounts of competing nucleotides. Bound ATP was compared to a reference where the competing nucleotide was replaced by buffer.

Results The nucleotide recognition by the cytoplasmic domain of ClC-5 is mediated by specific interactions of the protein with the adenosine base and the hydrogen bonding to the sugar moiety (Article: Figure 2a). Using equilibrium dialysis techniques it could be shown that the affinity for adenosine nucleotides is in the range of 100 μM and that the discrimination between the species AMP, ADP and ATP is poor (Article: Figure 3d). This finding is in line with the limited interaction of the β- and γ-phosphates of the nucleotide with the protein. It remained to be shown that the protein is able to discriminate adenosine nucleotides from related species like guanosine-5'-triphosphate,

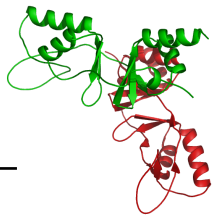

3'-5'-cyclic adenosine monophosphate or the metabolic precurser adenosine. To obtain a qualitative answer of whether the ClC-5 domains are able to bind these molecules a competition experiment was performed analogous to the results shown in the article in Figure 3d. The results indicate that the binding of these compounds to the nucleotide binding site in the cytoplasmic domains of ClC-5 is very low compared to the adenosine nucleotides. Thus they suggest that all the observed protein ligand interactions are contributing critically to the recognition of the molecule: 1. The interaction of T596 with the 6'-amino group of the base. 2. Hydrogen bonding of D727 to the 2'- and 3'-hydroxyls of the ribose moiety. 3. The backbone interaction of S618 with the α-phosphate.

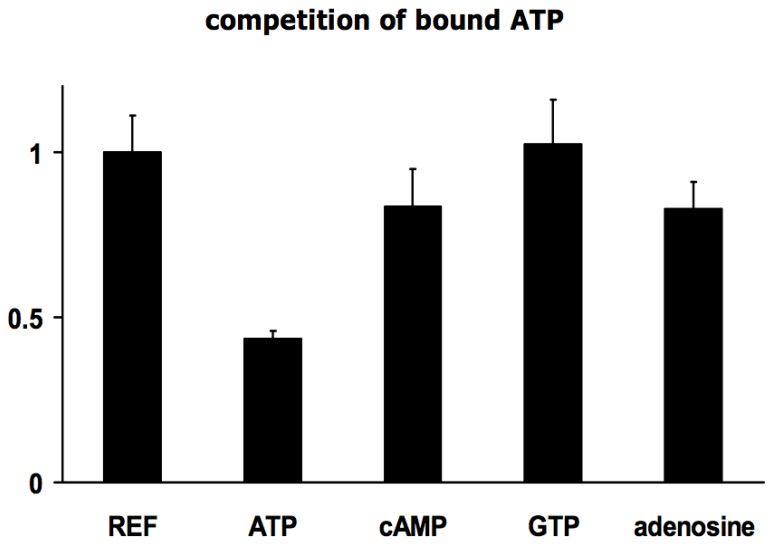

Figure S1: **Competition of Bound Radiolabeled ATP**
Equilibrium dialysis experiments of ATP binding to the purified C-terminal domain of ClC-5 in competition with unlabeled nucleotides. The reference shows the binding of 400 μM radiolabeled ATP to the protein. In competition experiments 400 μM of unlabeled ATP, cAMP, GTP and adenosine was added and the bound radiolabeled ligand was quantified and normalized to the reference value. Averages from 3-4 independent experiments and their standard deviations are shown.

Analytical Ultracentrifugation

Methods Sedimentation velocity experiments were performed with a Beckman XL-I analytical ultracentrifuge with an An 50-Ti rotor at 4 ^{circ}C. 12 mm epon double-sector cells were filled with 400 μl 150 mM NaCl, 50 mM Tris (pH 7.5), 5 mM MgCl2, 5 mM β-mercapto-ethanol, and protein sample. Experiments were performed at protein concentrations of 75 and 150 μM. Data were acquired using interference in continuous

scan mode in 0.003 cm intervals at a rotor speed of 42,000 rpm. The data analysis was performed with the c(S) module of Sedfit.[107,108] The buffer parameters and partial-specific volume of the protein were calculated by using Sednterp.[109]

Results The analytical ultracentrifugation experiments reveal that the protein exists in an equilibrium of two species in solution, the monomer and the dimer. This situation is similar but more pronounced than in the case of the ClC-0 cytoplasmic domains (Figure 3a[1]). The addition of ATP does not alter this equilibrium of the two species. At this point it is unclear, if these observed oligomeric states are of functional importance in the full-length transporter. However, it is likely that the high local concentration in the dimeric assembly of two transporters will drive the cytoplasmic domains towards dimerization.

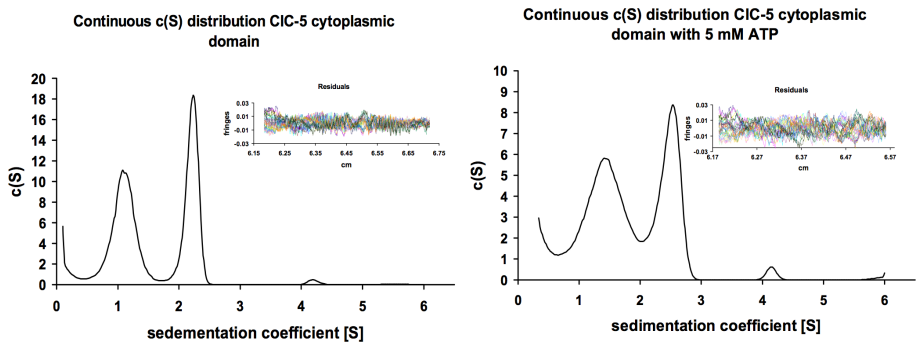

Figure S2: **Sedimentation Velocity Data of the ClC-5 Cytoplasmic Domain**
Distribution of sedimentation coefficients of the ClC-5 cytoplasmic domain without (a) and with addition of 5 mM ATP (b) measured at 4 °C. The data shows a monomer/dimer equilibrium of the protein with sedimentation values similar to those determined for the ClC-0 cytoplasmic domain. No significant change of the distribution is observed upon addition of ATP. The rms-deviation of the fits is 0.0063 and 0.0075 for a and b respectively.

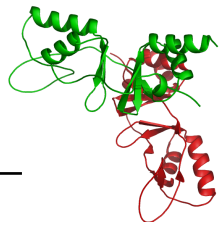

Two-electrode Voltage-Clamp In order to investigate the functional effects of nucleotide binding to the ClC-5 transporter the protein was heterologously expressed in *Xenopus l.* oocytes. After an expression of 3–4 days the ClC transporter dominated the current phenotype of the oocyte membrane and typical recordings of macroscopic ClC-5 currents[19] could be obtained by two-electrode voltage-clamp measurements (Figure S3). To assure that the observed currents were originating from the heterologously expressed protein and not from endogenous proteins, measurements of water injected oocytes were performed. These oocytes gave currents of 10- to 20-fold reduced amplitude. Additionally, it was routinely confirmed that the measured ClC-5 currents obeyed the reported chloride over iodide selectivity[19] causing a decrease in the current amplitudes upon exchange of the oocyte buffer. To assess the influence of nucleotide binding to the cytoplasmic domains the mutations that have been shown to abolish nucleotide binding by equilibrium dialysis were tested functionally in *Xenopus l.* oocytes. Due to the current-voltage characteristics of wt ClC-5 in heterologous expression, the protein is only active over a rather limited voltage range above +30 mV. This observation is seemingly contradictory to the function of the protein and will be discussed in more detail in the following chapter. However, to circumvent this problem the mutations under investigation were introduced in the background of the mutation E211A that has been recognized to abolish H^+ to Cl^- coupling thereby converting the protein in a constitutively open Cl^- conductor.[24–26] This experimental setup made the voltage range below +30 mV accessible to investigation and led to the discovery of the pronounced differences at negative voltages of ClC-5 bearing domains with impaired nucleotide binding ability (Figure S3 and S5).

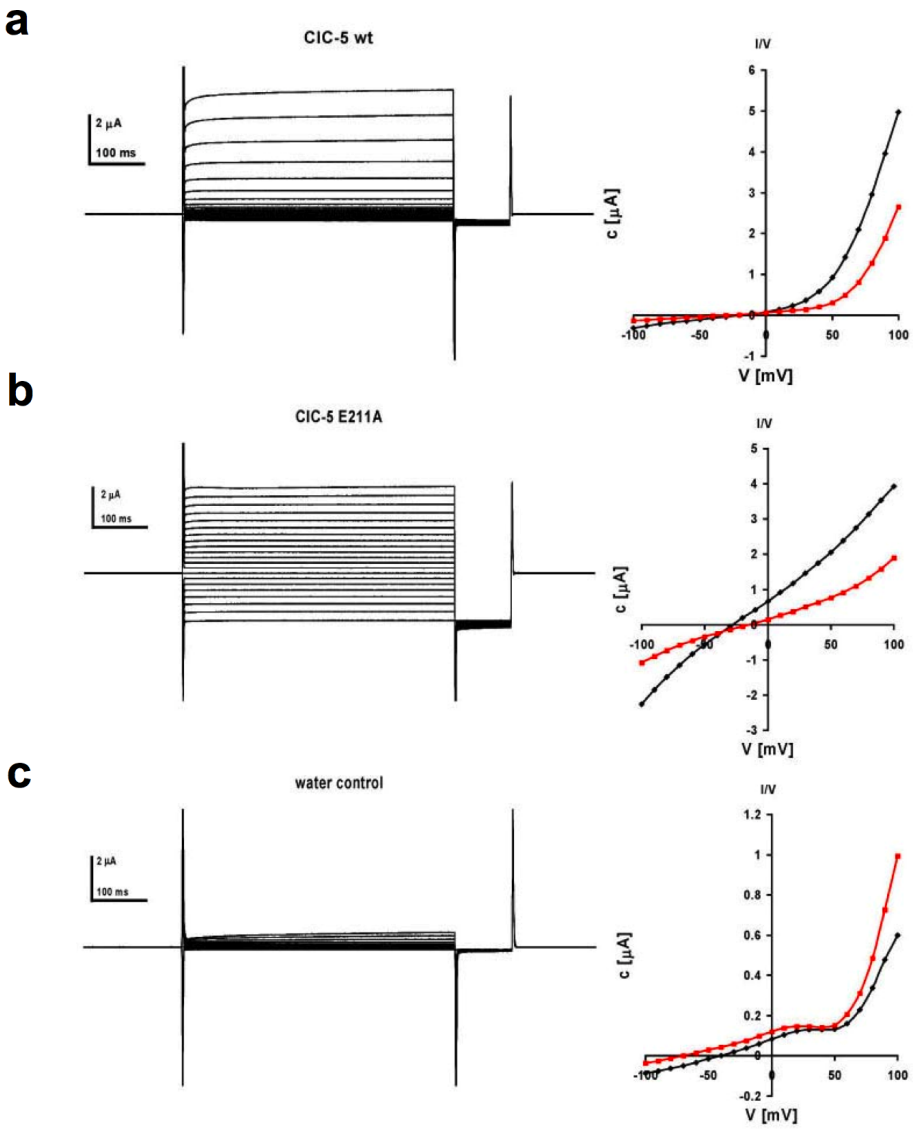

Figure S3: **Two-electrode Voltage-clamp Recordings of Human ClC-5 in *Xenopus l.* Oocytes**
(a) ClC-5 wt. Representative current traces of an oocyte injected with ClC-5 mRNA (left). Steady-state I-V curves were recorded at pH 7.4. Oocytes were clamped at -30 mV and a pulse protocol was applied starting from 100 mV to -100 mV in 10 mV steps. The corresponding current-voltage relationships in 96 mM Cl^- (black) and in 80 mM I^- (red) measured from the same oocyte are shown (right). (b) Data as in panel a is shown for a representative oocyte injected with ClC-5 E211A mRNA. (c) Data as in panel a is shown for a representative control oocyte injected with water.

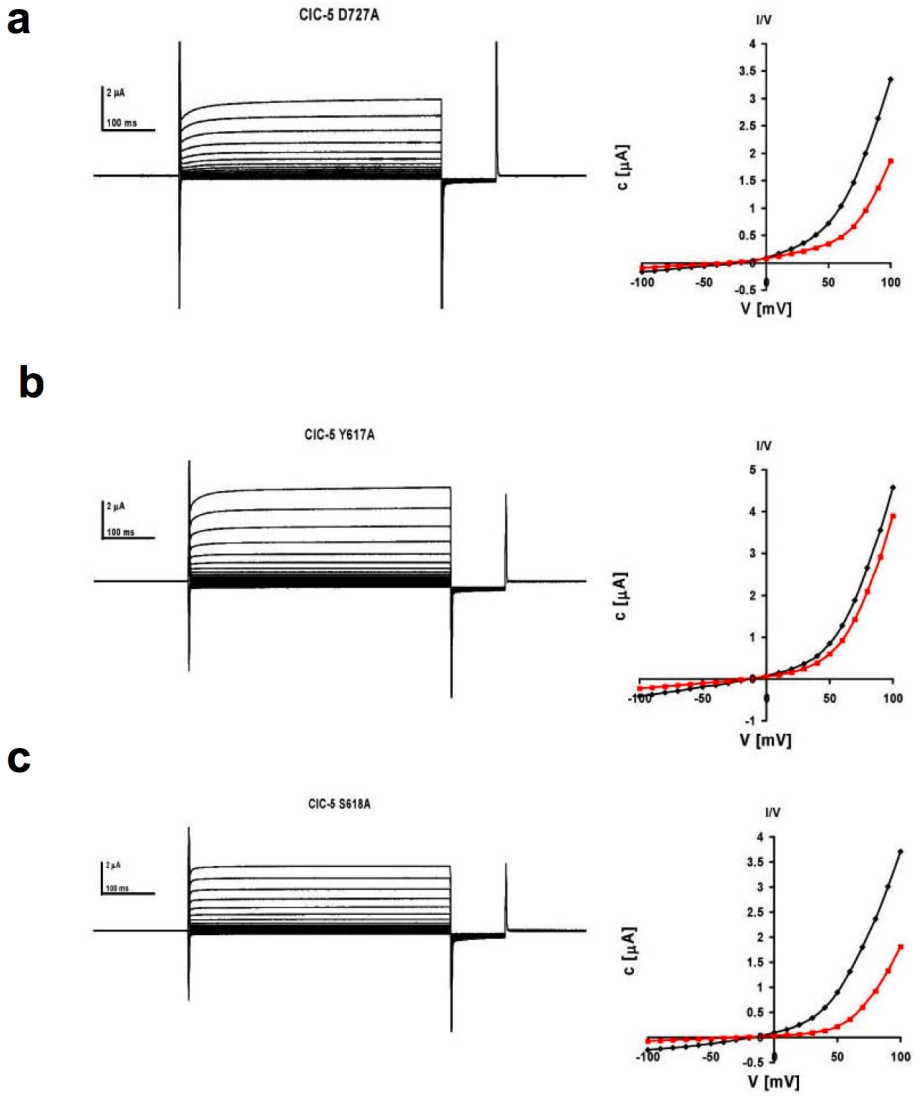

Figure S4: **Two-electrode Voltage-clamp Recordings of Human ClC-5 Mutants in *Xenopus l.* Oocytes**
(a) Representative current traces of an oocyte injected with ClC-5 D727A mRNA (left). The current protocol is as in Supplementary Figure S4a. The corresponding current-voltage relationships in 96 mM Cl^- (black) and in 80 mM I^- (red) measured from the same oocyte are shown (right). (b) Data as in panel a is shown for a representative oocyte injected with ClC-5 Y617A mRNA. (c) Data as in panel a is shown for a representative oocyte injected with ClC-5 S618A mRNA.

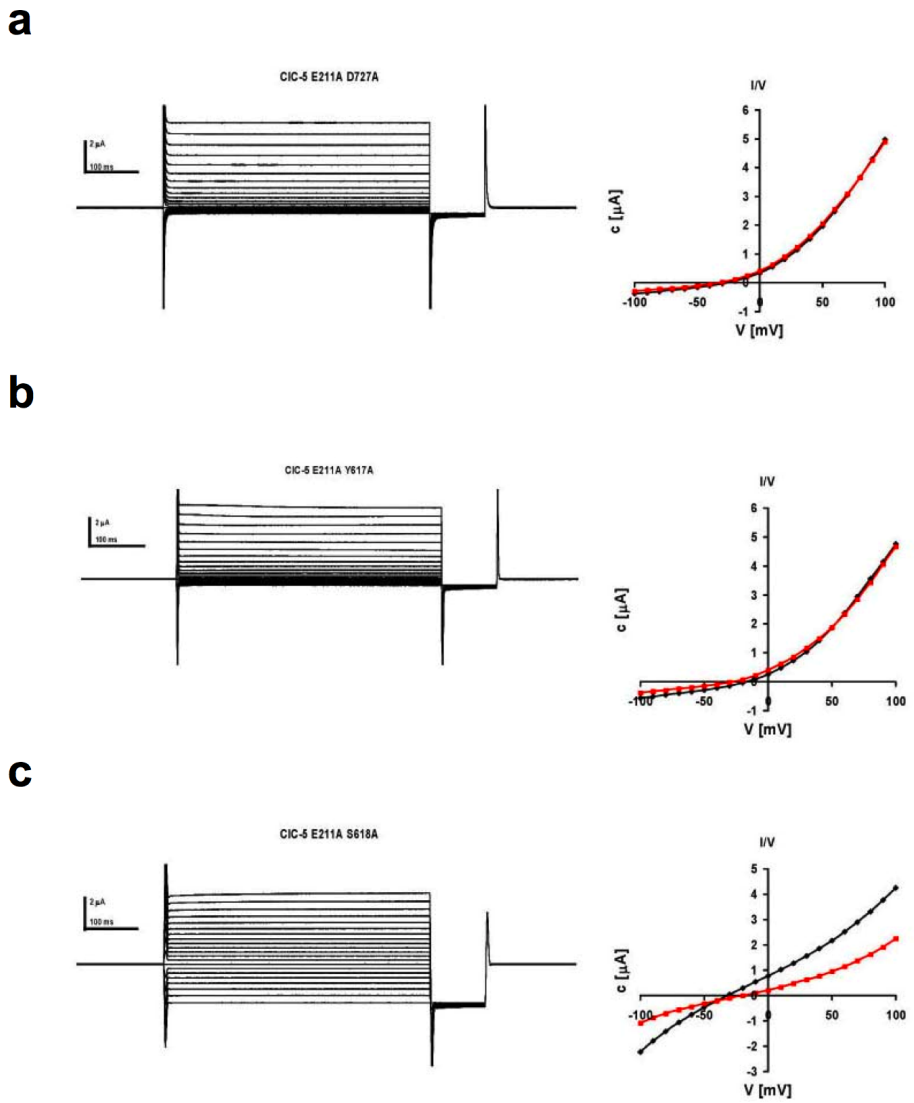

Figure S5: **Two-electrode Voltage-clamp Recordings of Human ClC-5 Mutants in *Xenopus l.* Oocytes**
(a) Representative current traces of an oocyte injected with ClC-5 E211A / D727A mRNA (left). The current protocol is as in Supplementary Figure S4a. The corresponding current-voltage relationships in 96 mM Cl^- (black) and in 80mM I^- (red) measured from the same oocyte are shown (right). (b) Data as in panel a is shown for a representative oocyte injected with ClC-5 E211A / Y617A mRNA. (c) Data as in panel a is shown for a representative oocyte injected with ClC-5 E211A / S618A mRNA.

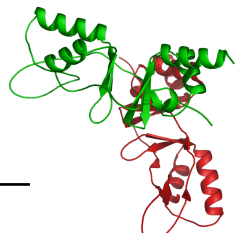

Structure Determination and Model Building The structure of the cytoplasmic domains of ClC-5 in complex with ATP was solved by multiwavelength anomalous diffraction at three wavelengths using a selenomethionine substituted protein crystal. Analysis of the solvent content of the crystals led to an assumption of 6 to 8 molecules in the asymmetric unit, as these would result in Matthew's coefficients of 2.8 to 2.1. The subsequent search for selenium sites in the crystal resulted in the identification of 29 sites, in the following the calculation of an experimental electron density map that allowed the tracing of 6 molecules in the asymmetric unit. An example of the electron density around one of the ATP ligands is shown in Figure S6, which illustrates the high quality of the experimental map in comparison to the final model.

The placement of the 6 molecules in the asymmetric unit revealed that the chains are

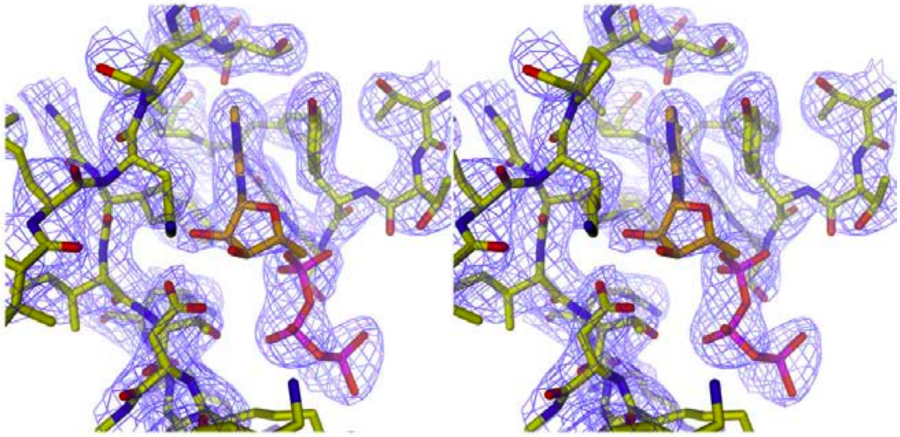

Figure S6: **Stereo View of Experimental Density of the Nucleotide Binding Region in One Protein Chain in the Asymmetric Unit of the ClC-5 Domain-ATP Complex** The electron density at 2.5 Å is shown contoured at 1 σ. The map was calculated from amplitudes and phases obtained from a three wavelength MAD experiment. The refined structure of the protein and the ATP molecule are shown as stick models, carbon atoms of the protein and the nucleotide are colored yellow and orange respectively.

arranged as three pairs of dimers related by an imperfect non-crystallographic threefold axis. The mode of interaction displayed by these dimers in the crystal is profoundly different from the dimerization interfaces observed in CBS proteins to this point.

Although five of the six different chains in the crystal were well-defined, the electron density of the chain F was of considerably lower quality. This resulted in parts of the molecule with missing or discontinous density for the amino acid side chains and peptide chain. Analysis of the crystal packing partly reveals the reason for the apparent disorder

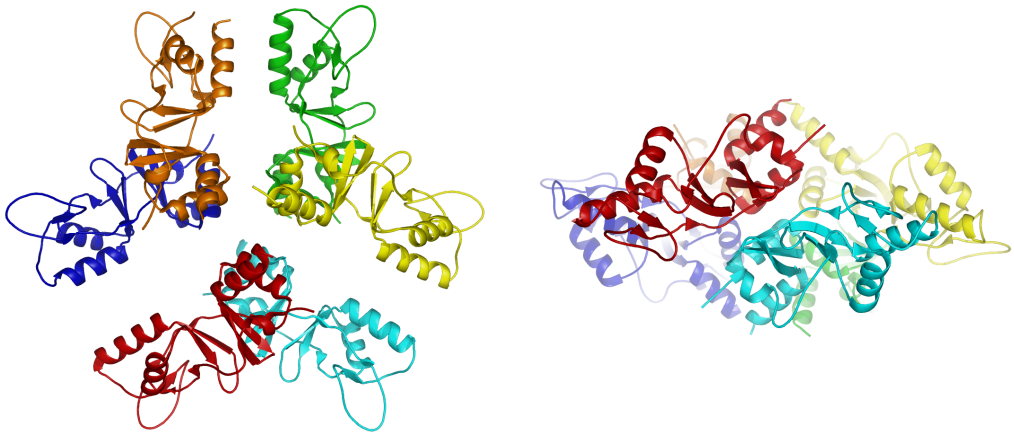

Figure S7: **View of the molecules in the asymmetric unit**
The six molecules are shown individually colored in a ribbon representation tracing the Cα positions. The proteins are depicted along the pseudo threefold axis (left) and rotated by 90 ° from the side.

of the chain F. While the proteins pack rather tightly in two dimensions of the crystal, namely along the axes y and z, only limited protein contacts are seen along the x-axis. This results in a layered appearance of the crystal lattice with large solvent cavities along the yz-plane. One of the CBS subdomains of chain F is exposed in this solvent channel resulting in the insufficient stabilization by crystal contacts. Due to the higher flexibility, this part of the chain could only be modeled with elevated B-factors compared to the other chains (Figure S8). In turn, the observed flexibility of parts of the asymmetric unit contributes to the relatively high R-factor of the structure, when compared to the average of structures at this resolution. Nevertheless, a model with good geometry could be build and refined using non-crystallographic symmetry restraints to the other chains.

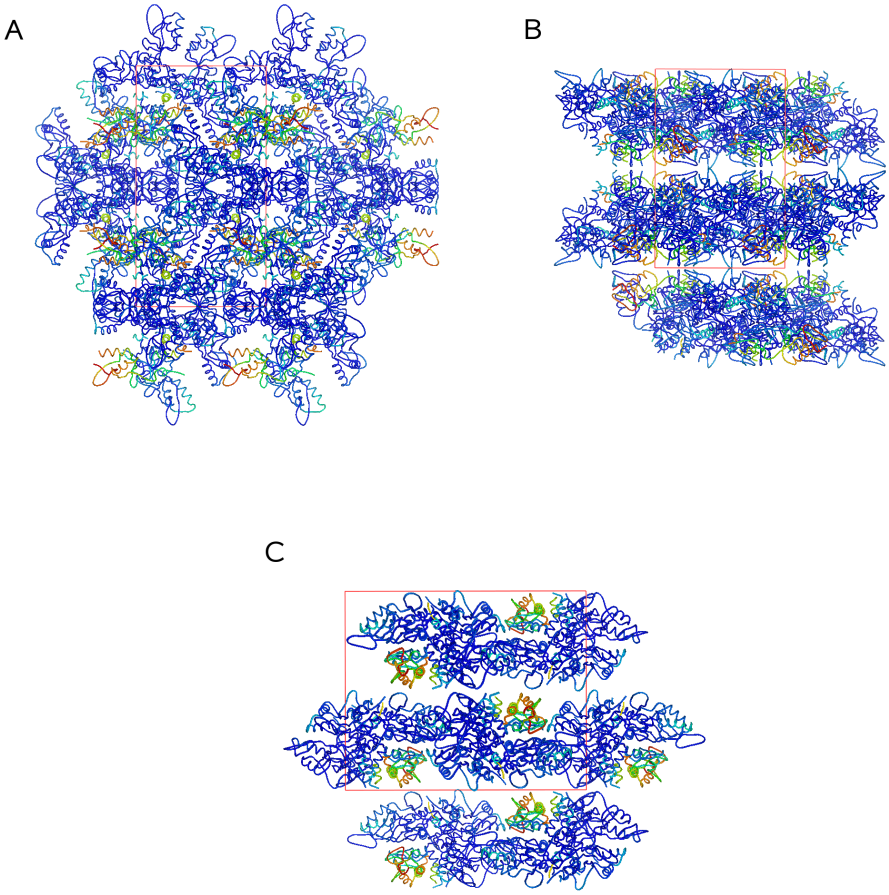

Figure S8: **View of the Crystal Packing**
The packing of the crystal lattice is shown by symmetry related molecules in ribbon representation. The molecules are colored according to the main chain B-factors with blue for the lowest and red for the highest values. The dimensions of one unit cell are depicted as red lines. The packing is displayed as a view along the cell axis, with (A) along x, (B) along y and (C) along z.

Chapter 3

General Discussion and Outlook

The family of ClC channels and transporters is ubiquitously expressed and involved in a variety of important physiological processes.[32] The high resolution structures of the membrane-embedded catalytic domain has led the field to begin to understand the molecular determinants of ion conduction in these complexly regulated proteins.[21,22] Nevertheless, structural and functional investigations have to go hand in hand in order to unravel the detailed mechanisms of ClC function. A striking example is the recent discovery of the transporter function of ecClC, the ClC homolog from *E.coli*, by electrophysiological[28] means and, on the other hand, the structure-guided identification of a glutamate residue that forms part of the proton pathway over the membrane.[27] These astonishing revelations have caused a change of paradigms concerning the mechanisms of channels and transporters, since these hitherto strictly separated functions can be attained by the same structural scaffold. This dualism of ClC function as voltage-gated chloride channels versus secondary active chloride proton transporters also extends to the human isoforms.[25,26] Another striking aspect of ClC function is the intricate regulation of the gating behavior that governs the ion conduction. Recently the cytoplasmic domains present in all eukaryotic ClCs have been recognized to be intimately involved in several regulatory processes. One of these is the association of the common gate with the domains and the coincidence of large movements in the cytoplasmic components upon gating.[83] This is in line with an observed large temperature dependence of the common gating process[70] and the identification of several point mutations in the intracellular domains that disrupt this gating mechanism.[76] A second emerging aspect is the regulation of ClC proteins in response to nucleotide binding to the cytoplasmic domains.[85–87] These studies have described this novel feature of the ClC family by electrophysiological meth-

ods in the muscle type channel ClC-1. In the case of ClC-1, intracellular ATP seems to inhibit the activity of the channel by decreasing the open probability. This effect is potentiated by low intracellular pH[85,87] and is therefore believed to underlie the increased excitability of skeletal muscle during acidosis caused by intense activity.[110] Yet, to understand the underlying mechanistic principles there is an increasing need for structural information.

In this work the cytoplasmic components of two ClC proteins have been studied, one from the voltage-gated chloride channel ClC-0 and the other from the secondary active transporter ClC-5. The structure of the cytoplasmic domains from ClC-0, as described in section 2.1.2, is the first high resolution model for the intracellular components in ClC proteins, setting the structural framework for the cytoplasmic domains in the ClC family. It was found that the two CBS subdomains are tightly interacting and that the N- and C-terminus are positioned on the same face of this well packed CBS tandem. Analytical ultracentrifugation experiments revealed the quaternary structure of the protein to be a dimer in solution alike to the assembly of the membrane domain. In contrast to the well-folded protein core, large parts of the linker connecting the CBS subdomains and the C-peptide were not resolved in the structure, possibly due to inherent flexibility. In a subsequent study (section 2.1.3) these stretches were characterized with NMR methods confirming the intrinsic disorder in solution. This novel feature in certain homologs of the α-subfamily, namely ClC-1, ClC-2 and ClC-0, had so far not been recognized. The functional importance is highlighted by altered functional behavior of some ClCs as a result of phosphorylation,[90,91] alternative splicing[82] or point mutations in these regions.[36] The underlying purpose of the disordered and highly mobile sequence segments is still poorly understood and requires further investigation.

The cytoplasmic domains of the secondary active transporter ClC-5 on the other hand lack these extended disordered segments. Although the fold of the CBS tandem appears very similar in ClC-5, the structure of the intracellular domains reveals two novel features: 1. The binding of ATP and ADP to the protein; 2. The dimeric assembly of two cytoplasmic domains later confirmed by a study on the domains of ClC-Ka.[88]

Several studies have previously suggested the direct interaction of adenosine nucleotides with the intracellular domains of different ClCs.[79,84,86] In an attempt to rationalize the molecular interaction with the ligands, homology modeling was used to map the binding site based on the CBS domains of IMPDH.[86] This binding site however does not match the interaction now observed in the complex structure, thus emphasizing the need for detailed structural information. Analysis of the binding pocket shows the nucleotide

bound in a novel conformation in comparison to known ATP binding sites. The base and the sugar moiety are inserted into a groove of the protein making several specific interactions, while the phosphate groups are pointing towards the solvent. This mode of nucleotide binding has thereafter been also observed in the CBS domains of the protein AMPK.[111,112] The binding affinities for the different nucleotides AMP, ADP and ATP of the cytoplasmic domains of ClC-5 have been determined and appear to be very similar in the range of 100 μM. Mutating residues involved in specific contacts with the nucleotide caused a drastic reduction of the binding affinities. Interestingly, the loss of nucleotide binding caused by these mutations did not alter the current phenotype of the transporter when studied in heterologous expression. Nonetheless, an altered current voltage relationship was observed when the mutations were introduced in the background of a mutation of the glutamate corresponding to the individual gate in the channels.[22] This well characterized mutant causes ClC-5 to uncouple chloride and proton transport resulting in selective chloride conduction over a broad voltage range. This includes the region of negative potentials where the wildtype protein is usually inactive.[24] At those voltages the transporter would be extruding chloride from the cytoplasm, while taking up protons from the extracellular space or the internalized vesicle. The results suggest that binding of nucleotides to the intracellular domains seems to affect the outward flux of chloride. In the case of ClC-5 the mutations that abolish the binding of nucleotides cause a pronounced reduction of the ion flow in the negative voltage range. Interestingly, in contrast to these findings the addition of ATP,[85–87] as well as AMP,[86] to the intracellular side of ClC-1 appears to inactivate the channel by decreasing the open probabilty. While results in ClC-1 can be conclusively integrated into its physiological role the situation in the case of ClC-5 is rather convoluted.

The physiological function of ClC-5 is proposed to be the shunt of chloride ions into endosomal vesicles that are getting acidified by V-type ATPases.[45] In this role the protein counteracts the building up of a large electric potential across the membrane, which would prevent further proton transport into the vesicle. The details of this function are still poorly understood and several observations seem paradox with regard to this task, especially the action as secondary active transporter.[25,26] For one, to serve the role as a chloride shunt the protein would need to allow chloride to flow in the outward direction with respect to the cytoplasm moving chloride to the extracellular space or inside the vesicles. However, this direction of chloride transport is not observed when the transporter is studied on the plasma membrane. Secondly, the exchange of chloride against protons of ClC-5 would counteract the efforts of the V-type ATPase to acidify the vesicle

by moving protons out of the lumen. In order to explain the obscure involvement of ClC-5 in the acidification of endosomal and lysosomal compartments one could imagine auxiliary factors that activate the transporter under physiological conditions. Another speculative idea would be to switch ClC-5 from a transporter to a channel during the maturation of an endocytotic to a lysosomal vesicle. In this scenario the transporter ClC-5 could use the initial high chloride concentration present in the early endosome, stemming from the extracellular milieu, to acidify the vesicle. Once the V-type ATPases are active on the maturing vesicle, a putative channel ClC-5 could then allow chloride ions to enter the vesicle dissipating the electric potential. Under both circumstances the required outward chloride flux might be activated and the regulation via nucleotide binding could become relevant. Still, the interesting observation that nucleotide binding has a functional effect does not directly explain the physiological rationale behind this regulatory mode. It has been hypothesized that CBS domains serve as energy-sensing modules for the metabolic state of the cell.[79] In order to fulfill this task by nucleotide binding the protein could either sense the concentration change of one of the adenosine nucleotide species or changes in the ratio of ATP:ADP:AMP by competitive interaction.[111,113] In light of this mechanism the experimentally determined binding affinities of the nucleotides to the isolated ClC-5 domains are puzzling, since ATP, with a cellular concentration of 2-5 mM, would be bound virtually all the time. Also a differential binding of ATP and AMP seems unlikely since this competition would require a much higher affinity for AMP due to its low cellular concentration.[114]
Although a number of valuable advances towards understanding of the regulatory role of the cytoplasmic domains in ClC channels and transporters have been made, a number of questions remain:

1. How are the domains positioned with respect to the catalytic domains and the pore?

2. How do the domains influence the conduction behavior of the channel or transporter and which conformational changes accompany the common gating?

3. What is the physiological relevance for the regulatory mode of nucleotide binding and how is it transduced?

To address these issues structural and functional methods have to be combined. Some aspects will have to be worked out by detailed electrophysiological analysis like the physiological importance of the ligand recognition by the cytoplasmic domains. To resolve

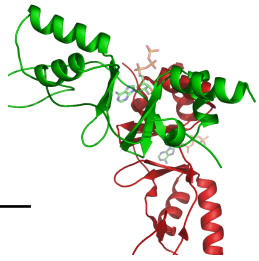

the organization and arrangement of the catalytic and intracellular domains it is crucial to determine a structure of a ClC protein that, in contrast to ecClC, contains both components, membrane embedded and cytosolic domains. The determination of membrane protein structures is still a challenging task, because of the various problems arising at all stages of a crystallization project starting from expression levels, acquisition of material at high purity and proper crystal packing to obtain well diffracting crystals. In a number of cases it has proven useful to turn to prokaryotic homologs for structural studies, since they are generally more readily expressed, biochemically more stable and more amenable to crystallization.[115–118] The structures of these prokaryotic homologs could serve as structural models for the physiological relevant eukaryotic relatives, like in the potassium channel field, where a number of crystal structures of the channel and its auxiliary modules (e.g. the voltage sensor or the ligand binding domains) led the field to the fundamental principles of ion selectivity and conduction.[119] In the case of the ClC family a number of prokaryotic homologs exist that share the domain architecture of the eukaryotic proteins, containing both the catalytic domain with all the conserved features of the selectivity filter and the cytoplasmic domains with both CBS subdomains. These proteins are promising candidates for structural and electrophysiological studies that address the questions raised above. In the appendix .1 preliminary experimental data of the characterization of the homologous ClC protein from the archaebacterial organism *Haloferax volcanii* is included.

Despite initial steps towards the understanding of the molecular function of ClCs, the challenges remaining in the field are numerous and much work still lies ahead to unravel the detailed mechanisms in this remarkable ambivalent family of proteins.

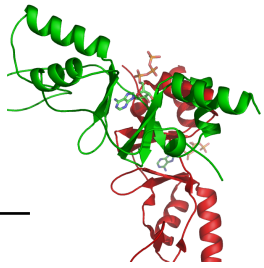

Appendix

.1 Cloning, Expression and Biochemical Characterization of Prokaryotic ClC Homologs

.1.1 Introduction

In order to address the pending questions of ClC mechanism and regulation, as they were outlined in Chapter 3, the combined structural and functional analysis of these proteins is required. In an effort towards this goal I have identified a number of prokaryotic ClC homologs that share the modular domain organization of the eukaryotic proteins. These proteins show the conserved hallmarks of the ClC selectivity filter and include the extended intracellular segments with a pair of CBS domains. Due to these attributes the prokaryotic homologs are excellent candidates to serve as model systems to resolve the molecular architecture and the mechanism of ligand regulation in the ClC family. In several similar cases it has been a successful approach to use prokaryotic proteins to develop structural models for their physiologically relevant eukaryotic homologs.
In the following I will give a summary of the employed strategy to obtain sufficient amounts of purified protein for structural studies or the reconstitution into lipid bilayers to carry out functional experiments. The description of the methodology applied for exploring detergent stability and purification conditions will be discussed mainly on the example of the ClC homolog from *Haloferax volcanii* summarizing the preliminary data towards the structural characterization.

.1.2 Results and Discussion

ClC homologs Prokaryotic ClC homologs were identified by sequence homology to different human ClC proteins, like ClC-1 or ClC-5, using tblastn.[120] In Table 1 the organisms are listed, from which homologs have been chosen for cloning into *E.coli* ex-

Homolog	Sequence homology / identity to hClC-5 [%]
Archaea	
Archaeoglobus fulgidus	30.5 / 16.7
Caldivirga maquilingensis	30.1 / 16.2
Haloferax volcanii	31.1 / 17.6
Hyperthermus butylicus	32.0 / 17.6
Methanoculleus marisnigri	30.1 / 15.9
Methanosaeta thermophila	31.1 / 16.2
Methanosarcina acetivorans	33.1 / 16.8
Methanosarcina mazei	32.9 / 17.5
Picrophilus torridus	31.0 / 17.1
Thermoplasma volcanium	31.0 / 15.4
Bacteria	
Gloeobacter violaceus	35.7 / 21.0 (excluding USP domain)
Nostoc punctiforme	36.1 / 20.2 (excluding USP domain)
Pelodictyon luteolum	33.0 / 18.2
Prosthecochloris vibrioformis	33.3 / 18.3
Rhodopirellula baltica	33.4 / 17.6
Streptomyces coelicolor	32.6 / 18.7
ClC-0	36.1 / 21.9
ecClC	33.3 / 16.6 (only pore domain)

Figure A1: **Prokaryotic ClC Homologs**
Table of the different ClC homologs that were cloned into *E.coli* expression vectors. The organisms are grouped into bacterial and archaebacterial origin and the sequence homology/identity to the human ClC-5 is stated according to a sequence alignment using the Blosum62 matrix of AlignX (Informax). For comparison the homology values for ClC-0 and the ecClC, in the latter case only with the transmembrane part of ClC-5, are given. The two cyanobacterial homologs *G.violaceus* and *N.punctiforme* include an additional protein domain at the C-terminus, the USP (universal stress protein) domain, which was excluded from the alignment.

pression vectors. Subsequently the strains were obtained from either DSMZ, ATCC or the Pasteur Institute.

Cloning, Expression and Membrane Preparation The genomic DNA from the different strains was prepared as described previously,[121] in short: DNA was prepared by resuspending pelleted cells in 500 μl lysis buffer (0.25 M Tris-HCl [pH 8.0], 25 % [wt/vol] sucrose, 10 μg/ml lysozyme) and incubated at 37 °C for 1 h. Sarkosyl (1 % [vol/vol]) and proteinase K (200 μg/ml) were then added, and the cell lysate was incubated at 65 °C for 1 h. Proteins were extracted once with phenol-chloroform (25:24) and once with chloroform-isoamyl alcohol (24:1) before precipitating nucleic acids with one volume of isopropanol and 0.4 volumes of 7.5 M ammonium acetate at room temperature.

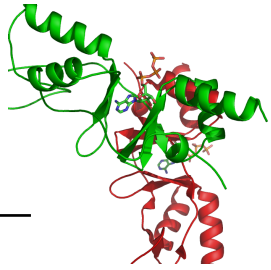

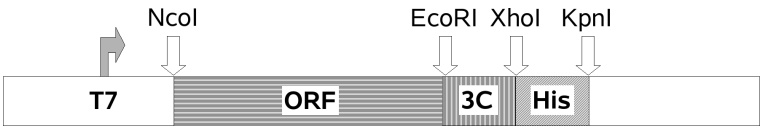

Figure A2: **Schematic Vector Map**
A schematic map of the hvClC expression construct in the pET28b vector. The sequence features are indicated as grey boxes from the 5' to the 3' direction on the vector. The open reading frame (ORF) followed by the 3C protease cleavage site and finally the histidine tag. On the top of the vector the different restriction sites used to assemble the construct are indicated by arrows. This cartoon is exemplary also for the different homologs mentioned in Appendix Figure A1.

Nucleic acids were recovered by centrifugation, washed once with 70 % (vol/vol) ethanol and resuspended in TE (10 mM Tris-HCl [pH 8.0], 0.1 mM EDTA) prior to storage at -20 °C. The cloning of the desired DNA sequences was performed by PCR with primers containing compatible restriction sites for different *E.coli* expression vectors, like pET28b or pQE60, containing poly-histidine affinity tags either at the N- or C-terminus of the protein.

Of the number of different homologs that were tested for expression in *E.coli* only about 25 % showed detectable signals in western blot analysis. This reduced the number of investigated candidates drastically and in the remainder I will limit the description of the protein analysis on one candidate protein. The homolog from the archaebacterium *Haloferax volcanii* (hvClC) that will be discussed in the following was cloned into a modified pET28b with a C-terminal His_{10} fusion tag.

For protein expression the construct was transformed into chemically competent BL21-(DE3) cells and the culture was grown in LB to an OD_{600} of 1 and induced for overnight expression at 20 °C with 0.5 mM IPTG. The cells were harvested by centrifugation and resuspended in lysis buffer: 50 mM sodium phosphate (pH 8), 300 mM NaCl, 200 mg/l lysozyme, 20 mg/l DNase, leupeptin, pepstatin and 1 mM phenylmethyl sulphonyl fluoride, all the following steps were carried out at 4 °C. The cells were disrupted using an EmulsiFlex (Avestin) and the lysate was cleared by centrifugation for 35 min at 12000 g. Subsequently, the membrane fraction was pelleted by centrifugation at 100000 g for 1 h. The isolated membranes were washed once in 50 mM sodium phosphate (pH 8), 300 mM NaCl (Buffer A) by resuspending followed by a second centrifugation step. Buffer A was used throughout the following steps. Membranes were flash-frozen in liquid nitrogen and stored at -80 °C.

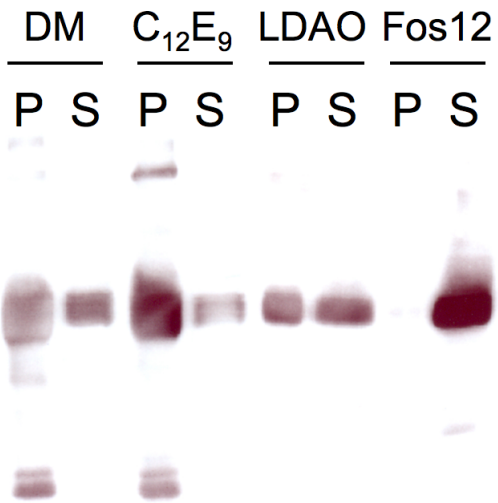

Figure A3: **Detergent-Extraction of hvClC**
Western blot analysis of a detergent extraction of the hvClC. The extraction performance of four different detergents was tested by analysis of the solubilized fraction (S) and the membrane pellet (P) after extraction and centrifugation. The signal for the hvClC is observed in the center of the lane and is in all cases the predominant band. The efficiency of the detergents n-Decyl-β-D-maltopyranoside (DM), Polyoxyethylene(9)dodecyl ether ($C_{12}E_9$), n-Dodecyl-N,N-dimethylamine-N-oxide (LDAO) and Fos-choline-12 (Fos12) is judged by comparison of the ratio of signal in the S to the P fraction.

Detergent Extraction The isolated membrane fraction was resuspended in Buffer A at a ratio of 10 ml per g of membrane and solubilized in 2 % of detergent for 2 h. Initial trials were carried out in 1 ml fractions using different detergents to analyze the efficiency of the solubilization. The unsolubilized lipid fraction was pelleted by centrifugation (100000 g for 1 h) and the two fractions were analyzed by western blot detecting the expressed protein via an α-his antibody (Roche). The analysis (Figure A3) revealed that all of the tested detergents were suitable to extract a large portion of the protein from the membrane, although the efficiency differed from almost complete extraction in Fos-choline-12 (Fos12) to partial extraction in n-Decyl-β-D-maltopyranoside (DM), n-Dodecyl-N,N-dimethylamine-N-oxide (LDAO) and Polyoxyethylene(9)dodecyl ether ($C_{12}E_9$).

Detergent Stability Analysis In order to assess the protein stability in different detergents the migration behavior on a gelfiltration column was exploited to differentiate mono-disperse from aggregated sample. In a simple assay, similar to a previously described approach,[122] the crude membrane extract from the small scale detergent solubilization is filtered with a 0.45 μm spin-filter and applied on a Superdex200 column (GE Healthcare). The retention volume of the protein of interest was determined by western blot analysis of the elution fractions starting from the void volume of 7 ml up to 13 ml. To confirm that the technique faithfully reflects the elution profile of the purified pro-

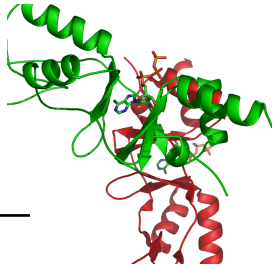

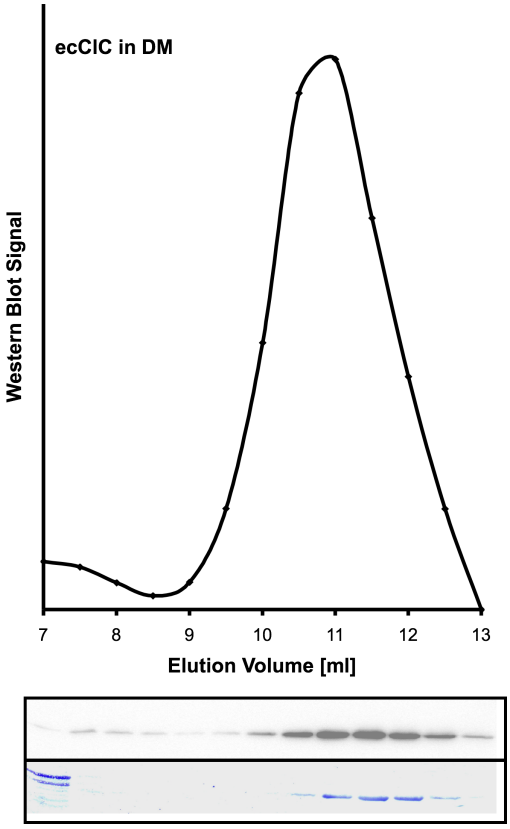

Figure A4: **Gelfiltration Analysis of ecClC**
Comparison of the elution profile of crude membrane extract versus purified ecClC from a Superdex200 size exclusion column in DM. The upper panel shows the plot of the western blot quantification of the crude membrane fraction gelfiltration (middle panel). The lower panel shows a coomassie stained SDS-PAGE of a gelfiltration run of purified ecClC. The slight shift towards higher elution volume is due to the increased volume of the tubing of the system with connected UV detector.

tein gelfiltration was initially performed on samples of ecClC, both purified and as crude extract in DM. The protein was expressed and purified as described previously[21] and the elution profiles were analyzed by UV280 absorbance and coomassie staining for the purified protein and by western blot for the unpurified sample. The western blot analysis was carried out with the chemiluminescent western blot detection kit (Millipore) and the signals were evaluated as integrated peak intensities using the software AIDA (Raytest). The comparison, as shown in Figure A4, showed a good agreement of the retention volumes.

In order to determine the detergent stability of hvClC in crude membrane extracts, the samples were loaded on the gelfiltration column and 500 μl fractions were collected starting at the void volume of the column (Figure A5). The protein amount in the fractions was quantified and plotted in comparison to the values for the ecClC as reference. The results indicate that the protein shows heavy aggregation in DM with the majority of the protein eluting in the void volume. In the case of C12E9 an intermediate behavior could be observed with part of the protein eluting at about 10.5 ml corresponding to

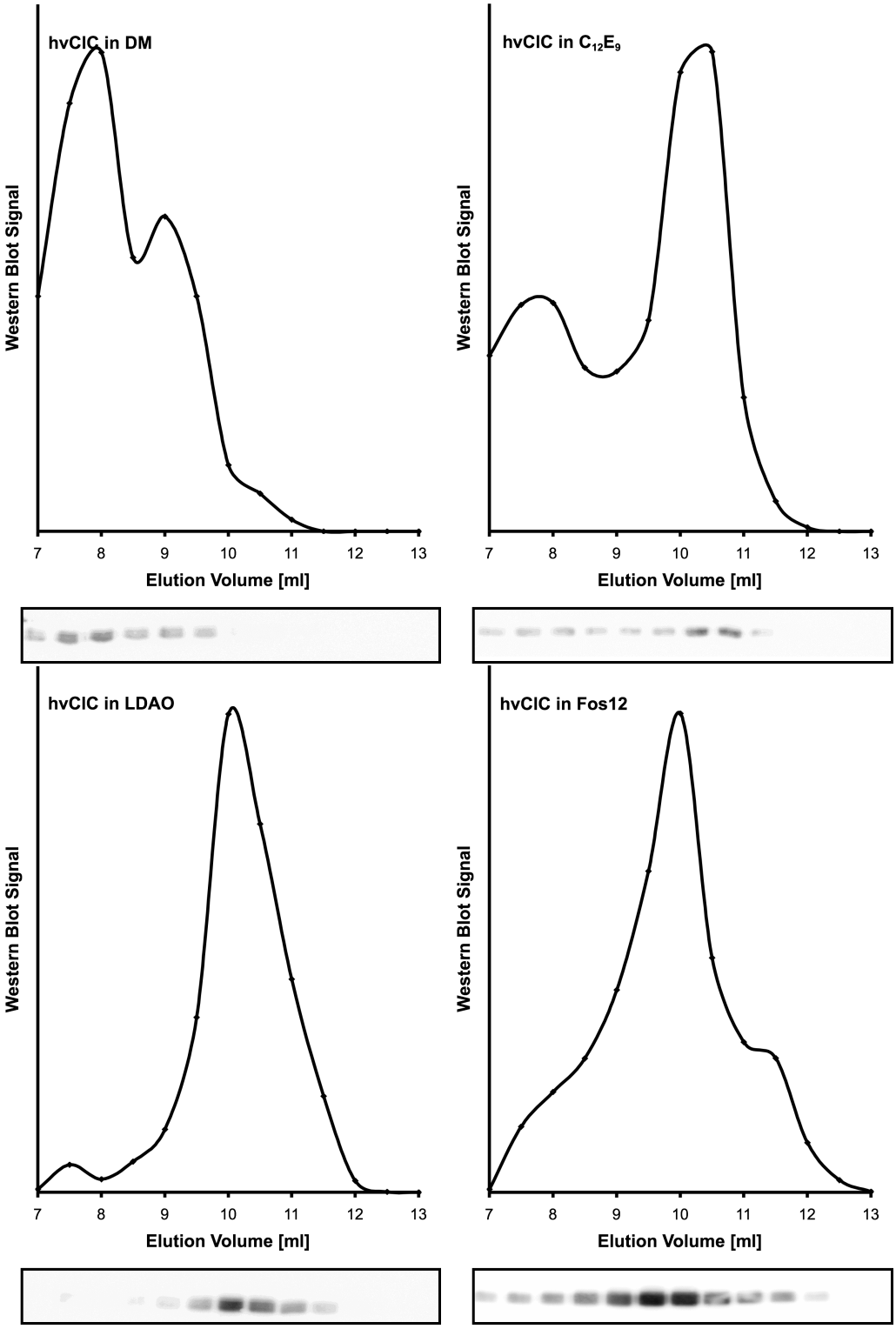

Figure A5: **Gelfiltration Analysis of hvClC**
Western blot analysis of the Superdex200 size exclusion elution profiles of crude membrane extracts of hvClC. Membrane extracts of hvClC in four different detergents were separated by gelfiltration and analysed by western blot quantification. The western blots and the resulting plots are depicted.

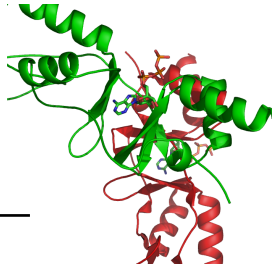

an appropriate molecular weight of the dimeric hvClC, which is shifted towards a lower elution volume with respect to the ∼30 kDa smaller ecClC. Nevertheless, a large amount of the protein showed aggregation suggesting limited stability in $C_{12}E_9$. For the detergents Fos12 and LDAO on the other hand the analysis revealed a preferential elution at 10.5 ml suggesting these detergents extract the hvClC natively from the membrane and the protein remains stable in solution during the course of the experiment. The asymmetry in the peakshape of Fos12 sample is most likely due to the strong signals on the western blot caused by the comparatively higher amounts of extracted protein. Hence, these results led to the choice of the LDAO and Fos12 for extraction and purification in the subsequent experiments.

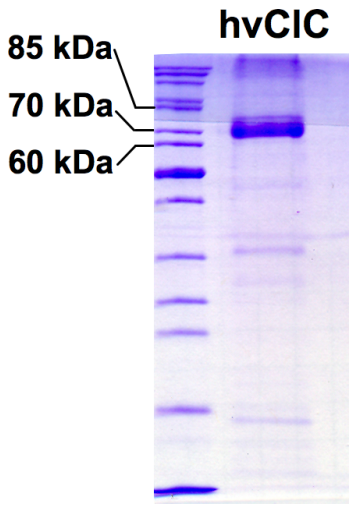

Figure A6: **Coomassie Stained Gel of Purified hvClC**
SDS PAGE of the hvClC (∼70 kDa) elution fractions after IMAC.

Protein Purification For the purification of the hvClC membrane extracts were prepared using either LDAO or Fos12 and the protein was bound in batch for 2 h to Protino Ni-IDA resin (Macherey-Nagel) in a ratio of about 1 ml bed volume per 10 ml of extract. The loaded resin was applied to a Econo-chromatography column (Bio-Rad) and washed with 12 column volumes of buffer containing 15 mM of imidazole. The protein was eluted with buffer containing 300 mM imidazole and the purity was assessed by SDS-PAGE and coomassie staining (Figure A6).

As an additional purification step and to further evaluate the oligomeric state of the protein and potential aggregation behavior the purified protein was subjected to size exclusion chromatography on a Superdex200 column. The elution pool from the immobilized metal affinity chromatography was concentrated and separated by size exclusion chromatography. The analysis of the elution profile revealed that during the purification higher molecular aggregates of the protein are being formed causing the hvClC to elute in the void volume of about 8 ml (Figure A7). Only a minor fraction of the protein was found to migrate as the dimer, when a not concentrated sample was analyzed. This dramatic aggregation behavior was observed regardless whether the protein was digested with 3C protease to remove the affinity-tag or prepared in LDAO or Fos12.

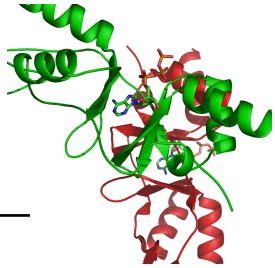

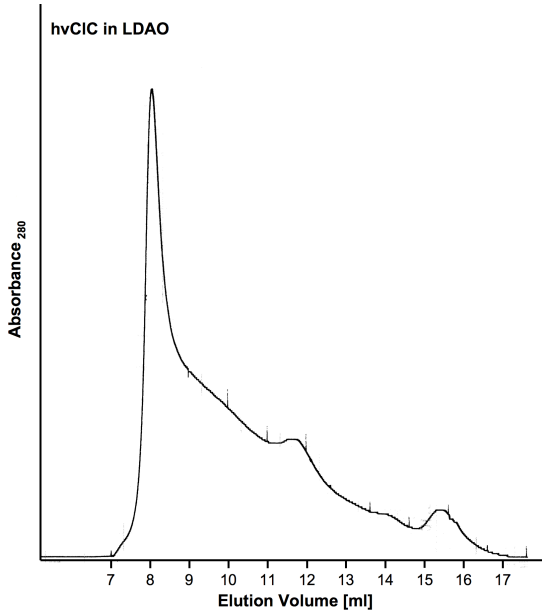

Figure A7: **Gelfiltration of Purified hvClC** Gelfiltration elution profile of the purified hvClC, plot of the absorbance at 280 nm. The concentrated sample of the hvClC was loaded on a Superdex200 size exclusion column and the protein elution was monitored by plotting the Abs_{280}. An example of the purification in LDAO is shown, however, comporable results were also obtained in Fos-12.

In summary, the screening of several prokaryotic ClC homologs led to the identification of a potential candidate for structural analysis. During the further biochemical characterization of the ClC protein from *Haloferax volcanii* an extraction and purification protocol could be established for two detergents. However, the assessment of the protein quality revealed that during the purification process the hvClC formed higher molecular aggregates making it unsuitable for crystallographic studies.

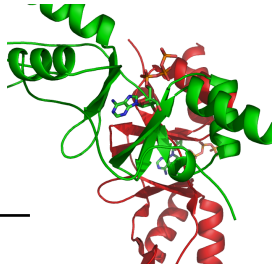

References

[1] S. Meyer and R. Dutzler. Crystal structure of the cytoplasmic domain of the chloride channel ClC-0. *Structure*, 14(2):299–307, Feb 2006.

[2] S. Alioth, S. Meyer, R .Dutzler, and K. Pervushin. The cytoplasmic domain of the chloride channel ClC-0: structural and dynamic characterization of flexible regions. *J Mol Biol*, 369(5):1163–1169, Jun 2007.

[3] S. Meyer, S. Savaresi, I. C. Forster, and R. Dutzler. Nucleotide recognition by the cytoplasmic domain of the human chloride transporter ClC-5. *Nat Struct Mol Biol*, 14(1):60–67, Jan 2007.

[4] M. C. Sanguinetti and M. Tristani-Firouzi. hERG potassium channels and cardiac arrhythmia. *Nature*, 440(7083):463–469, Mar 2006.

[5] M. L. Mayer. Glutamate receptors at atomic resolution. *Nature*, 440(7083):456–462, Mar 2006.

[6] S. M. Sine and A. G. Engel. Recent advances in Cys-loop receptor structure and function. *Nature*, 440(7083):448–455, Mar 2006.

[7] C. Kung. A possible unifying principle for mechanosensation. *Nature*, 436(7051):647–654, Aug 2005.

[8] T. J. Jentsch, V. Stein, F. Weinreich, and A. A. Zdebik. Molecular structure and physiological function of chloride channels. *Physiol Rev*, 82(2):503–568, Apr 2002.

[9] D. B. Mount and M. F. Romero. The SLC26 gene family of multifunctional anion exchangers. *Pflugers Arch*, 447(5):710–721, Feb 2004.

[10] A. Vandewalle. Expression and function of CLC and cystic fibrosis transmembrane conductance regulator chloride channels in renal epithelial tubule cells: pathophysiological implications. *Chang Gung Med J*, 30(1):17–25, 2007.

[11] C. Miller. ClC chloride channels viewed through a transporter lens. *Nature*, 440(7083):484–489, Mar 2006.

[12] S. Sile, C. G. Vanoye, and A. L. George. Molecular physiology of renal ClC chloride channels/transporters. *Curr Opin Nephrol Hypertens*, 15(5):511–516, Sep 2006.

[13] M. M. White and C. Miller. A voltage-gated anion channel from the electric organ of Torpedo californica. *J Biol Chem*, 254(20):10161–10166, Oct 1979.

[14] T. J. Jentsch, K. Steinmeyer, and G. Schwarz. Primary structure of Torpedo marmorata chloride channel isolated by expression cloning in Xenopus oocytes. *Nature*, 348(6301):510–514, Dec 1990.

[15] K. Steinmeyer, R. Klocke, C. Ortland, M. Gronemeier, H. Jockusch, S. Gründer, and T. J. Jentsch. Inactivation of muscle chloride channel by transposon insertion in myotonic mice. *Nature*, 354(6351):304–308, Nov 1991.

[16] A. Thiemann, S. Gründer, M. Pusch, and T. J. Jentsch. A chloride channel widely expressed in epithelial and non-epithelial cells. *Nature*, 356(6364):57–60, Mar 1992.

[17] S. Kieferle, P. Fong, M. Bens, A. Vandewalle, and T. J. Jentsch. Two highly homologous members of the ClC chloride channel family in both rat and human kidney. *Proc Natl Acad Sci U S A*, 91(15):6943–6947, Jul 1994.

[18] S. Sasaki, S. Uchida, M. Kawasaki, S. Adachi, and F. Marumo. ClC family in the kidney. *Jpn J Physiol*, 44 Suppl 2:S3–S8, 1994.

[19] K. Steinmeyer, B. Schwappach, M. Bens, A. Vandewalle, and T. J. Jentsch. Cloning and functional expression of rat CLC-5, a chloride channel related to kidney disease. *J Biol Chem*, 270(52):31172–31177, Dec 1995.

[20] S. Brandt and T. J. Jentsch. ClC-6 and ClC-7 are two novel broadly expressed members of the CLC chloride channel family. *FEBS Lett*, 377(1):15–20, Dec 1995.

[21] R. Dutzler, E. B. Campbell, M. Cadene, B. T. Chait, and R. MacKinnon. X-ray structure of a ClC chloride channel at 3.0 Å reveals the molecular basis of anion selectivity. *Nature*, 415(6869):287–294, Jan 2002.

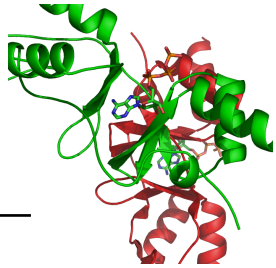

[22] R. Dutzler, E. B. Campbell, and R. MacKinnon. Gating the selectivity filter in ClC chloride channels. *Science*, 300(5616):108–112, Apr 2003.

[23] M. Maduke, C. Miller, and J. A. Mindell. A decade of CLC chloride channels: structure, mechanism, and many unsettled questions. *Annu Rev Biophys Biomol Struct*, 29:411–438, 2000.

[24] T. Friedrich, T. Breiderhoff, and T. J. Jentsch. Mutational analysis demonstrates that ClC-4 and ClC-5 directly mediate plasma membrane currents. *J Biol Chem*, 274(2):896–902, Jan 1999.

[25] O. Scheel, A. A. Zdebik, S. Lourdel, and T. J. Jentsch. Voltage-dependent electrogenic chloride/proton exchange by endosomal CLC proteins. *Nature*, 436(7049):424–427, Jul 2005.

[26] A. Picollo and M. Pusch. Chloride/proton antiporter activity of mammalian CLC proteins ClC-4 and ClC-5. *Nature*, 436(7049):420–423, Jul 2005.

[27] A. Accardi, M. Walden, W. Nguitragool, H. Jayaram, C. Williams, and C. Miller. Separate ion pathways in a Cl-/H+ exchanger. *J Gen Physiol*, 126(6):563–570, Dec 2005.

[28] A. Accardi and C. Miller. Secondary active transport mediated by a prokaryotic homologue of ClC Cl- channels. *Nature*, 427(6977):803–807, Feb 2004.

[29] R. Estévez, T. Boettger, V. Stein, R. Birkenhäger, E. Otto, F. Hildebrandt, and T. J. Jentsch. Barttin is a Cl- channel beta-subunit crucial for renal Cl- reabsorption and inner ear K+ secretion. *Nature*, 414(6863):558–561, Nov 2001.

[30] P. F. Lange, L. Wartosch, T. J. Jentsch, and J. C. Fuhrmann. ClC-7 requires Ostm1 as a beta-subunit to support bone resorption and lysosomal function. *Nature*, 440(7081):220–223, Mar 2006.

[31] S. Waldegger, N. Jeck, P. Barth, M. Peters, H. Vitzthum, K. Wolf, A. Kurtz, M. Konrad, and H. W. Seyberth. Barttin increases surface expression and changes current properties of ClC-K channels. *Pflugers Arch*, 444(3):411–418, Jun 2002.

[32] T. J. Jentsch, M. Poët, J. C. Fuhrmann, and A. A. Zdebik. Physiological functions of CLC Cl- channels gleaned from human genetic disease and mouse models. *Annu Rev Physiol*, 67:779–807, 2005.

[33] T. J. Jentsch, I. Neagoe, and O. Scheel. CLC chloride channels and transporters. *Curr Opin Neurobiol*, 15(3):319–325, Jun 2005.

[34] A. L. Hodgkin and P. Horwicz. The influence of potassium and chloride ions on the membrane potential of single muscle fibres. *J Physiol*, 148:127–160, Oct 1959.

[35] M. C. Koch, K. Steinmeyer, C. Lorenz, K. Ricker, F. Wolf, M. Otto, B. Zoll, F. Lehmann-Horn, K. H. Grzeschik, and T. J. Jentsch. The skeletal muscle chloride channel in dominant and recessive human myotonia. *Science*, 257(5071):797–800, Aug 1992.

[36] C. L. Beck, C. Fahlke, and A. L. George. Molecular basis for decreased muscle chloride conductance in the myotonic goat. *Proc Natl Acad Sci U S A*, 93(20):11248–11252, Oct 1996.

[37] K. Haug, M. Warnstedt, A. K. Alekov, T. Sander, A. Ramírez, B. Poser, S. Maljevic, S. Hebeisen, C. Kubisch, J. Rebstock, S. Horvath, K. Hallmann, J. S. Dullinger, B. Rau, F. Haverkamp, S. Beyenburg, H. Schulz, D. Janz, B. Giese, G. Müller-Newen, P. Propping, C. E. Elger, C. Fahlke, H. Lerche, and A. Heils. Mutations in CLCN2 encoding a voltage-gated chloride channel are associated with idiopathic generalized epilepsies. *Nat Genet*, 33(4):527–532, Apr 2003.

[38] J. Blanz, M. Schweizer, M. Auberson, H. Maier, A. Muenscher, C. A. Hübner, and T. J. Jentsch. Leukoencephalopathy upon disruption of the chloride channel ClC-2. *J Neurosci*, 27(24):6581–6589, Jun 2007.

[39] S. Waldegger and T. J. Jentsch. Functional and structural analysis of ClC-K chloride channels involved in renal disease. *J Biol Chem*, 275(32):24527–24533, Aug 2000.

[40] S. M. Stobrawa, T. Breiderhoff, S. Takamori, D. Engel, M. Schweizer, A. A. Zdebik, M. R. Bösl, K. Ruether, H. Jahn, A. Draguhn, R. Jahn, and T. J. Jentsch. Disruption of ClC-3, a chloride channel expressed on synaptic vesicles, leads to a loss of the hippocampus. *Neuron*, 29(1):185–196, Jan 2001.

[41] R. Mohammad-Panah, R. Harrison, S. Dhani, C. Ackerley, L. J. Huan, Y. Wang, and C. E. Bear. The chloride channel ClC-4 contributes to endosomal acidification and trafficking. *J Biol Chem*, 278(31):29267–29277, Aug 2003.

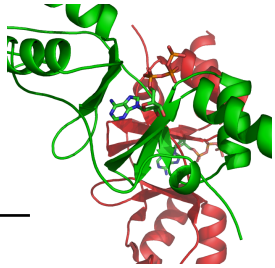

[42] C. G. Vanoye and A. L. George. Functional characterization of recombinant human ClC-4 chloride channels in cultured mammalian cells. *J Physiol*, 539(Pt 2):373–383, Mar 2002.

[43] T. Wang and S. A. Weinman. Involvement of chloride channels in hepatic copper metabolism: ClC-4 promotes copper incorporation into ceruloplasmin. *Gastroenterology*, 126(4):1157–1166, Apr 2004.

[44] N. Piwon, W. Günther, M. Schwake, M. R. Bösl, and T. J. Jentsch. ClC-5 Cl- -channel disruption impairs endocytosis in a mouse model for Dent's disease. *Nature*, 408(6810):369–373, Nov 2000.

[45] W. Günther, A. Lüchow, F. Cluzeaud, A. Vandewalle, and T. J. Jentsch. ClC-5, the chloride channel mutated in Dent's disease, colocalizes with the proton pump in endocytotically active kidney cells. *Proc Natl Acad Sci U S A*, 95(14):8075–8080, Jul 1998.

[46] S. E. Lloyd, S. H. Pearce, S. E. Fisher, K. Steinmeyer, B. Schwappach, S. J. Scheinman, B. Harding, A. Bolino, M. Devoto, P. Goodyer, S. P. Rigden, O. Wrong, T. J. Jentsch, I. W. Craig, and R. V. Thakker. A common molecular basis for three inherited kidney stone diseases. *Nature*, 379(6564):445–449, Feb 1996.

[47] M. Poët, U. Kornak, M. Schweizer, A. A. Zdebik, O. Scheel, S. Hoelter, W. Wurst, A. Schmitt, J. C. Fuhrmann, R. Planells-Cases, S. E. Mole, C. A. Hübner, and T. J. Jentsch. Lysosomal storage disease upon disruption of the neuronal chloride transport protein ClC-6. *Proc Natl Acad Sci U S A*, 103(37):13854–13859, Sep 2006.

[48] U. Kornak, D. Kasper, M. R. Bösl, E. Kaiser, M. Schweizer, A. Schulz, W. Friedrich, G. Delling, and T. J. Jentsch. Loss of the ClC-7 chloride channel leads to osteopetrosis in mice and man. *Cell*, 104(2):205–215, Jan 2001.

[49] D. Kasper, R. Planells-Cases, J. C. Fuhrmann, O. Scheel, O. Zeitz, K. Ruether, A. Schmitt, M. Poët, R. Steinfeld, M. Schweizer, U. Kornak, and T. J. Jentsch. Loss of the chloride channel ClC-7 leads to lysosomal storage disease and neurodegeneration. *EMBO J*, 24(5):1079–1091, Mar 2005.

[50] R. E. Middleton, D. J. Pheasant, and C. Miller. Homodimeric architecture of a ClC-type chloride ion channel. *Nature*, 383(6598):337–340, Sep 1996.

[51] F. Weinreich and T. J. Jentsch. Pores formed by single subunits in mixed dimers of different CLC chloride channels. *J Biol Chem*, 276(4):2347–2353, Jan 2001.

[52] C. Miller. Open-state substructure of single chloride channels from Torpedo electroplax. *Philos Trans R Soc Lond B Biol Sci*, 299(1097):401–411, Dec 1982.

[53] A. Bateman. The structure of a domain common to archaebacteria and the homocystinuria disease protein. *Trends Biochem Sci*, 22(1):12–13, Jan 1997.

[54] E. Gouaux and R. Mackinnon. Principles of selective ion transport in channels and pumps. *Science*, 310(5753):1461–1465, Dec 2005.

[55] C. Miller and M. M. White. Dimeric structure of single chloride channels from Torpedo electroplax. *Proc Natl Acad Sci U S A*, 81(9):2772–2775, May 1984.

[56] M. Pusch, K. Steinmeyer, and T. J. Jentsch. Low single channel conductance of the major skeletal muscle chloride channel, ClC-1. *Biophys J*, 66(1):149–152, Jan 1994.

[57] C. Saviane, F. Conti, and M. Pusch. The muscle chloride channel ClC-1 has a double-barreled appearance that is differentially affected in dominant and recessive myotonia. *J Gen Physiol*, 113(3):457–468, Mar 1999.

[58] M. Walden, A. Accardi, F. Wu, C. Xu, C. Williams, and C. Miller. Uncoupling and turnover in a Cl-/H+ exchange transporter. *J Gen Physiol*, 129(4):317–329, Apr 2007.

[59] R. Estévez, B. C. Schroeder, A. Accardi, T. J. Jentsch, and M. Pusch. Conservation of chloride channel structure revealed by an inhibitor binding site in ClC-1. *Neuron*, 38(1):47–59, Apr 2003.

[60] W. Hanke and C. Miller. Single chloride channels from Torpedo electroplax. Activation by protons. *J Gen Physiol*, 82(1):25–45, Jul 1983.

[61] U. Ludewig, M. Pusch, and T. J. Jentsch. Two physically distinct pores in the dimeric ClC-0 chloride channel. *Nature*, 383(6598):340–343, Sep 1996.

[62] T.Y. Chen. Structure and function of ClC channels. *Annu Rev Physiol*, 67:809–839, 2005.

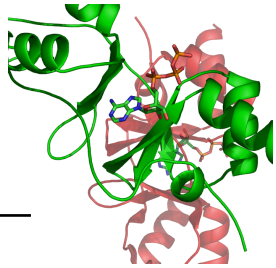

[63] M. Pusch, U. Ludewig, A. Rehfeldt, and T. J. Jentsch. Gating of the voltage-dependent chloride channel CIC-0 by the permeant anion. *Nature*, 373(6514):527–531, Feb 1995.

[64] S. B. Long, E. B. Campbell, and R. Mackinnon. Voltage sensor of Kv1.2: structural basis of electromechanical coupling. *Science*, 309(5736):903–908, Aug 2005.

[65] S. B. Long, E. B. Campbell, and R. Mackinnon. Crystal structure of a mammalian voltage-dependent Shaker family K+ channel. *Science*, 309(5736):897–903, Aug 2005.

[66] Y. W. Lin, C. W. Lin, and T. Y. Chen. Elimination of the slow gating of ClC-0 chloride channel by a point mutation. *J Gen Physiol*, 114(1):1–12, Jul 1999.

[67] P. Fong, A. Rehfeldt, and T. J. Jentsch. Determinants of slow gating in ClC-0, the voltage-gated chloride channel of Torpedo marmorata. *Am J Physiol*, 274(4 Pt 1):C966–C973, Apr 1998.

[68] T. Y. Chen and C. Miller. Nonequilibrium gating and voltage dependence of the ClC-0 Cl- channel. *J Gen Physiol*, 108(4):237–250, Oct 1996.

[69] M. Pusch, S. E. Jordt, V. Stein, and T. J. Jentsch. Chloride dependence of hyperpolarization-activated chloride channel gates. *J Physiol*, 515 (Pt 2):341–353, Mar 1999.

[70] M. Pusch, U. Ludewig, and T. J. Jentsch. Temperature dependence of fast and slow gating relaxations of ClC-0 chloride channels. *J Gen Physiol*, 109(1):105–116, Jan 1997.

[71] C. Miller and M. M. White. A voltage-dependent chloride conductance channel from Torpedo electroplax membrane. *Ann N Y Acad Sci*, 341:534–551, 1980.

[72] A. Accardi, S. Lobet, C. Williams, C. Miller, and R. Dutzler. Synergism between halide binding and proton transport in a CLC-type exchanger. *J Mol Biol*, 362(4):691–699, Sep 2006.

[73] W. Nguitragool and C. Miller. Uncoupling of a CLC Cl-/H+ exchange transporter by polyatomic anions. *J Mol Biol*, 362(4):682–690, Sep 2006.

[74] M. Maduke, C. Williams, and C. Miller. Formation of CLC-0 chloride channels from separated transmembrane and cytoplasmic domains. *Biochemistry*, 37(5):1315–1321, Feb 1998.

[75] T. Schmidt-Rose and T. J. Jentsch. Reconstitution of functional voltage-gated chloride channels from complementary fragments of CLC-1. *J Biol Chem*, 272(33):20515–20521, Aug 1997.

[76] R. Estévez, M. Pusch, C. Ferrer-Costa, M. Orozco, and T. J. Jentsch. Functional and structural conservation of CBS domains from CLC chloride channels. *J Physiol*, 557(Pt 2):363–378, Jun 2004.

[77] S. Ignoul and J. Eggermont. CBS domains: structure, function, and pathology in human proteins. *Am J Physiol Cell Physiol*, 289(6):C1369–C1378, Dec 2005.

[78] M. D. Miller, R. Schwarzenbacher, F. von Delft, P. Abdubek, E. Ambing, T. Biorac, L. S. Brinen, J. M. Canaves, J. Cambell, H. J. Chiu, X. Dai, A. M. Deacon, M. DiDonato, M. A. Elsliger, S. Eshagi, R. Floyd, A. Godzik, C. Grittini, S. K Grzechnik, E. Hampton, L. Jaroszewski, C. Karlak, H. E. Klock, E. Koesema, J. S. Kovarik, A. Kreusch, P. Kuhn, S. A. Lesley, I. Levin, D. McMullan, T. M. McPhillips, A. Morse, K. Moy, J. Ouyang, R. Page, K. Quijano, A. Robb, G. Spraggon, R. C. Stevens, H. van den Bedem, J. Velasquez, J. Vincent, X. Wang, B. West, G. Wolf, Q. Xu, K. O. Hodgson, J. Wooley, and I. A. Wilson. Crystal structure of a tandem cystathionine-beta-synthase (CBS) domain protein (TM0935) from Thermotoga maritima at 1.87 Å resolution. *Proteins*, 57(1):213–217, Oct 2004.

[79] J. W. Scott, S. A. Hawley, K. A. Green, M. Anis, G. Stewart, G. A. Scullion, D. G. Norman, and D. G. Hardie. CBS domains form energy-sensing modules whose binding of adenosine ligands is disrupted by disease mutations. *J Clin Invest*, 113(2):274–284, Jan 2004.

[80] B. Schwappach, S. Stobrawa, M. Hechenberger, K. Steinmeyer, and T. J. Jentsch. Golgi localization and functionally important domains in the NH2 and COOH terminus of the yeast CLC putative chloride channel Gef1p. *J Biol Chem*, 273(24):15110–15118, Jun 1998.

[81] M. Schwake, T. Friedrich, and T. J. Jentsch. An internalization signal in ClC-5, an endosomal Cl-channel mutated in dent's disease. *J Biol Chem*, 276(15):12049–12054, Apr 2001.

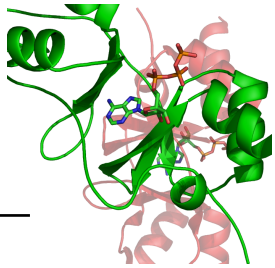

[82] J. Denton, K. Nehrke, X. Yin, A. M. Beld, and K. Strange. Altered gating and regulation of a carboxy-terminal ClC channel mutant expressed in the Caenorhabditis elegans oocyte. *Am J Physiol Cell Physiol*, 290(4):C1109–C1118, Apr 2006.

[83] E. A. Bykova, X. D. Zhang, T. Y. Chen, and J. Zheng. Large movement in the C terminus of CLC-0 chloride channel during slow gating. *Nat Struct Mol Biol*, 13(12):1115–1119, Dec 2006.

[84] L. Wellhauser, H. H. Kuo, F. L. L. Stratford, M. Ramjeesingh, L. J. Huan, W. Luong, C. Li, C. M. Deber, and C. E. Bear. Nucleotides bind to the C-terminus of ClC-5. *Biochem J*, 398(2):289–294, Sep 2006.

[85] B. Bennetts, M. W. Parker, and B. A. Cromer. Inhibition of skeletal muscle CLC-1 chloride channels by low intracellular pH and ATP. *J Biol Chem*, Aug 2007.

[86] B. Bennetts, G. Y. Rychkov, H. L. Ng, C. J. Morton, D. Stapleton, M. W. Parker, and B. A. Cromer. Cytoplasmic ATP-sensing domains regulate gating of skeletal muscle ClC-1 chloride channels. *J Biol Chem*, 280(37):32452–32458, Sep 2005.

[87] P. Y. Tseng, B. Bennetts, and T. Y. Chen. Cytoplasmic ATP inhibition of CLC-1 is enhanced by low pH. *J Gen Physiol*, 130(2):217–221, Aug 2007.

[88] S. Markovic and R. Dutzler. The structure of the cytoplasmic domain of the chloride channel ClC-Ka reveals a conserved interaction interface. *Structure*, 15(6):715–725, Jun 2007.

[89] S. Hebeisen, A. Biela, B. Giese, G. Müller-Newen, P. Hidalgo, and C. Fahlke. The role of the carboxyl terminus in ClC chloride channel function. *J Biol Chem*, 279(13):13140–13147, Mar 2004.

[90] J. Cuppoletti, K. P. Tewari, A. M. Sherry, C. J. Ferrante, and D. H. Malinowska. Sites of protein kinase A activation of the human ClC-2 Cl(-) channel. *J Biol Chem*, 279(21):21849–21856, May 2004.

[91] J. Denton, K. Nehrke, X. Yin, R. Morrison, and K. Strange. GCK-3, a newly identified Ste20 kinase, binds to and regulates the activity of a cell cycle-dependent ClC anion channel. *J Gen Physiol*, 125(2):113–125, Feb 2005.

[92] K. Pervushin, R. Riek, G. Wider, and K. Wüthrich. Attenuated T2 relaxation by mutual cancellation of dipole–dipole coupling and chemical shift anisotropy

indicates an avenue to NMR structures of very large biological macromolecules in solution. *Proc Natl Acad Sci U S A*, 94(23):12366–12371, Nov 1997.

[93] M. Salzmann, K. Pervushin, G. Wider, H. Senn, and K. Wüthrich. [13C]-constant-time [15N,1H]-TROSY-HNCA for sequential assignments of large proteins. *J Biomol NMR*, 14(1):85–88, May 1999.

[94] M. Salzmann, K. Pervushin, G. Wider, H. Senn, and K. Wüthrich. TROSY in triple-resonance experiments: new perspectives for sequential NMR assignment of large proteins. *Proc Natl Acad Sci U S A*, 95(23):13585–13590, Nov 1998.

[95] S. Talluri and G. Wagner. An optimized 3D NOESY-HSQC. *J Magn Reson B*, 112(2):200–205, Aug 1996.

[96] G. Zhu, Y. Xia, L. K. Nicholson, and K. H. Sze. Protein dynamics measurements by TROSY-based NMR experiments. *J Magn Reson*, 143(2):423–426, Apr 2000.

[97] A. M. Mandel, M. Akke, and A. G. Palmer. Backbone dynamics of Escherichia coli ribonuclease HI: correlations with structure and function in an active enzyme. *J Mol Biol*, 246(1):144–163, Feb 1995.

[98] A. G. Palmer, M. Rance, and P. E. Wright. Intramolecular Motions of a Zinc Finger DNA-Binding Domain from Xfin Characterized by Proton-Detected Natural Abundance C-12 Heteronuclear Nmr-Spectroscopy. *Journal of the American Chemical Society*, 113:4371–4380, 1991.

[99] V. Y. Orekhov, D. M. Korzhnev, K. V. Pervushin, E. Hoffmann, and A. S. Arseniev. Sampling of protein dynamics in nanosecond time scale by 15N NMR relaxation and self-diffusion measurements. *J Biomol Struct Dyn*, 17(1):157–174, Aug 1999.

[100] A. J. Dingley, J. P. Mackay, G. L. Shaw, B. D. Hambly, and G. F. King. Measuring macromolecular diffusion using heteronuclear multiple-quantum pulsed-field-gradient nmr. *Journal of Biomolecular NMR*, 10:1–8, 1997.

[101] A. J. Dingley, J. P. Mackay, B. E. Chapman, M. B. Morris, P. W. Kuchel, B. D. Hambly, and G. F. King. Measuring protein self-association using pulsed-field-gradient NMR spectroscopy: application to myosin light chain 2. *J Biomol NMR*, 6(3):321–328, Nov 1995.

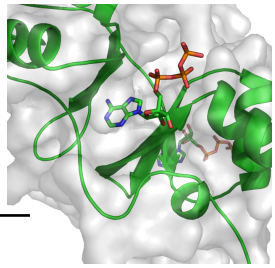

[102] M. R. Hansen, P. Hanson, and A. Pardi. Filamentous bacteriophage for aligning RNA, DNA, and proteins for measurement of nuclear magnetic resonance dipolar coupling interactions. *Methods Enzymol*, 317:220–240, 2000.

[103] M. R. Hansen, L. Mueller, and A. Pardi. Tunable alignment of macromolecules by filamentous phage yields dipolar coupling interactions. *Nat Struct Biol*, 5(12):1065–1074, Dec 1998.

[104] R. Keller. *The Computer Aided Resonance Assignment Tutorial*. Cantina Verlag, Goldau., 2004.

[105] J. E. Masse and R. Keller. AutoLink: automated sequential resonance assignment of biopolymers from NMR data by relative-hypothesis-prioritization-based simulated logic. *J Magn Reson*, 174(1):133–151, May 2005.

[106] D. S. Wishart, C. G. Bigam, A. Holm, R. S. Hodges, and B. D. Sykes. 1H, 13C and 15N random coil NMR chemical shifts of the common amino acids. I. Investigations of nearest-neighbor effects. *J Biomol NMR*, 5(1):67–81, Jan 1995.

[107] P. Schuck. Size-distribution analysis of macromolecules by sedimentation velocity ultracentrifugation and lamm equation modeling. *Biophys J*, 78(3):1606–1619, Mar 2000.

[108] P. Schuck, M. A. Perugini, N. R. Gonzales, G. J. Howlett, and D. Schubert. Size-distribution analysis of proteins by analytical ultracentrifugation: strategies and application to model systems. *Biophys J*, 82(2):1096–1111, Feb 2002.

[109] T. Ridgeway T. Laue, B. Shah and S. Pelletier. *Computer aided interpretation of analytical sedimentation data for proteins.* The Royal Society of Chemistry, Cambridge, UK, 1992.

[110] T. H. Pedersen, F. de Paoli, and O. B. Nielsen. Increased excitability of acidified skeletal muscle: role of chloride conductance. *J Gen Physiol*, 125(2):237–246, Feb 2005.

[111] X. Jin, R. Townley, and L. Shapiro. Structural Insight into AMPK Regulation: ADP Comes into Play. *Structure*, 15(10):1285–1295, Oct 2007.

[112] R. Townley and L. Shapiro. Crystal structures of the adenylate sensor from fission yeast AMP-activated protein kinase. *Science*, 315(5819):1726–1729, Mar 2007.

[113] J. Jämsen, H. Tuomunen, A. Salminen, G. Belogurov, N. Magretova, A. Baykov, and R. Lahti. A CBS domain-containing pyrophosphatase of Moorella thermoacetica is regulated by adenine nucleotides. *Biochem J*, Aug 2007.

[114] F. I. Ataullakhanov and V. M. Vitvitsky. What determines the intracellular ATP concentration. *Biosci Rep*, 22(5-6):501–511, 2002.

[115] D. A. Doyle, J. Morais Cabral, R. A. Pfuetzner, A. Kuo, J. M. Gulbis, S. L. Cohen, B. T. Chait, and R. MacKinnon. The structure of the potassium channel: molecular basis of K+ conduction and selectivity. *Science*, 280(5360):69–77, Apr 1998.

[116] K. P. Locher, A. T. Lee, and D. C. Rees. The E. coli BtuCD structure: a framework for ABC transporter architecture and mechanism. *Science*, 296(5570):1091–1098, May 2002.

[117] H. Luecke, B. Schobert, J. K. Lanyi, E. N. Spudich, and J. L. Spudich. Crystal structure of sensory rhodopsin II at 2.4 angstroms: insights into color tuning and transducer interaction. *Science*, 293(5534):1499–1503, Aug 2001.

[118] A. Yamashita, S. K. Singh, T. Kawate, Y. Jin, and E. Gouaux. Crystal structure of a bacterial homologue of Na+/Cl–dependent neurotransmitter transporters. *Nature*, 437(7056):215–223, Sep 2005.

[119] R. MacKinnon. Potassium channels and the atomic basis of selective ion conduction (Nobel Lecture). *Angew Chem Int Ed Engl*, 43(33):4265–4277, Aug 2004.

[120] S. F. Altschul, W. Gish, W. Miller, E. W. Myers, and D. J. Lipman. Basic local alignment search tool. *J Mol Biol*, 215(3):403–410, Oct 1990.

[121] T. Berkelman, P. Garret-Engele, and N. E. Hoffman. The pacL gene of Synechococcus sp. strain PCC 7942 encodes a Ca(2+)-transporting ATPase. *J Bacteriol*, 176(14):4430–4436, Jul 1994.

[122] T. Kawate and E. Gouaux. Fluorescence-detection size-exclusion chromatography for precrystallization screening of integral membrane proteins. *Structure*, 14(4):673–681, Apr 2006.

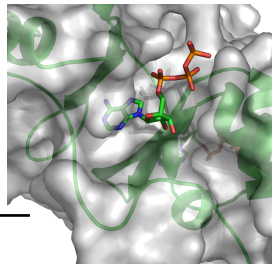

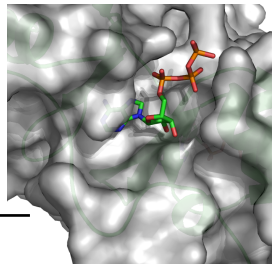

Curriculum Vitae

SEBASTIAN MEYER

Born:	06 September 1977
Place:	Hamburg
Nationality	German

Education

01/2004 – 01/2008	PhD thesis at the Universtiät Zürich and Molecular Life Science PhD Program/
2003	Diploma thesis at the Center for Molecular Neurobiology; Title: "Struktur-Funktionsanalyse von ClC-Kb und Barttin"
1998 – 2003	Studiengang Biochemie / Molekularbiologie, University Hamburg
1988 – 1997	Allgemeine Hochschulreife Gymnasium Dörpsweg, Hamburg

Professional Development

03/2007	Postgraduate Course – Zurich Center for integrative Human Physiology; Title:"Electrophysiology"
07/2006	Poster Presentation – Gordon Research Conference "Ion Channels" Tilton, NH, USA; Title: "Regulatory Domains of the Chloride Transporter ClC-5"

09/2006	Postgraduate Course – Swiss Light Source at the Paul Scherrer Institute, Villigen, Switzerland; Title: "Synchrotron Data Acquisition Techniques in Macromolecular Crystallography"

Publications

1. Alioth, S., **Meyer, S.**, Dutzler, R. & Pervushin, K. The Cytoplasmic Domain of the Chloride Channel ClC-0: Structural and Dynamic Characterization of Flexible Regions. J Mol Biol 369, 1163-1169 (2007)

2. **Meyer, S.**, Savaresi, S., Forster, I.C. & Dutzler, R. Nucleotide recognition by the cytoplasmic domain of the human chloride transporter ClC-5. Nat Struct Mol Biol 14, 60-7 (2007)

3. **Meyer, S.** & Dutzler, R. Crystal structure of the cytoplasmic domain of the chloride channel ClC-0. Structure 14, 299-307 (2006)

Zürich, March 14, 2008